R-09-45

Hydraulic Features of the Excavation Disturbed Zone – Laboratory investigations of samples taken from the Q- and S-tunnels at Äspö HRL

Lars O. Ericsson, Petra Brinkhoff,
Gunnar Gustafson, Sara Kvartsberg
Division of GeoEngineering, Department of Civil and Environmental Engineering, Chalmers University of Technology

December 2009

Svensk Kärnbränslehantering AB
Swedish Nuclear Fuel
and Waste Management Co

Box 250, SE-101 24 Stockholm
Phone +46 8 459 84 00

ISSN 1402-3091
SKB Rapport R-09-45

Hydraulic Features of the Excavation Disturbed Zone – Laboratory investigations of samples taken from the Q- and S-tunnels at Äspö HRL

Lars O. Ericsson, Petra Brinkhoff,
Gunnar Gustafson, Sara Kvartsberg
Division of GeoEngineering, Department of Civil
and Environmental Engineering, Chalmers
University of Technology

December 2009

Preface

The project "Hydraulic features in EDZ – Laboratory investigations and introductory field measurements" was part of the overall SKB programme ZUSE (*störda **Z**onens mekaniska och hydra**U**li**S**ka **E**genskaper*- 'Mechanical and hydraulic features of the excavation disturbed zone') in order to increase our understanding of the mechanical and hydraulic features in the zone around a tunnel affected by blasting. This report is the concluding report in this sub-project.

The majority of the work has been carried out at the Division of GeoEngineering at the Department of Civil and Environmental Engineering at Chalmers University of Technology, Gothenburg. For those parts of the project that dealt with analysis of microfracturing, the services of Dr. Urban Åkesson at SP in Borås were enlisted. *In situ* measurements in the form of single-hole tests were made in co-operation with POSIVA, Finland and within the framework of the Tunnel Sealing Project at Äspö. Core-drilling at Äspö was carried out by Miro Diamantborrning. Scoping calculations on rock stresses surrounding the Q- and S-tunnels at Äspö Hard Rock Laboratory were performed by Dr. I. Olofsson and Prof. D. Martin.

There has been close co-operation between the project at Chalmers and another sub-project within the ZUSE programme, the aim of which was to provide a better understanding of the geometrical spread of a disturbed or damaged zone, both radially and axially. This second sub-project, which was run by Swebrec and Golder Associates, involved sawing blocks from the tunnel wall, measuring the blocks, sawing the blocks into slabs, fracture detection with the aid of penetrants, positioning and photographing of the slabs, digitisation and 3-D modelling of the fractures. Furthermore close co-operation has been taking place with a separate ZUSE-project on international EDZ-experiences /Bäckblom 2008/.

Gothenburg, October 21, 2009

Lars O. Ericsson
Project Leader

Contents

1	**Introduction**	**7**
2	**Objectives**	**9**
3	**Sampling locations**	**11**
3.1	The Q-tunnel	11
3.2	The S-tunnel	13
4	**Laboratory testing of fracture transmissivity**	**17**
4.1	Triaxial cell Permeameter	18
4.2	Test method	18
4.3	Confining pressure	19
4.4	Flow measurements	20
5	**Drilling and sampling**	**21**
5.1	Drilling of Q-tunnel samples	21
5.2	Drilling of S-tunnel samples	22
5.3	Rock samples from the Q-tunnel	22
	5.3.1 Smaller samples	22
	5.3.2 Larger samples	23
5.4	Rock samples from the S-tunnel	24
5.5	Ultrasonic scanlines in the Q-tunnel and S-tunnel	24
6	**Hydraulic tests in S-tunnel**	**25**
7	**Brief descriptions of the analysis methods**	**27**
7.1	Transmissivity calculations	27
	7.1.1 Laboratory testing	27
	7.1.2 *In situ* testing	27
7.2	Microfracturing	27
	7.2.1 Ultrasonics	27
	7.2.2 Matrix porosity	29
	7.2.3 Microscoping	29
7.3	QA checks and uncertainties	29
8	**Results**	**31**
8.1	Transmissivities in the disturbed zone	31
	8.1.1 Q-tunnel	31
	8.1.2 S-tunnel	32
	8.1.3 Hydromechanical coupling	33
8.2	*In situ* measurements in the S-tunnel	37
	8.2.1 Transmissivities for all boreholes	37
	8.2.2 Transmissivities for all test sections	38
	8.2.3 Water pressure in the boreholes	40
8.3	Microfracturing	40
	8.3.1 Ultrasonics	40
	8.3.2 Matrix porosity, Q-tunnel	44
	8.3.3 Microscoping	45
9	**Discussion and conclusions**	**47**
References		**51**

Appendix 1	Investigations in the Q-tunnel Äspö HRL. Database	53
Appendix 2	Investigations in the S-tunnel Äspö HRL, Database	61
Appendix 3	Field investigations in the S-tunnel Äspö HRL. Database	89
Appendix 4	Characterisation of micro cracks in EDZ	91
Appendix 5	Investigation of natural fracture traces used in EDZ 3D-model	97
Appendix 6	Survey of natural fractures in EDZ slabs	105
Appendix 7	Length of fractures in EDZ 3D model	119
Appendix 8	Length of the sorted natural fractures	125

1 Introduction

During underground work the prevailing features in the bedrock in the immediate vicinity of a tunnel or a facility for nuclear waste are affected in terms of the mechanical stress distribution and the groundwater conditions. If conventional tunnelling is used, with charge drilling and subsequent blasting, a damaged zone or disturbed zone may be created in the tunnel perimeter. The extent of the zone depends, among other things, on the drilling precision, specific charge and the shape of the tunnel cross-section. A general conceptual understanding of hydraulic conditions in the zone is essential when describing the groundwater flows and possible nuclide transport around a nuclear waste repository /see e.g. Hudson et al. 2009/.

In order to increase our understanding of the mechanical and hydraulic features in the zone around a tunnel affected by blasting SKB initiated a R&D activity: ZUSE (*störda* ***Z****onens mekaniska and hydra****U****li****S****ka* ***E****genskaper*- 'Mechanical and hydraulic features of the excavation disturbed zone'). The activity has comprised literature surveys /Bäckblom 2008/, extensive geometrical fracture mapping and 3D-modelling on slabs from a tunnel wall /Olsson et al. 2009/, hydraulic a hydrochemical modelling /Laaksoharju et al. 2009/.

Furthermore and consequently, a separate project focusing on hydraulic features in the immediate zone along a tunnel wall was carried out within the ZUSE program. Examinations of rock samples have been carried out in the laboratory. In addition, *in situ* measurements were made in the form of hydraulic tests directly in the tunnel wall. In the project, samples and drilling cores were taken from slabs sawn out of the tunnel walls in the Q- and S-tunnels at the Äspö Hard Rock Laboratory, HRL, in Oskarshamn. The samples were examined at the laboratory with regard to fracture transmissivity, microfracturing and matrix porosity.

2 Objectives

The general aim of the project has been to contribute to the SKB safety and assessment analysis with realistic figures of hydraulic properties in an excavation disturbed zone. The project had the following more detailed objectives:

- Develop a laboratory method to determine fracture transmissivity under water-saturated conditions.
- Provide magnitudes for realistic values for fracture transmissivity in the disturbed or damaged zone due to excavation.
- Map micro cracks radially from the tunnel wall.
- Map the spread of matrix porosity radially from the tunnel wall.
- Develop single-hole hydraulic testing methodology in tunnel wall for saturated conditions.
- Integration of fracture geometries and transmissivity investigations for conceptual hydraulic modelling of the bedrock along a tunnel wall.

3 Sampling locations

The samples, i.e. drill cores investigated in this project, were taken from rock slabs originating in the Q- and S-tunnels at Äspö HRL, see Figure 3-1. The bedrock at the Äspö HRL consists of diorite, intersected by granitic and pegmatitic dykes.The rock slabs from the Q-tunnel are described in more detail in /Olsson et al. 2004/. The samples from the rock slabs taken from the S-tunnel were drilled out *in situ* at Äspö in December 2008. For further information about the rock slabs in the S-tunnel, reference can be made to /Olsson et al. 2009/.

3.1 The Q-tunnel

The Q-tunnel was blasted in a particular way to create high *in situ* stress between the test holes in the tunnel floor. This was achieved by making the quotient between height and width large and by creating a semicircular floor /Andersson 2007/. A simple numerical model of the stress situation in the tunnel is shown in Figure 3-2. There were strict demands regarding the blasting of the tunnel to minimise the excavation disturbed or damaged zone using careful blasting, which made extraordinary demands on the location and charging of the charge boreholes /Olsson et al. 2004/.

In order to study the damage to the remaining rock, a number of sections were sawn out from the tunnel wall – five vertical slots and one horizontal. Slabs were then sawn out from each vertical slot, making a total of 15 slabs. The sides of the slabs were then mapped with the aid of penetrant fluid to determine the type of fractures and their spread from the tunnel wall or the blasting core. A section was also sawn in the floor. The fractures were categorised as natural, blast-induced and directly from the charge borehole. The results are presented in /Olsson et al. 2004/.

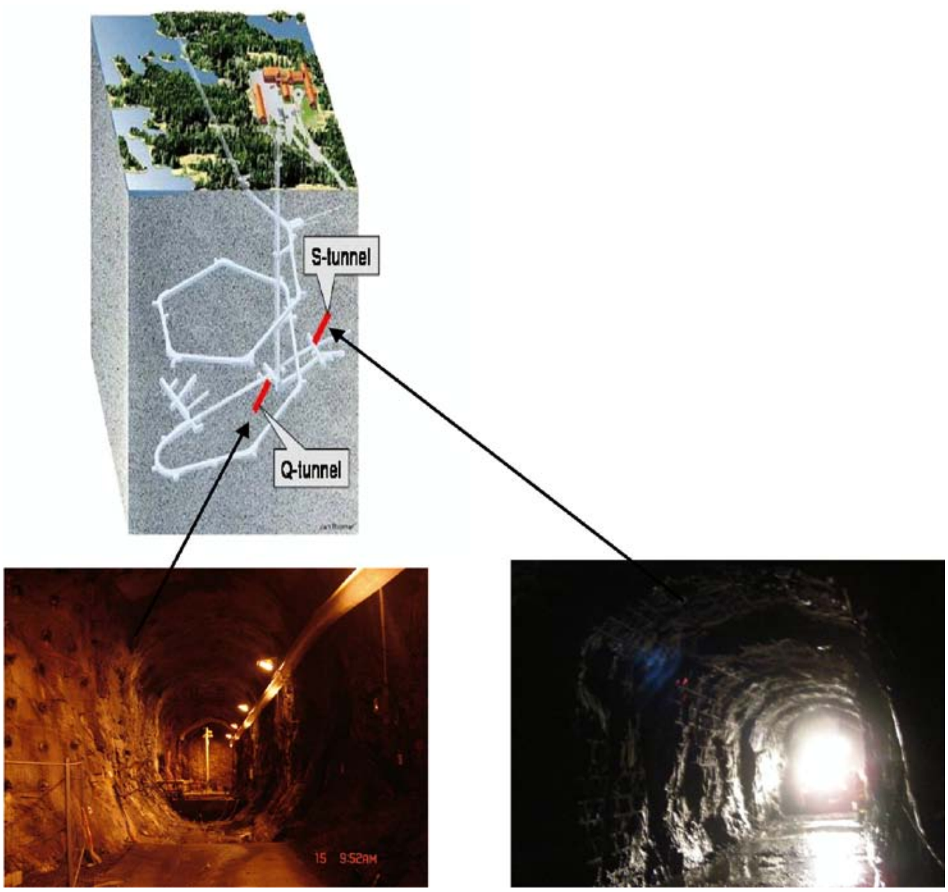

Figure 3-1. *Location of the Q- and S-tunnels at Äspö HRL.*

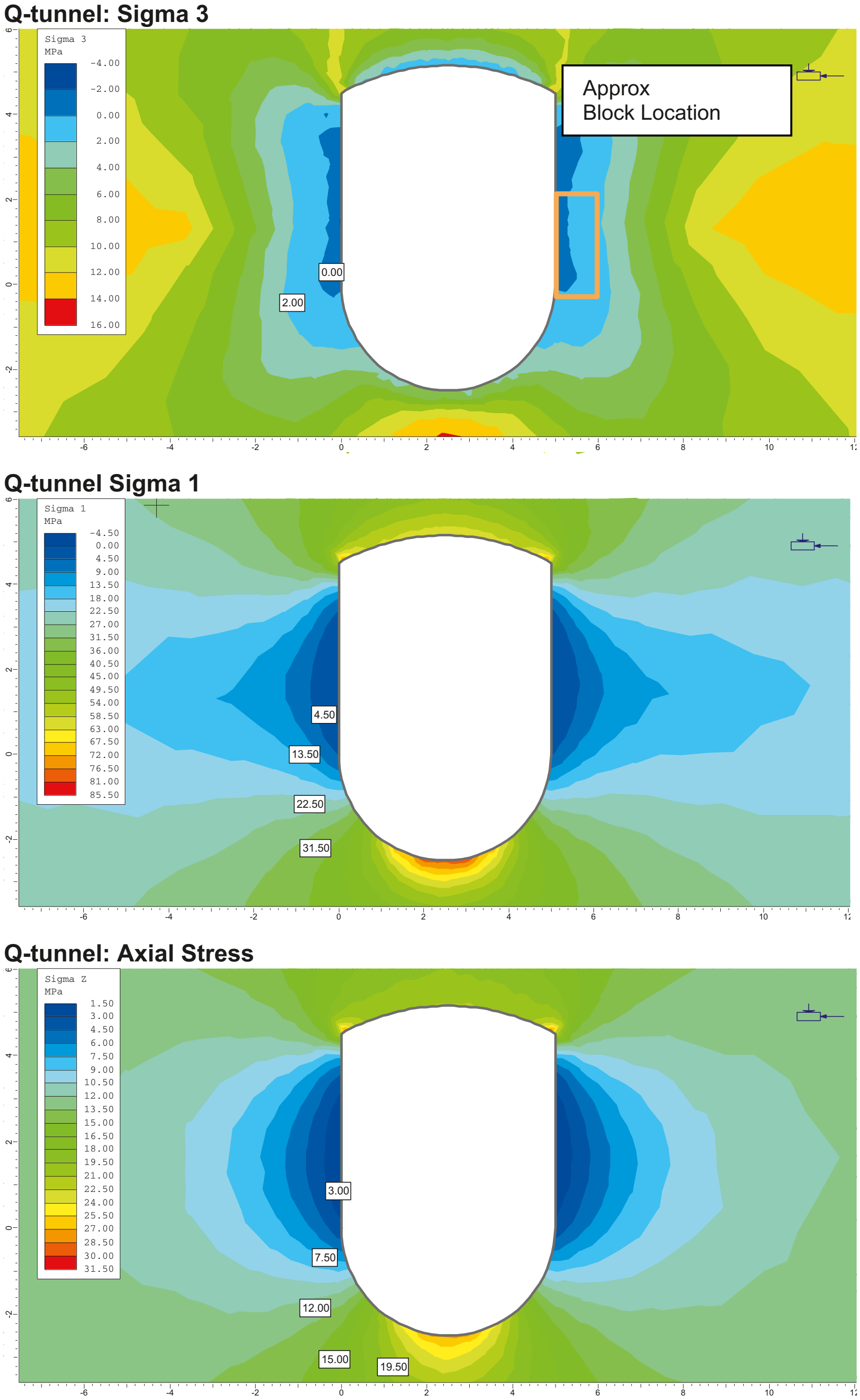

Figure 3-2. *The stress situation in the Q-tunnel, which shows the vertical stress Sigma 3, the horizontal stress Sigma 1 and the axial stress.*

Six of the slabs were examined by /Olsson et al. 2008/ as part of a method study for documentation and 3-D modelling of blast-induced fractures. In the present investigation, five vertical slabs and one horizontal slab were used, AD-AA and BD (see Figure 3-3). Four of the slabs are from test area 2 (the so-called A group) and one from test area 3 (the so-called B group), see also /Olsson et al. 2008/.

In the present project partial use was made of the same slabs that were used in the method study by /Olsson et al. 2008/. Table 3-1 shows which slabs are common to the two studies and additional slabs in this study.

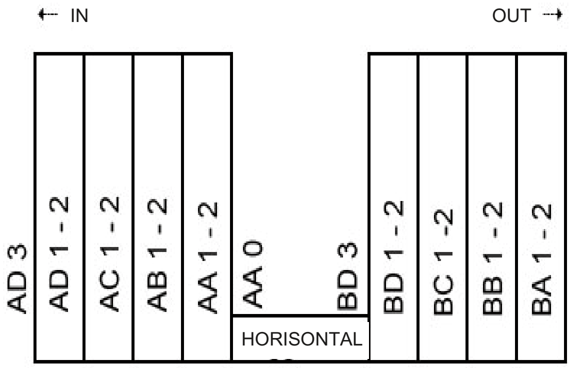

Figure 3-3. *The principle behind which slabs in the method study for documentation and 3-D modelling of blast-induced cracks are sawn out from the tunnel wall and into the rock /from Olsson et al. 2008/.*

Table 3-1. Slabs which are common to the study in the Q-tunnel by /Olsson et al. 2008/ and the id of other slabs in this study.

Common slabs	Other slabs in this project
AA 1-2	BC 1-2
AB 1-2	BB 1-2
AC 1-2	4:1 lower
BD 1-2	2:2:2
	XX

3.2 The S-tunnel

The primarily objective with the S-tunnel was to develop strategies and technology for grouting a tunnel to meet high demands on restricted inflow. The secondary objective was to explore how high requirements on smooth and careful blasting are feasible to achieve. High effort was put on the drilling of the contour and helper holes. Furthermore the excavation was based on recent research on parameters of importance for careful blasting findings. This included use of electronic detonators to reduce damage in the contour.

The S-tunnel is located at 450 m depth. The crystalline rock mass is dominated by diorite and cross-cut by two sub-vertical joint sets, trending NW and NE. The S-tunnels is aligned in a large angle to the NW joint set, which is also found to be the most water bearing set. In addition, there is also a gently dipping joint set. The rock quality is good, average RMR value for the tunnel is 70.4, ranging between 66 and 81. The uniaxial strength is in the range of 210–225 MPa, and a Young's modulus of 75–80 GPa.

The major horizontal stress is in the order of 28–30 MPa at the 450-m level, trending NW–SE, sub-parallel to the NW joint set and consequently perpendicular to the tunnel. The minor horizontal stress and the vertical stress are both close to the the weight of the overburden, 12–13 MPa.

The S-tunnel was blasted in a traditional horseshoe shape as opposed to the Q-tunnel. General numerical modelling of the stress situation in the tunnel is shown in Figure 3-4.

In the tunnel, eight blocks, each 1.5 m high, 1 m wide and 0.6–1.0 m deep, were sawn from the tunnel wall using a diamond wire saw to allow the zone of expected disturbance or damage to be studied in more detail. The blocks were then sawn into 75 slabs in order to categorise, using a penetrant fluid and photography, direct blast induced fractures from charge holes and induced and natural fractures in the surroundings of the tunnel. The categorisation resulted in a 3-D image of the spread of the fractures and the connectivity in the rock mass. Figure 3-5 shows a 3-D model of fractures in the block from the S-tunnel, /Olsson et al. 2009/. In order to distinguish between different kinds of natural fractures a succeeding mapping survey was performed. Thus the natural fractures were divided into healed, closed/tight and open fractures (See Appendices 5–8).

S-tunnel: Sigma 3

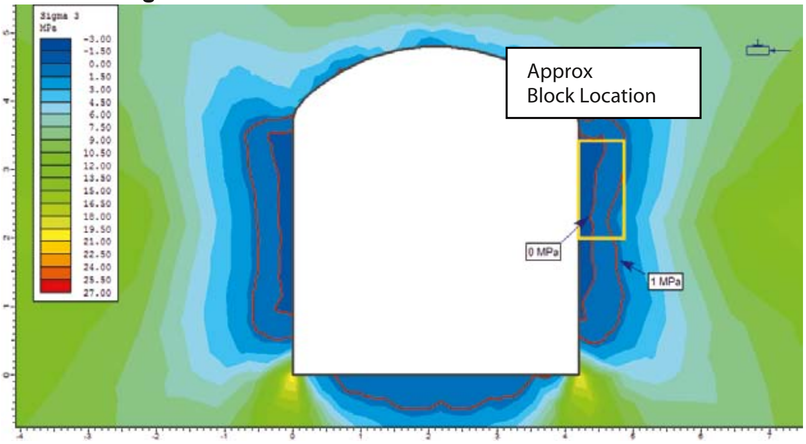

S-tunnel: Sigma 1

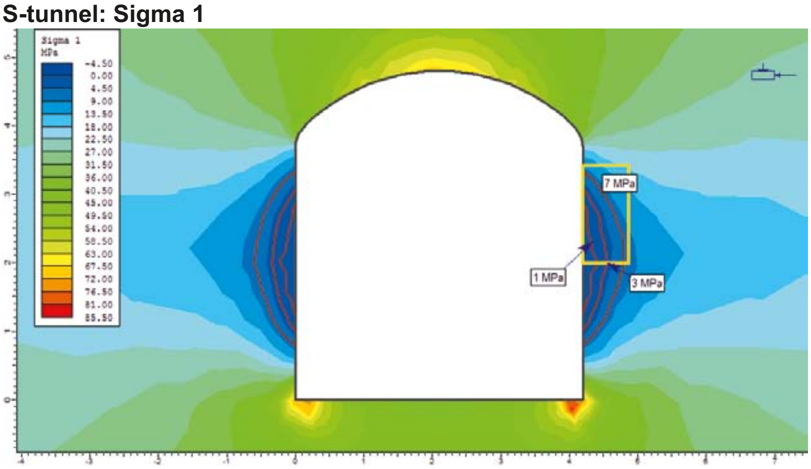

S-tunnel: Sigma Z - Axialstress

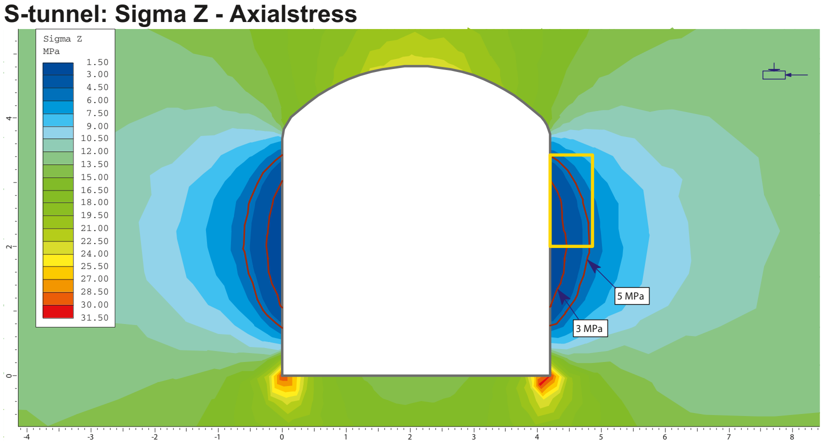

Figure 3-4. *Estimated stress situation in the S-tunnel based on elastic assumptions, material properties and in situ stresses as in Figure 3-2; vertical stress Sigma 3, horizontal stress Sigma 1 and axial stress.*

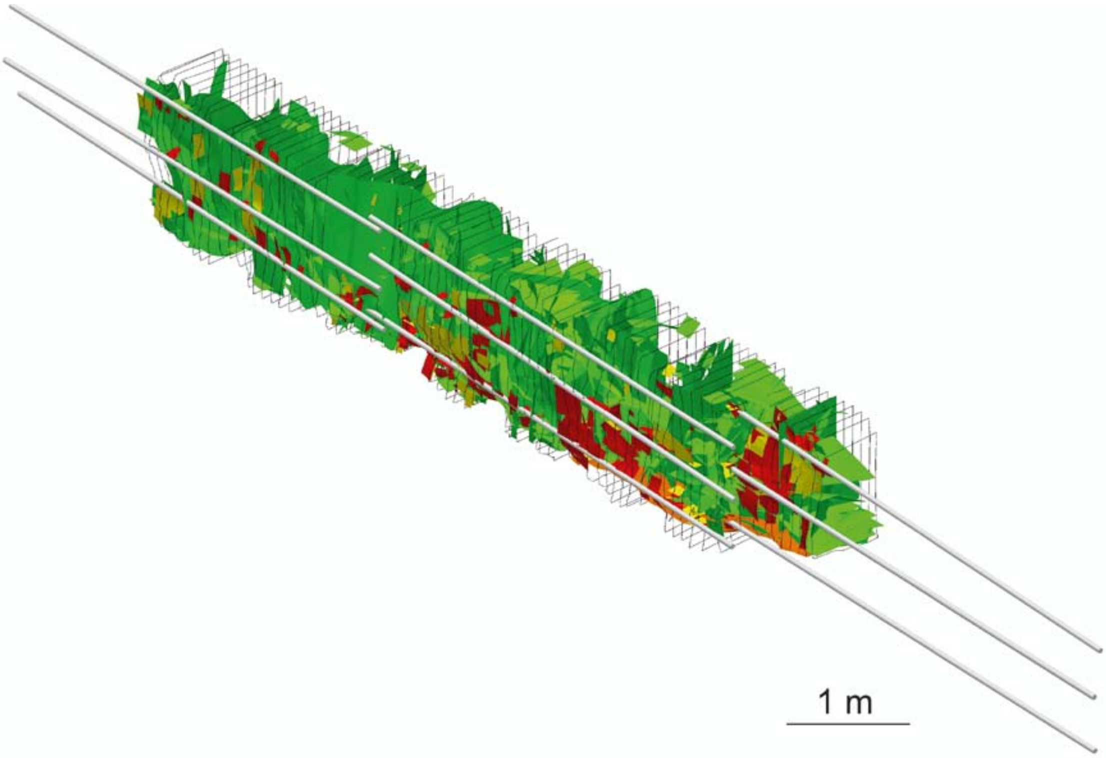

Figure 3-5. *A 3-D model of the fractures in the block sawn from the S-tunnel. The figure shows the slabs and contour holes as well as interpreted natural fractures (green), induced fractures (yellow) and direct blast-induced fractures (red) /from Olsson et al. 2009/.*

4 Laboratory testing of fracture transmissivity

The test equipment in the laboratory is purposely built and comprised a triaxial cell permeameter, a water container, a graduated measuring glass where the water that passes through the permeameter is collected, a pressure tube with compressed air as well as pipes. The pipes connect the water container to the permeameter and then the permeameter to the measuring glass. The pressure of the air that is forced into the triaxial cell but outside the sample membrane is measured using a manometer. Figures 4-1 and 4-2 show the test equipment. In total, 11 rock samples from the Q-tunnel and 19 from the S-tunnel were tested. For further information about the rock samples and other conditions in conjunction with the tests, see Appendices 1 and 2.

Figure 4-1. *Equipment used for testing rock samples from the Q- and S-tunnel. The red vertical line represents the fall in pressure, dh, through the sample.*

Figure 4-2. *To the left is the triaxial cell permeameter and its different parts and to the right is a sample placed on the bottom plate. The sample is surrounded by double rubber membranes and a total of four o-rings.*

4.1 Triaxial cell Permeameter

The permeameter which makes it possible to examine cores with a diameter of 200 mm and height approximately 100 mm, was made at the Division of GeoEngineering at Chalmers University of Technology. The cell is triaxial and is set up for pressures of up to 4 MPa. In the triaxial cell the radial and axial load were the same. The maximum confining pressure in this case was 2.5 MPa. The cell comprises:

- a bottom plate with a net,
- a top plate with a net as a holding tool with a steel pipe to channel the water out of the cell,
- a steel cylinder,
- a steel lid,
- 12 long, threaded bolts.

In addition to the above there are two rubber membranes and 4–6 o-rings, which are placed around/on the drilling core to keep it tight against the compressed air inside the cell. The water that enters the cell should only pass through the core and not between the core and the membrane. Nor should it leak out through the membrane, hence the use of a double membrane, see Figure 4-2.

4.2 Test method

Following an initial test of the methodology, the test equipment was adjusted to optimise the measurements (three tests for samples from the Q-tunnel were carried out using a simplified test arrangement). The test arrangement meant that the water that was used first was boiled in a vacuum for at least 1.5 hours to reduce the volume of air. The air proved to be a probable reason for the reduced flow over time during the methodology test (see Figure 4-3).

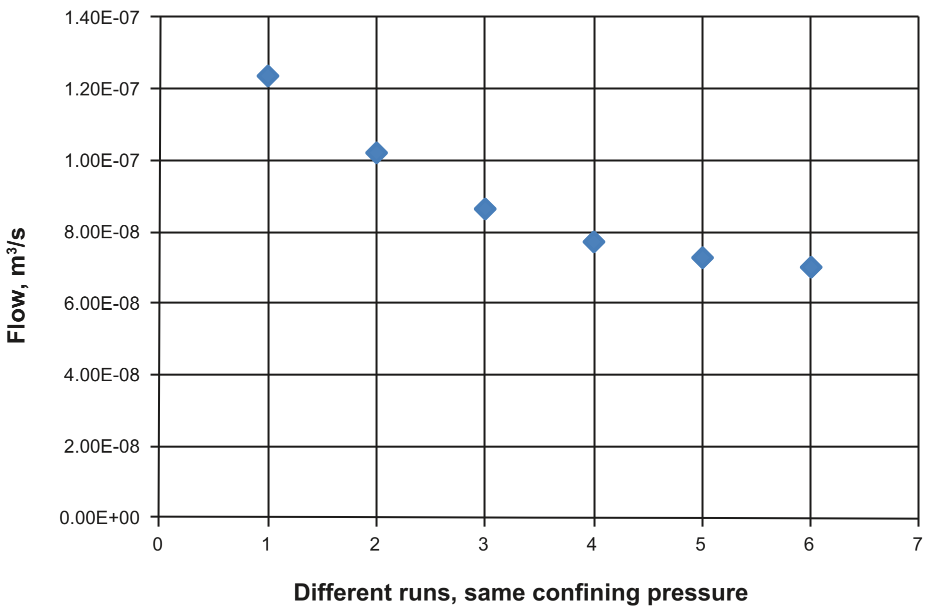

Figure 4-3. *The graph shows the flow through a rock sample in conjunction with six different measurements and under constant confining pressure. The flow decreased in conjunction with each measurement despite a constant confining pressure.*

The core itself was subjected to vacuum suction for 20–30 minutes after being placed in the cell. This was done to remove as much air as possible. The de-aerated water was then sucked into the core under vacuum conditions before measurement commenced. To maintain a constant gradient across the sample, the water tank was placed on a pallet truck, which was raised as the water in the tank fell. The water tank also had a plastic lid to prevent contact between the air and the water inside the tank.

Due to the very low porosity figures, it was necessary in the case of 11 of the rock samples from the S-tunnel to further modify the test method. The (incoming) water pressure to the sample was increased to approximately 0.35 MPa with the aid of air forced into the water tank, which was transformed into a sealed vessel.

4.3 Confining pressure

Based on the general numerical calculations, presented in Chapters 3.1 and 3.2, the tests were conducted with generalised confining pressures, i.e. corresponding fracture normal stresses of **0.5** and **1.0** MPa /Larsson 1997/. The stress levels were deliberately chosen to reflect a conservative flow situation, i.e. an over-estimation of the fracture transmissivities in fractures close to a tunnel wall. The flow estimations in the test procedure are in accordance with increased normal stress from 0.5 to 1.0 MPa.

By performing a sequence of measurements with more stress-levels and where the confining pressure first increased and then decreased, it however became clear that the fractures are unable to revert to their original width once the stress is decreased. In Figure 4-4 this can be seen clearly as the flow in conjunction with stress relief remains largely the same or is marginally higher compared with the maximum confining flow figure. A number of separate test series have been conducted to study the change in stiffness with regard to load cycles through an individual fracture, see Section 8.1.3.

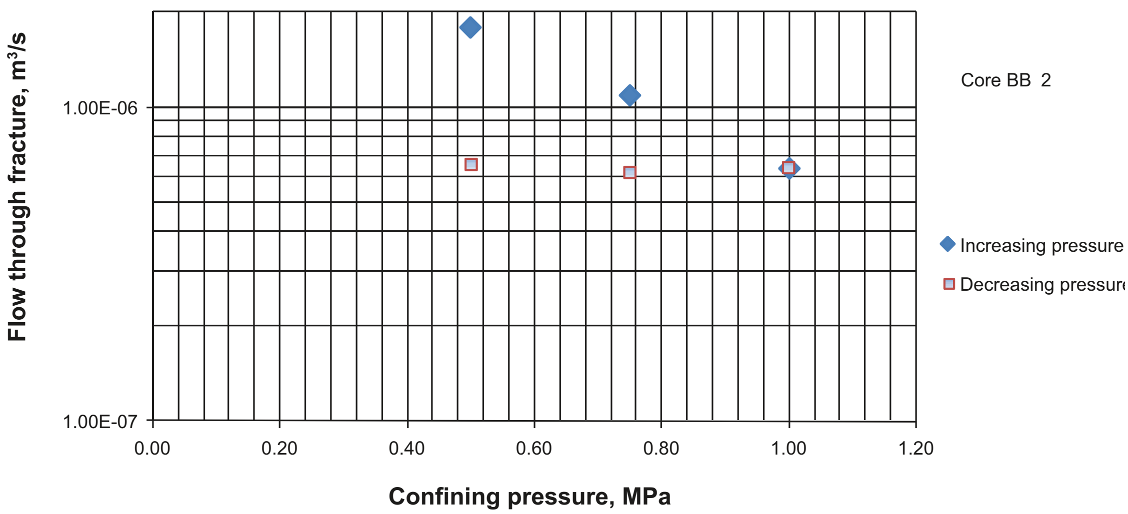

Figure 4-4. *Diagram showing the flow through a rock sample at different confining pressures. The sample is first exposed to increasing stress and then decreasing stress.*

4.4 Flow measurements

Normally, the flow through the permeameter is measured with the aid of a graduated measuring glass with a resolution of one millilitre. In those cases where the flow was very small, a time estimate for filling a certain small volume was applied.

5 Drilling and sampling

5.1 Drilling of Q-tunnel samples

The rock samples from the Q-tunnel slabs were drilled at Chalmers University of Technology. Two different drilling arrangements were used: one for the smaller samples (diameter 42 mm), see Figure 5-1 and the description in Section 5.3.1, and one for the larger rock samples (diameter 200 mm). For the larger rock samples no protective plate was used at first over the rock sample although later on drilling took place with a steel plate attached to the rock surface to avoid the fracture opening up during drilling (see Figure 5-2).

Figure 5-1. *Drilling of smaller samples from slab BC.*

Figure 5-2. *Drilling of a larger sample (diameter 200 mm) with a protective steel plate.*

5.2 Drilling of S-tunnel samples

The rock samples from the S-tunnel were drilled at Äspö where the rock slabs are stored. The preparatory work included selecting fractures varying in origin from the rock slabs. Fractures with *one* clear vertical spread were chosen where possible.

5.3 Rock samples from the Q-tunnel

For the slabs from the Q-tunnel, the sampling can be regarded as random across available individual fractures. Two sample sizes were drilled from slab BC, three small and one large. From the remaining slabs only large samples were drilled. A total of seven small rock samples were taken, see Table 5-1, as well as 11 large rock samples, see Table 5-2.

5.3.1 Smaller samples

A smaller borehole (designated h) with a diameter of 42 mm was drilled in rock slab BC at right angles to the direction of the tunnel. The sample was drilled from the charge borehole marking and into the slab, which is the same as into the tunnel wall. The total length was 40.5 cm, see Figure 5-3. It was not possible to extract the core fully intact. The first 16 cm were broken up into a large number of small parts, see Figure 5-4. The remaining part of the core was in two parts. Samples varying in length were made from these.

A further two smaller samples were drilled from slab BC (see Figure 5-5). These were drilled in the direction of the tunnel (designated v), one closer to the charge borehole and one farther away. The samples were thus cylindrical in shape with ground, intact ends.

Table 5-1. The ID of the smaller samples from slab BC and also the direction in which they were drilled in relation to the blasting direction.

Sample ID, small cores	Location in the slab
v1a	Core in the direction of the tunnel, 20 cm from tunnel wall
v1b	Core in the direction of the tunnel, 34.5 cm from tunnel wall
h1a	Core at right angles to the direction of the tunnel
h1b	Core at right angles to the direction of the tunnel
h1c	Core at right angles to the direction of the tunnel, approx. 16 cm
h1d	Core at right angles to the direction of the tunnel, approx. 25 cm
h1e	Core at right angles to the direction of the tunnel, approx. 35 cm

Figure 5-3. *The whole of the first core taken from slab BC1-2, total 40.5 cm.*

Figure 5-4. A close-up of the damaged part closest to the charge borehole, the first 16 cm.

Figure 5-5. Drilled cores v1a and v1b from slab BC.

5.3.2 Larger samples

A total of 11 larger rock samples with a diameter of 200 mm and a height of approximately 100 mm were taken from slabs BC 1-2, BB 1-2, BD1-2, AB1-2, AC1-2, AA 1-2, 4:1 lower, 2.2.2 and XX. The ID of the rock samples is related to the ID listed in Table 5-2.

The samples BD1–BD2, 2:AB1–AB2, 3:AC1–AC2, 1:4 upper, 2:2:2 and XX were drilled in a different way compared to the BC and BB cores. As samples BC and BB tended to disintegrate, a stabilising steel plate was placed over the fracture before drilling the slab. This was done to avoid the fracture opening up during drilling. The cores could thus be kept intact prior to the permeameter tests, see Figure 5-2.

The larger samples were drilled parallel to the blast holes. In those cases where the ends of the large samples were damaged, these were filled in with silicone. Silicone was also used to fill in the holes that arose when attaching the protective plate.

Table 5-2. The ID of the larger rock samples and the slabs from the Q-tunnel.

Sample ID, larger rock samples	Slab
BC	BC 1-2
BB1	BB 1-2
BB2	BB 1-2
BB3	BB 1-2
BD1–BD2	BD 1-2
2, AB1–AB2	AB 1-2
3, AC1–AC2	AC 1-2
1:4 upper	AA 1-2
4:1 lower	4:1 lower
2:2:2	2:2:2
XX	XX

5.4 Rock samples from the S-tunnel

A total of 21 rock samples with a diameter of 190–200 mm and varying in height were drilled out from the slabs from the S-tunnel, see Table 5-3. **PS** stands for **P**rov i **S**kiva (sample in slab) the number after 00 is the number of the block (= number of running metres into the tunnel) and the second to last figure is the running number of the slab in each block. The last figure is the running number of the sample taken from the slab. Two rock samples were destroyed after extraction and are not included in the examination as they were too damaged to be tested in the permeameter. These are rock samples PS0037071 and PS0037091. Classified sampling of fractures was carried out on the S-tunnel block. The fractures were interpreted as natural /Olsson et al. 2009/ divided into healed, tight/closed and open (see Appendices 5–8).

The samples in the S-tunnel were also drilled in parallel to the blast holes (the tunnel). In those cases where the ends of the large samples were damaged, these were filled in with silicone. Silicone was also used to fill in the holes that arose when attaching the protective plate.

The location of the samples was determined using the internal co-ordinate system in the Äspö project. An account can found in Appendix 2.

Table 5-3. ID of samples from the S-tunnel included in the examination.

ID, samples from slabs from the S-tunnel				
PS0036091	PS0037061	PS0039013	PS0039051	PS0040042
PS0037051	PS0037062	PS0039021	PS0039061	PS0040071
PS0037052	PS0039011	PS0039022	PS0039071	PS0040072
PS0037053	PS0039012	PS0039023	PS0040041	

5.5 Ultrasonic scanlines in the Q-tunnel and S-tunnel

Ultrasonic examinations were made directly of slab BC from the Q-tunnel.

An ultrasonic examination of slabs from the S-tunnel was carried out *in situ* at Äspö. The scan lines are designated **LS** for **L**ine in the slab, see Table 5-4 for the scan lines included in the examination and Appendix 2 for the location of the slabs. The scan lines were determined using the Äspö project's own co-ordinate system, Appendix 2.

Table 5-4. ID of the scan lines in the ultrasonic examination from the S-tunnel.

ID, lines in slabs from the S-tunnel	
LS0036041	LS0040071
LS0039061	LS0040041
LS0039062	LS0040061

6 Hydraulic tests in S-tunnel

In the S-tunnel, Äspö HRL, 11 short investigation holes were drilled to check the hydraulic features in the excavation disturbed or damaged zone. The drill holes were 50–60 cm deep. The aim was to make a comparison with the data obtained from the permeameter tests using the cores taken from the blocks that were sawn from the tunnel wall on the right-hand side. Five of the tests were carried out on the same wall as the block extraction, known as the right-hand wall, and six tests were carried out on the opposite tunnel wall in the same section.

The tests were carried out with the aid of single-packer equipment where pressure and water flow to and from the boreholes could be measured with a high degree of accuracy. In each borehole the tests commenced with static water pressure (after 15 minutes) and the inflow into the tunnel with an open valve was then registered for five minutes. This provides a good starting point for the subsequent water injection measurements (see Figures 6-1, 6-2).

In the boreholes one or several water injection measurements were then made by stepwise moving the packer into the borehole and injecting water under pressure for each measurement step. The injected water volume and injection pressure were registered during the test. The test results and raw data can be seen in Appendix 3.

The different test locations in the right-hand wall of the S-tunnel can be seen in Figure 6-3.

Figure 6-1. *Drilling, diameter 32 mm, for the purpose of single-hole testing.*

Figure 6-2. *Equipment for single-hole testing.*

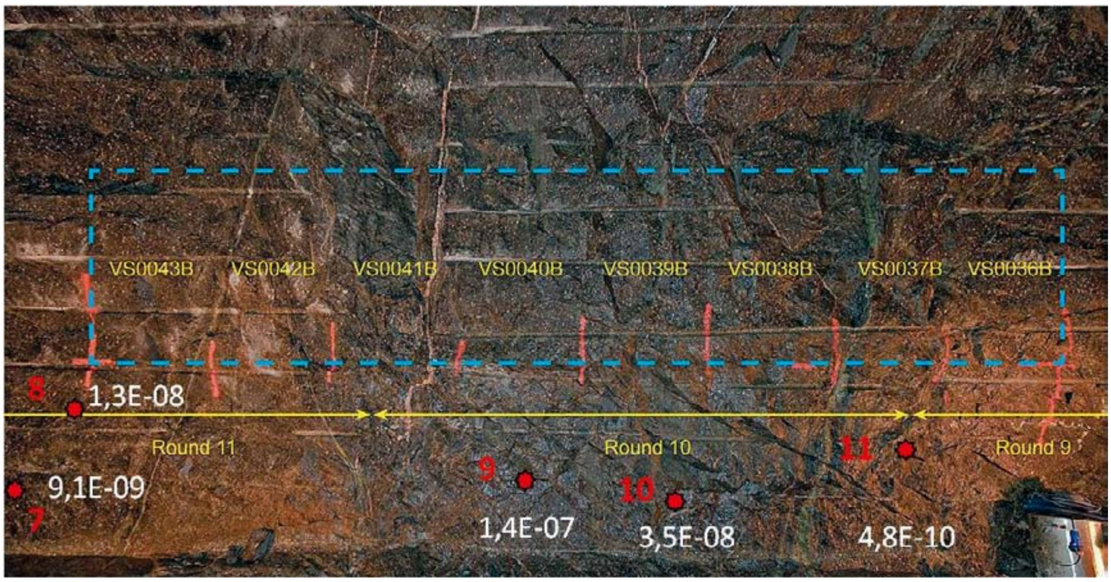

Figure 6-3. *Single-hole testing – Borehole positions, right-hand wall as well as determined total borehole values of transmissivity in the disturbed zone.*

7 Brief descriptions of the analysis methods

All methods used in the laboratory study were first tested on slab BC from the Q-tunnel and were then evaluated to determine whether they were suitable for continued use in the project.

7.1 Transmissivity calculations

7.1.1 Laboratory testing

With the aid of a triaxial cell permeameter the fracture transmissivity was analysed for the larger rock samples from the Q-tunnel and S-tunnel. The flow through the drilling core takes place mainly in a single fracture or, in some cases, in several fractures. The flow was measured with the core fixed firmly in the permeameter, which is described in Sections 4.1 and 4.2. If an average value is calculated for the trace length B (m) and if the flow length (L) and the pressure difference (dh) in the sample are determined it is possible to recalculate the flow to the transmissivity $T = Q/B \cdot (dh/L)$. The input parameters for evaluating fracture transmissivities are stated in Appendix 1 for the Q-tunnel and in Appendix 2 for the S-tunnel. The measurement limit for the determination of the transmissivity is estimated to $5 \cdot 10^{-12}$ m^2/s.

7.1.2 *In situ* testing

When calculating the water recharges to the zone nearby the wall in the S-tunnel, the injected water volume and injection pressure were registered. Data has been evaluated in such a way that specific capacity, *Q/dh,* was calculated for each measurement step. This value has proved to be a good approximation for the transmissivity value for the section for these short test periods /Gustafson 2009/. The measurement limit for the determination of the transmissivity is estimated to $1 \cdot 10^{-11}$ m^2/s.

7.2 Microfracturing

7.2.1 Ultrasonics

Microfracturing can be analysed by measuring the time it takes for a compression wave to pass through rock with a specific geometry. The travelling time is then related to the thickness of the rock. Using this method, the velocity of the wave through the rock is calculated. The velocity differences can be attributed to the varying mechanical characteristics of the rock. A more fractured section in the rock could produce lower throughflow velocities. This method is for comparison purposes only, which means that the results can only be interpreted within the group of samples/slabs examined in this study.

Ultrasonic scanlines, Q-tunnel

When measuring directly on the BC slab from the Q-tunnel, a surface area was first marked out on each side of the slab using a ruler and a spirit level. The surface area was equivalent to the diameter of an envisaged sample, approximately 2.17 cm. The surfaces overlap each other to provide more measurements (in effect running averages), see Figure 7-1. To ensure optimum contact, a contact gel was used on the surfaces of the sensor and the receiver.

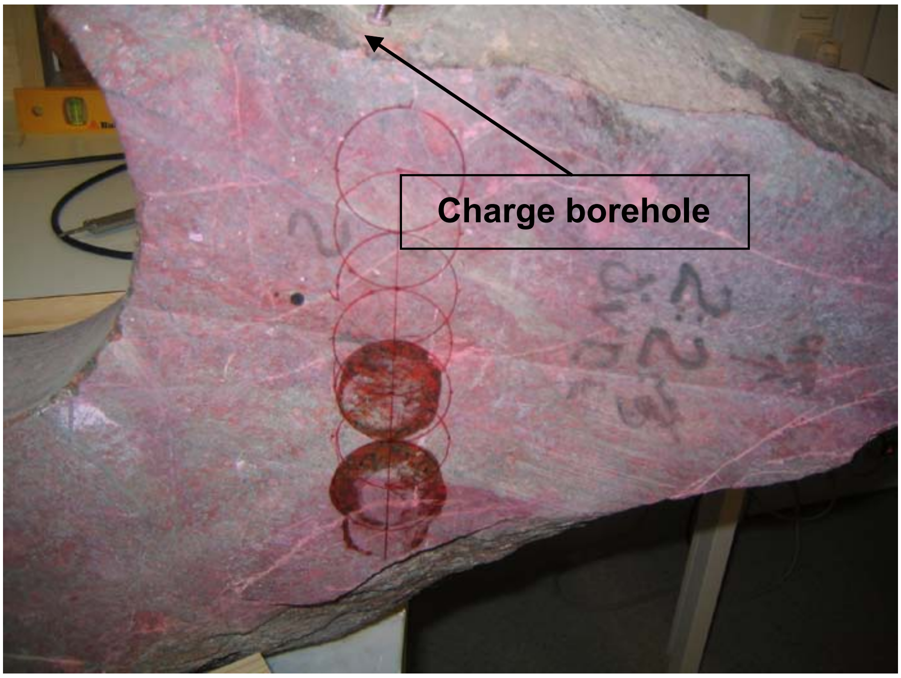

Figure 7-1. *Slab BC with surfaces marked for ultrasonic measurement.*

Ultrasonic scanlines, S-tunnel

A number of slabs were selected in accordance with Chapter 5.5 and placed in such a way that the sensor and receiver could be fixed with the aid of a constructed steel frame on either side of the slab, see Figure 7-2. To keep the sensor and receiver in the steel frame, each slot was milled to half the length of the sensor. Measurement can thus be carried out every half-sensor length, 2.05 cm, and upwards. To ensure optimum contact, a contact gel was used on the surfaces of the sensor and receiver.

Figure 7-2. *The steel frame placed on the slab so that the sensor and the receiver of the compression wave are fixed, both in relation to the scan line and to each other.*

7.2.2 Matrix porosity

The varying porosity could tell us something about possible blast-induced damage to the rock. With an increase in fracture frequency one might expect an increase in porosity. The porosity determinations should be regarded as comparative in the same way as the ultrasonic examinations.

The matrix porosity is the relationship between the total volume of the sample and the pore volume. The pore volume was determined using vacuum chamber technology. A sample was weighed following drying at 105°C for 24 h to a level of accuracy of 0.01 g. The sample was then treated in a vacuum for 90 minutes. This was done to extract the air from the pores. The core was then saturated with distilled water in a vacuum for 5.5 hours. Following the vacuum treatment, the sample was reweighed. The difference in weight before and after the vacuum treatment produces the weight of the water that has penetrated the pores. Knowing the density of the water, the volume of the penetrating water and thus the volume of the pores in the core can be calculated.

To obtain the volume of irregular samples comprising pieces of stone fractions, the Archimedes principle is used. The weight of the displaced fluid and the density of the water are used to determine the volume of the sample pieces. In the case of pore volumes in the irregular samples, the same method was used as for the intact cores.

7.2.3 Microscoping

A characterisation in a microscope of micro cracks from drilling cores extracted from the stone slabs in the Q-tunnel was also analysed, see Chapter 5.3.1. Five samples were analysed, of which three were placed at right angles to the tunnel wall (the h-samples). These samples were taken consecutively from the same drilling core. Two samples were placed parallel to the tunnel wall (the v-samples). The relative distances between the samples and the tunnel wall are shown in Table 7.1.

The samples were sawn up and a thin section, placed parallel to the drilling core, was made from each sample. In order to detect micro cracks, the samples were vacuum-impregnated with fluorescent epoxy.

Table 7.1. The relative distances to the tunnel wall of the microscoped samples.

Sample	Relationship to the tunnel wall
h1 C	Closest, approx. 16 cm
h1 D	Middle, approx. 25 cm
h1 E	Farthest away, approx. 35 cm
v1 A	Closest, approx. 20 cm
v1 B	Farthest away approx. 34.5 cm

7.3 QA checks and uncertainties

In order to verify that the permeameter was sealed and that no air has entered the sample through the cell membrane and that no water has infiltrated between the sample and the membrane, the permeameter was tested using a plastic dummy at confining pressures of 0.5 and 1.0 MPa. The dummy test was conducted for pressure differences across the sample of dh = 0.64 m.vp and dh = 35 m.vp. It was confirmed that the permeameter was tight.

The ultrasonic measurements were carried out by one person and as the method is for comparison purposes only this was deemed satisfactory for measurement accuracy. If any type of incorrect reading occurred it was probably the same in all measurements.

Ultrasonic measurements of small sample pieces or relatively thin sections can be problematic as larger, individual mineral grains can either increase or decrease the velocity. This could, in turn, mean that the measurement does not present a representative picture of the part of the rock being studied and simply reflects the mineral content.

Measurement accuracy when measuring the length of smaller samples was checked through repeated measurement (8) of both the height and width. For the height the deviation was at most 0.41% and the width 0.3%.

Regarding the in situ transmissivity determinations by means of single hole testing it was observed that the pressure was zero in approximately 50% of the boreholes. Thus underpressures in some testholes may have occurred but not been registered. The transmissivity determinations could thus be underestimated slightly as they possibly not represented water-saturated conditions (see Section 8.2.3).

8 Results

8.1 Transmissivities in the disturbed zone

In the light of the previously described methods and sampling, the transmissivity values listed below for the Q-tunnel and the S-tunnel were obtained. For the S-tunnel, the results from single-hole tests carried out in the field are also presented.

8.1.1 Q-tunnel

Tables 8-1 shows the transmissivity values for the samples analysed in the permeameter cell from the slabs from the Q-tunnel. See also Appendix 1. For the slabs from the Q-tunnel, the sampling can be regarded as random across available individual fractures. Log distributions for the resulting values are shown in Figure 8-1. In summary, the following was obtained:

At confining pressure 0.5 MPa – Mean value [log]: $T = 3.1 \cdot 10^{-7}$ m²/s, STD[log] = 0.62

At confining pressure 1.0 MPa – Mean value [log]: $T = 1.7 \cdot 10^{-7}$ m²/s, STD[log] = 0.62

By comparison, it can be noted that for a corresponding rock volume under undisturbed conditions, the preliminary examinations produced a Mean value [log]: $T = 4.9 \cdot 10^{-8}$ m²/s, STD[log] = 0.78 /Hernqvist et al. 2009/.

Table 8-1. Transmissivity values, samples from the Q-tunnel. Confining pressure 0.5 and 1.0 MPa.

Sample ID	T, m²/s at 0.5 MPa	T, m²/s at 1.0 MPa	Comments
BB1	5.922E-07	3.258E-07	One main fracture
BB3	0.000E+00	0.000E+00	No visible fracture
BC1	2.583E-06	1.575E-06	Confining pressure 0.6 MPa, One main fracture
BD1–BD2	5.449E-08	2.946E-08	Complex system of fractures
2, AB1–AB2	1.899E-07	9.585E-08	One fracture
3, AC1–AC2	3.641E-07	2.573E-07	One main fracture
1:4 upper	1.725E-06	1.050E-06	One main fracture
4:1 lower	0.000E+00	0.000E+00	Healed fractures
2.2.2	1.302E-07	9.223E-08	Complex system of fractures
Core XX	3.901E-07	1.651E-07	One main fracture
BB2	1.604E-06	5.723E-07	One main fracture, spline

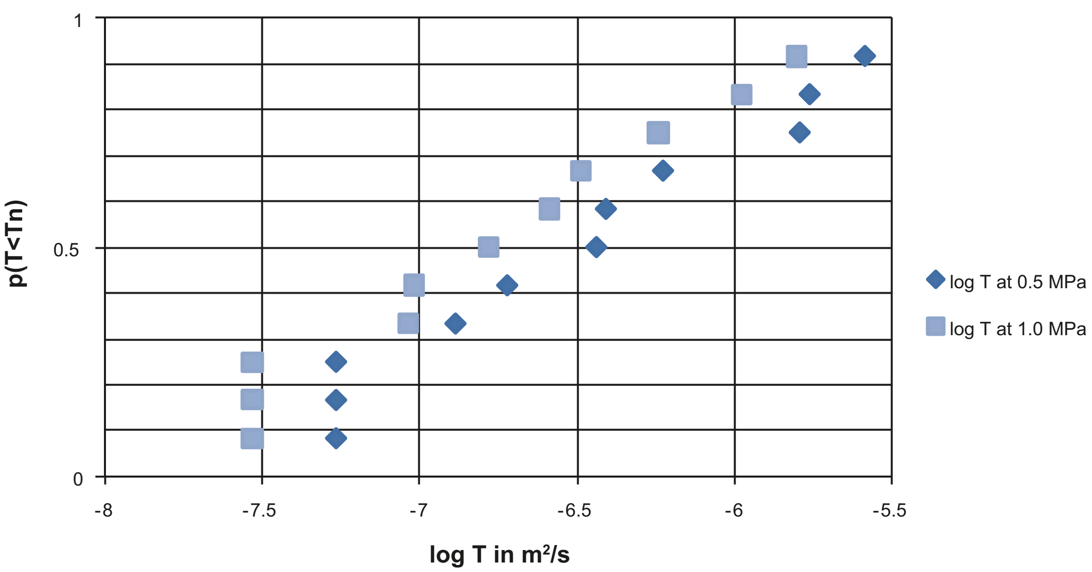

Figure 8-1. *Cumulative distribution, fracture transmissivities in the wall, Q-tunnel.*

8.1.2 S-tunnel

Table 8-2 shows the transmissivity values for the samples analysed in the permeameter cell from the slabs taken from the S-tunnel (see also Appendix 2). Classified sampling of fractures was carried out on the S-tunnel block. The fractures were interpreted as induced or natural /Olsson et al. 2009/ divided into healed, tight/closed and open (see Appendices 5–8). Figures 8-2 and 8-3 show the transmissivity values for the confining pressures 0.5 and 1.0 MPa as a function of the distance to the tunnel wall. If one regards the naturally open fractures as being taken from an undifferentiated population, a distribution graph according to Figure 8-4 is obtained. For the open, natural fractures:

At confining pressure 0.5 MPa – Mean value: $T = 3.7\cdot10^{-6}$ m²/s, STD[log] = 0.31
At confining pressure 1.0 MPa – Mean value: $T = 2.1\cdot10^{-6}$ m²/s, STD[log] = 0.34

Table 8-2. Transmissivity values, samples from the S-tunnel. Confining pressure 0.5 and 1.0 MPa.

Sample ID	T, m²/s at 0.5 MPa	T, m²/s at 1.0 MPa	Fracture type	Comments	Distance to wall, mm
PS0036091	4.84E-09	6.28E-10	Induced open (1/2)	Complex	138
PS0037051	0.00E+00	0.00E+00	Natural healed		325
PS0037052	0.00E+00	0.00E+00	Natural healed		50
PS0037053	3.46E-06	1.66E-06	Natural open		150
PS0037061	5.59E-06	2.71E-06	Natural open		75
PS0037062	3.32E-10	2.67E-10	Natural closed	Two fractures	538
PS0039011	0.00E+00	0.00E+00	Induced closed		53
PS0039012	1.36E-06	7.31E-07	Natural open		453
PS0039013	2.00E-09	5.69E-10	Natural closed		466
PS0039021	8.63E-11	5.00E-11	Induced open (1/2)		66
PS0039022	2.33E-06	1.33E-06	Natural open		413
PS0039023	5.68E-10	2.52E-10	Natural healed		493
PS0039051	1.12E-05	7.58E-06	Natural open	Three fractures	26
PS0039061	4.07E-06	2.23E-06	Natural open		280
PS0039071	4.69E-09	2.19E-09	Natural closed		333
PS0040041	4.79E-09	2.98E-09	Natural healed		31
PS0040042	0.00E+00	0.00E+00	Natural closed		354
PS0040071	0.00E+00	0.00E+00	Natural healed		280
PS0040072	5.67E-11	6.60E-12	Natural closed		173

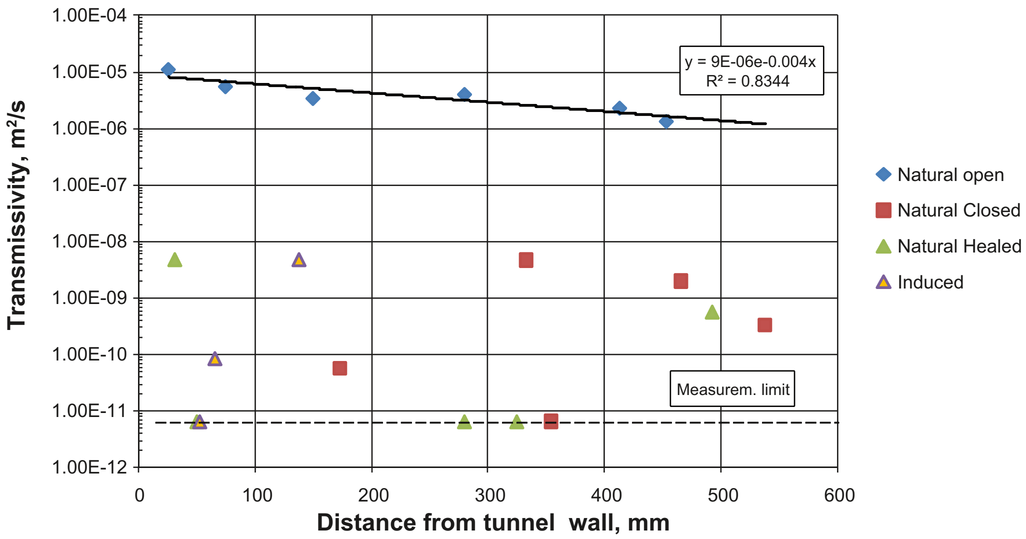

Figure 8-2. Transmissivity for different fracture types vs distance from the tunnel wall, confining pressure 0.5 MPa.

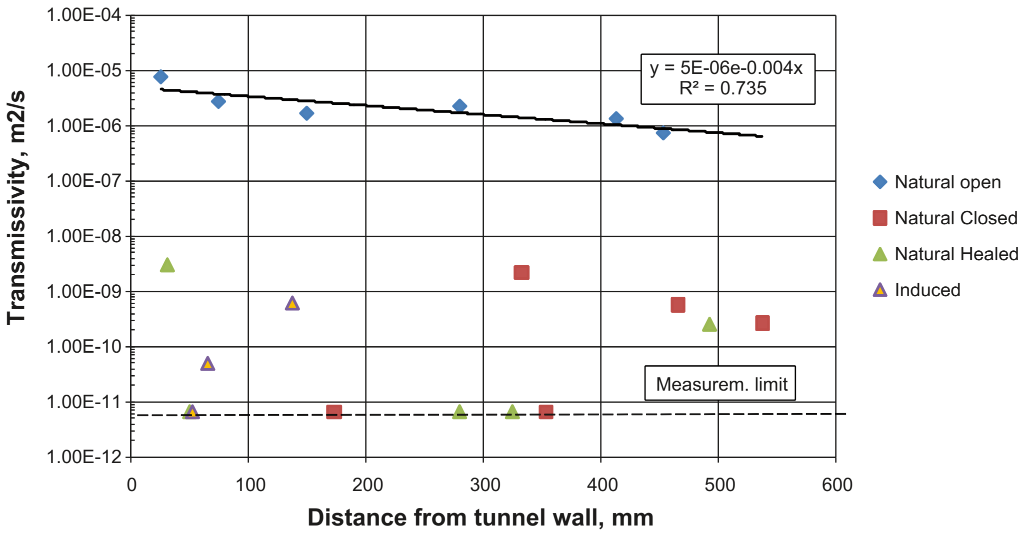

Figure 8-3. Transmissivity for different fracture types vs distance from the tunnel wall, confining pressure 1.0 MPa.

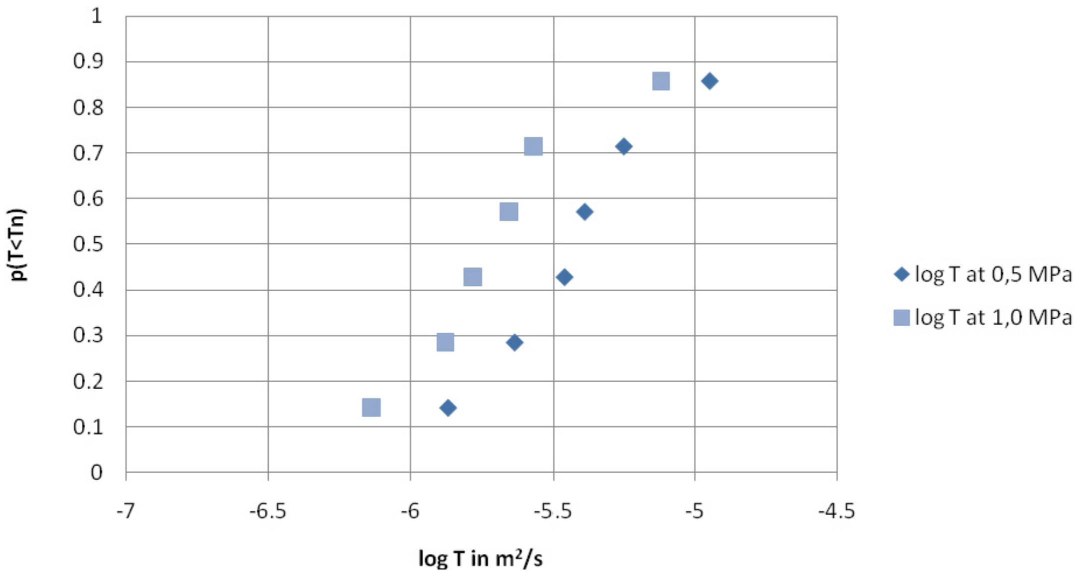

Figure 8-4. Cumulative distribution, Fracture transmissivities in natural, open fractures in the wall for the S-tunnel.

8.1.3 Hydromechanical coupling

The tests were conducted under the generalised normal stresses of **0.5** and **1.0** MPa, see Chapter 4.3. It is known that the fracture stiffness and thus the resulting fracture apertures can be stress-dependent. This applies in particular to low stress levels. The purpose of achieving a qualitative image of the hydromechanical conditions in conjunction with an increasing load and a decreasing load, flow tests were carried out on a number of samples in conjunction with a stepwise increase in load with a subsequent decrease, see Figures 8-5, 8-6, 8-7. Tests were also carried out with two and three loading and unloading cycles respectively, see Figures 8-8 and 8-9. It can be seen from the figures that the fractures are closed non-linearly in conjunction with increasing confining stress. It can also be seen from Figures 8-8 and 8-9 that an incomplete hysteresis appears. Clear consolidation has taken place of the fracture apertures following discrete loading levels.

Based on the test with the three cycles, Figure 8-9, the fracture transmissivities and corresponding fracture apertures ('cubic law') can be calculated easily using the maximum values of the loading steps and a graph can be obtained according to Figures 8-10 and 8-11 for the links to interpreted normal stresses. The hydraulic aperture changes for normal stress increases to 1.0, 2.0 and 2.5 MPa approximately correspond to the normal stiffnesses 16, 27 and 46 GPa/m see e.g. /Fransson 2009/.

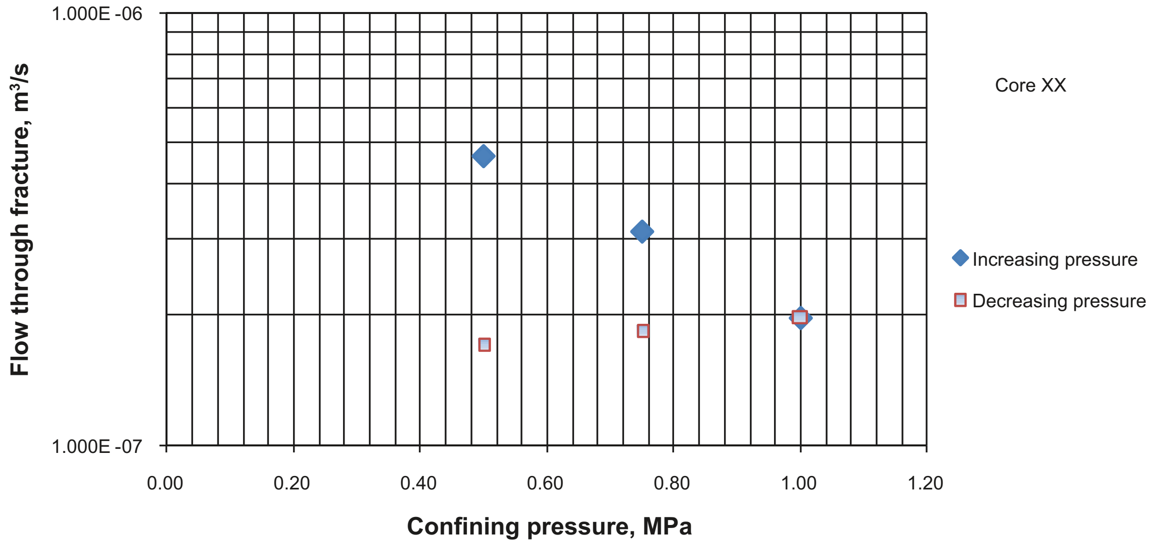

Figure 8-5. *Results showing fracture flow changes during stepwise increased and decreased confining pressure, sample XX from the Q-tunnel.*

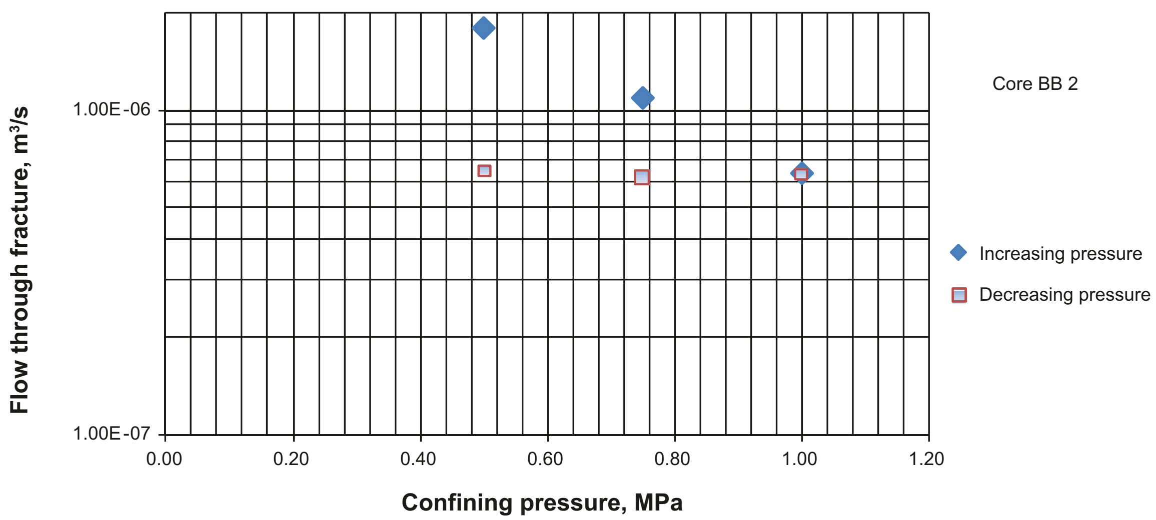

Figure 8-6. *Results showing fracture flow changes during stepwise increase and decreased confining pressure, sample BB2 from the Q-tunnel.*

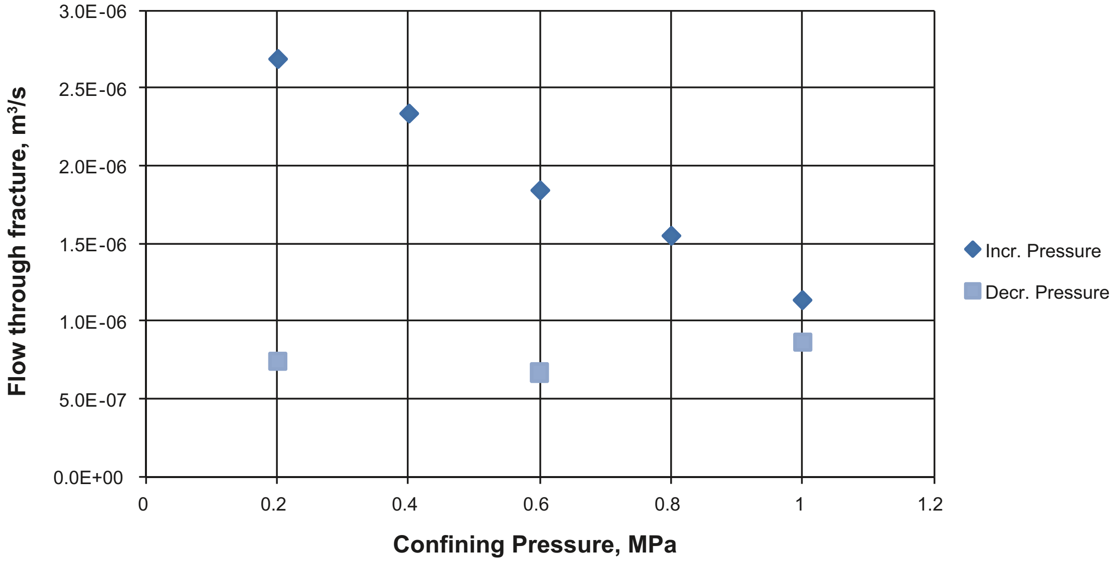

Figure 8-7. *Results showing fracture flow changes during stepwise increased and decreased confining pressure, sample BC1 from the Q-tunnel.*

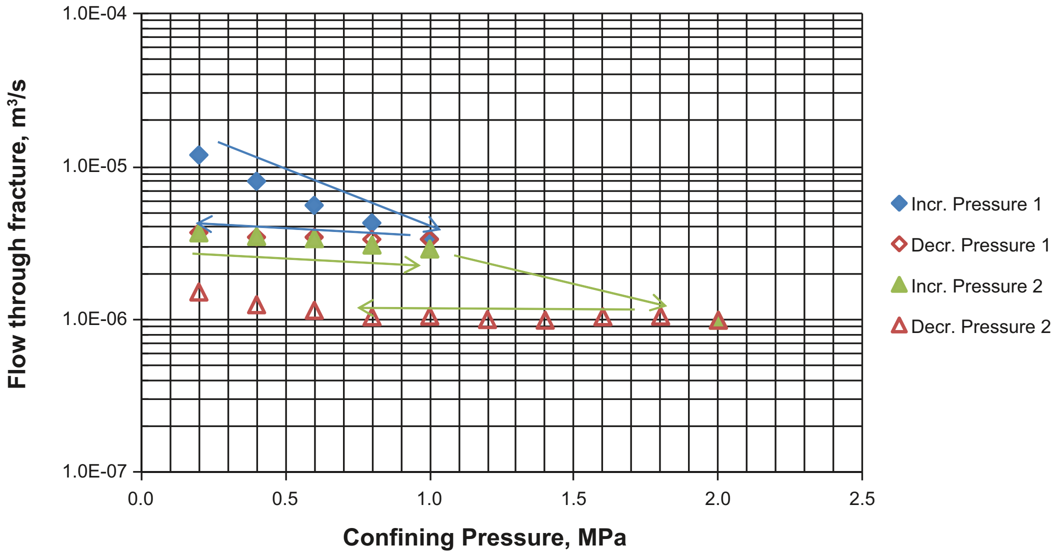

Figure 8-8. *Two stepwise loading cycles of the permeameter cell, sample no. PS0037061 from the S-tunnel.*

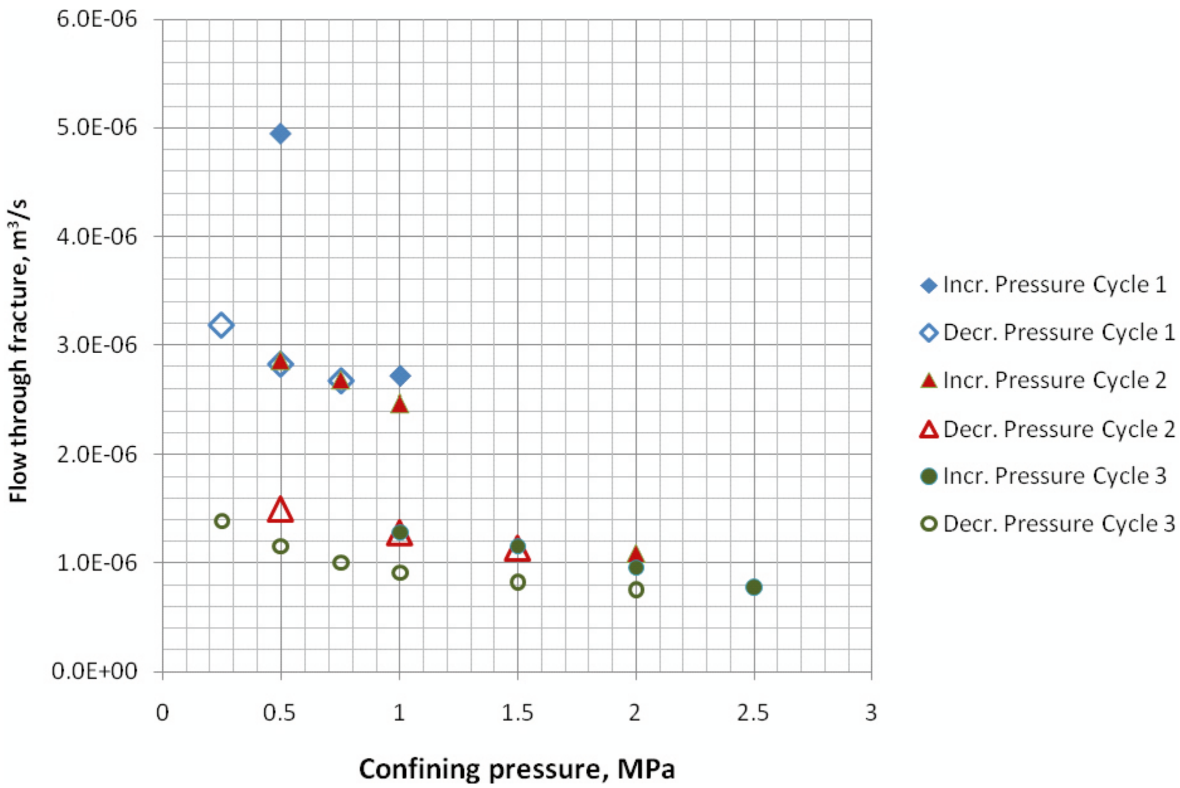

Figure 8-9. *Three stepwise loading cycles (in bars) of the permeameter cell, sample no. PS0039061 from the S-tunnel.*

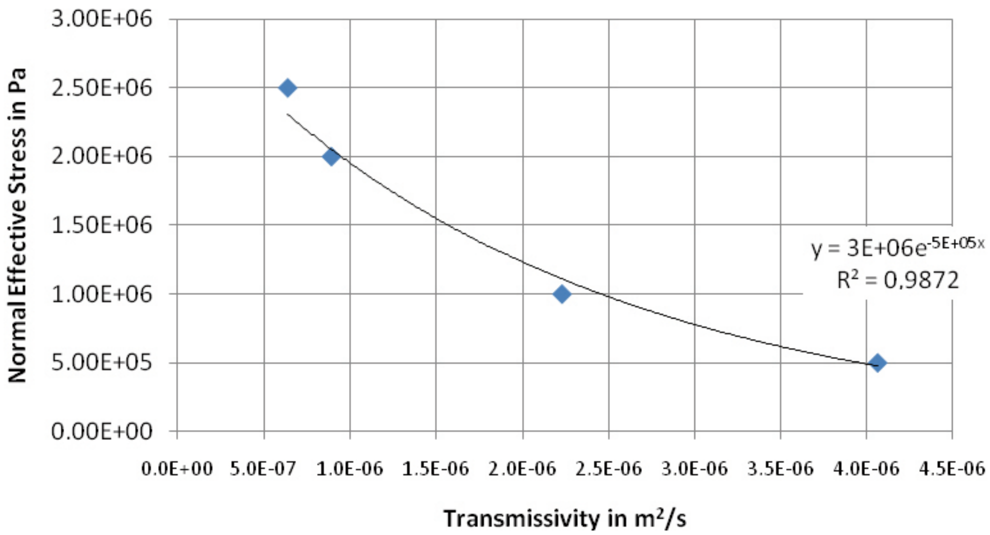

Figure 8-10. *Change in the transmissivity in the light of the load cycle's maximum values for an open fracture in sample no. PS0039061 from the S-tunnel.*

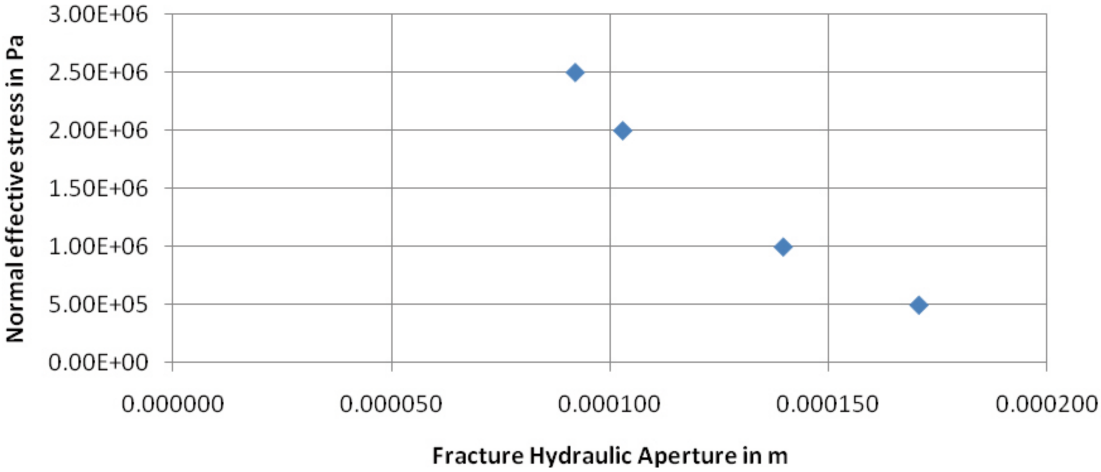

Figure 8-11. *The change in the fracture aperture in the light of the load cycle's maximum values for an open fracture in sample PS003906 from the S-tunnel. The apertures are calculated using the cubic law.*

8.2 *In situ* measurements in the S-tunnel

As stated previously in Chapter 6, single-hole field tests were carried out in the S-tunnel using water injection to determine fracture transmissivities and general transmissivity values in the tunnel wall. Below is a presentation of both transmissivity estimates for the whole length of the boreholes tested, i.e. approximating to the whole disturbed zone, as well as for individual, transmissive fractures in the zone.

8.2.1 Transmissivities for all boreholes

The measurement using the outer packer position, which in effect is the transmissivity for the whole borehole, ought to provide the total transmissivity for the disturbed zone in the proximity. The Table 8-3 contains a summary of these.

A cumulative distribution graph for these is shown below in Figure 8-12. The median, which can be seen as a characteristic value for the whole of the disturbed zone, is 9.2·E-9 m^2/s and the spread is approximately 10^3.

Table 8-3. Transmissivity determinations for water injection tests in a tunnel wall. The transmissivities are based on values for tests using packer positions close to the tunnel wall. $p(T< T_n)$ expresses the probability for the value of being less than the actual value.

Test no.	Max. Depth Packer Position (cm)	Total borehole depth (cm)	Test interval L (m)	T = Q/dh (m^2/s)	$p(T<T_n)$
1_1	7.3	59	0.517	4.24E-09	0.33
2_2	1.9	53	0.511	8.51E-09	0.42
3_1	2.3	54	0.517	1.58E-09	0.25
4_1	3.4	53	0.496	2.8E-07	0.92
5_1	2.6	58	0.554	4.74E-08	0.75
6_2	21.4	52	0.306	4.45E-10	0.08
7_1	3.6	60	0.564	9.16E-09	0.50
8_1	4	60	0.56	1.32E-08	0.58
9_1	2.3	60	0.577	1.48E-07	0.83
10_1	4	52	0.48	3.59E-08	0.67
11_2	13.8	53	0.392	4.83E-10	0.17

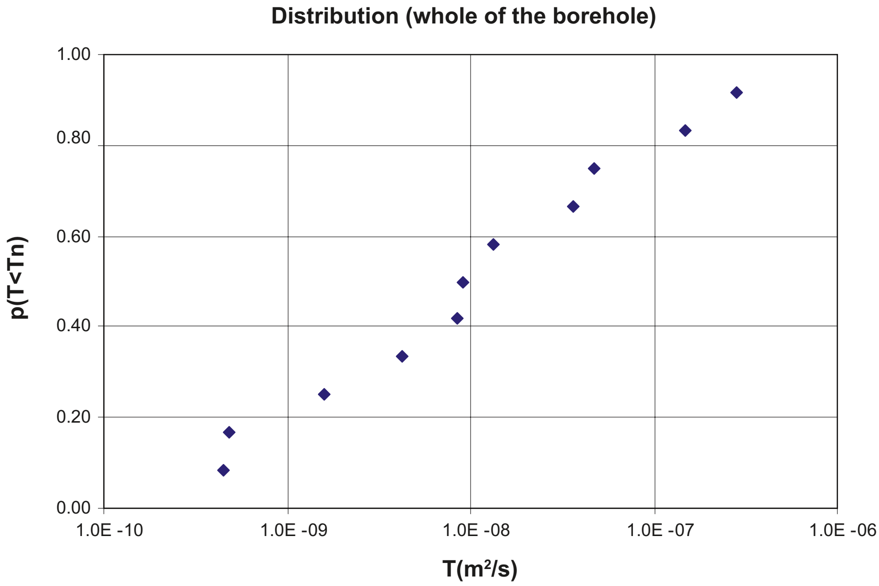

Figure 8-12. *Cumulative distribution, Transmissivities based on single-hole testing in the wall of the S-tunnel.*

8.2.2 Transmissivities for all test sections

The packer was put in another position according to the occurrence of inferred single fractures in the drill-cores. The transmissivity for the different test intervals was thus calculated in such a way that the difference in transmissivity between two packer positions in the same borehole was calculated and was assumed to represent the transmissivity for this interval. For the innermost interval, the transmissivity for the innermost packer position was used directly. Data is reported in Table 8-4 below.

Table 8-4. Transmissivity determinations for water injection tests in a tunnel wall. The transmissivities are based on values for each test interval.

Test no.	Upper limit interval (cm)	Lower limitinterval (cm)	Average depth (cm)	Interval length (m)	T = Q/dh for the interval (m^2/s)	Log T
1_1	7.3	21.2	14.25	0.52	4.19E-09	–8.37824
1_2	21.2	59	40.1	0.38	5.14E-11	–10.2889
2_2	1.9	14.7	8.3	0.51	8.49E-09	–8.07098
2_3	14.7	53	33.85	0.38	2.16E-11	–10.6661
3_1	2.3	3.4	2.85	0.52	1.58E-09	–8.80169
4_1	3.4	24.5	13.95	0.50	3.02E-08	–7.52063
4_2	24.5	30.5	27.5	0.29	2.40E-07	–6.62066
4_4	30.5	53	41.75	0.23	1.06E-08	–7.97317
5_1	2.6	11.2	6.9	0.55	1.53E-09	–8.81558
5_2	11.2	20.8	16	0.47	3.53E-08	–7.45172
5_3	20.8	31.1	25.95	0.37	1.05E-08	–7.97756
5_4	31.1	58	44.55	0.27	1.00E-11	–11
6_2	21.4	52	36.7	0.31	4.45E-10	–9.35187
7_1	3.6	60	31.8	0.56	9.16E-09	–8.03792
8_1	4	60	32	0.56	3.32E-07	–6.47845
9_1	2.3	10	6.15	0.58	1.00E-11	–11
9_2	10	24.5	17.25	0.50	1.00E-11	–11
9_3	24.5	42.7	33.6	0.36	3.32E-07	–6.47898
9_4	42.7	60	51.35	0.17	4.00E-10	–9.39811
10_1	4	23.7	13.85	0.48	3.54E-08	–7.4507
10_2	23.7	13.8	18.75	0.28	1.00E-11	–11
11_2	13.8	53	33.4	0.39	4.83E-10	–9.31568

A cumulative distribution graph for these values is shown in Figure 8-13 below. The transmissivities can to some extent be said to better represent the fracture transmissivities in the boreholes. The median value is 2.9·E-9 m^2/s. For comparison the corresponding rock volume under undisturbed conditions in the pre-investigation produced a median value of $T = 8 \cdot 10^{-10}$ m^2/s for the fracture transmissivities /Funehag 2008/.

Using this data as a starting point, an attempt has been made to evaluate whether the interval transmissivities decrease with the depth of the borehole. This ought to be expected if the blast disturbance or damage decreases with the distance outside the tunnel wall. In Figure 8-14 below, a logarithm for the interval transmissivity has been plotted as a function of the depth to the outer packer position. As can be seen from the figure, there is considerable spread and the transmissivity has a vague decreasing trend with the depth of the borehole. However, due to the large spread the significance is very low.

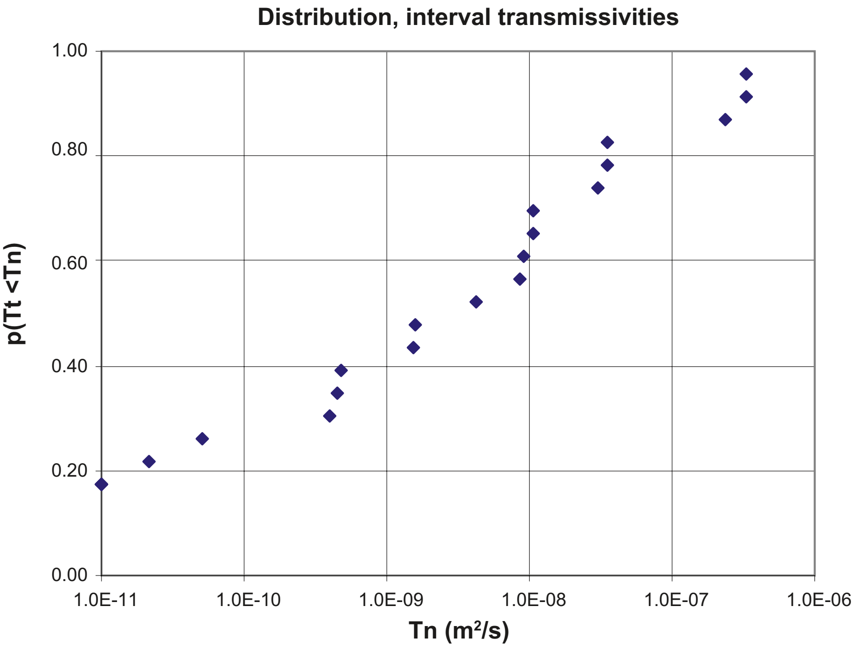

Figure 8-13. Cumulative distribution of transmissivities for all test intervals in all injection test holes in the walls of the S-tunnel.

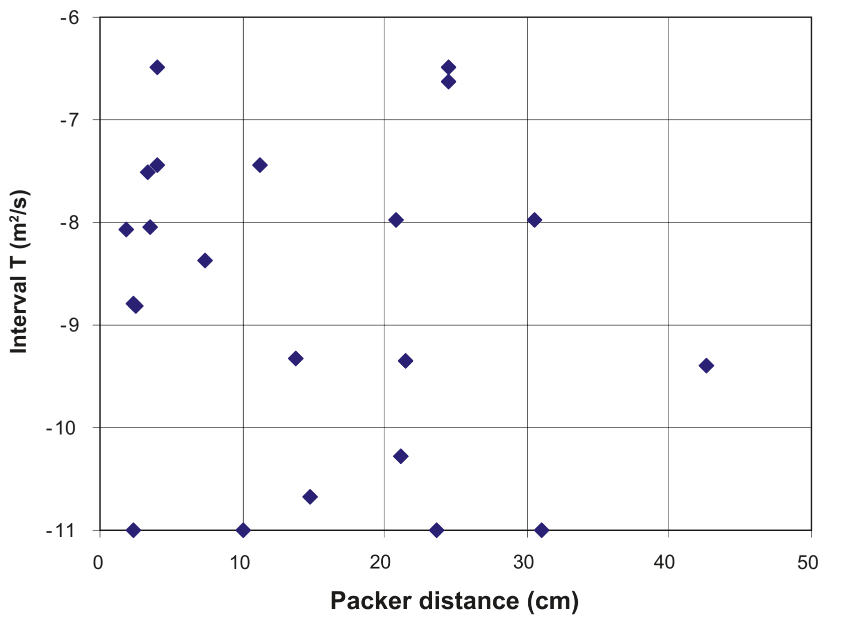

Figure 8-14. Transmissivities in sealed-off test intervals vs. "upper" packer distances from the tunnel wall.

8.2.3 Water pressure in the boreholes

Prior to each test the static water pressure in the boreholes was measured. Preliminary modelling /Christiansson et al. 2009/ has shown that the water pressure in the disturbed zone and the tunnel wall ought to be low or even negative. As Table 8-5 shows, the pressure is zero in approximately 50% of the boreholes. There could very well also be underpressure as negative pressure was not registered. In the light of the recorded pressure measurements, the transmissivity determinations could thus be underestimated slightly as they have not always represented water-saturated conditions.

Table 8-5. Initial water pressure in each borehole.

Borehole no.	Packer distance (cm)	Borehole depth (cm)	Interval length (m)	Static pressure (bar)
1	7.3	59	0.517	0.2
2	1.9	53	0.511	0
3	2.3	54	0.517	0
4	3.4	53	0.496	0
5	2.6	58	0.554	0
6	21.4	52	0.306	0.4
7	3.6	60	0.564	0.5
8	4	60	0.56	0.5
9	2.3	60	0.577	0
10	4	52	0.48	0
11	13.8	53	0.392	0.1

8.3 Microfracturing

An analysis of microfracturing, as presented earlier, was conducted using ultrasonic measurements, analysis of matrix porosity and microscoping. The extent of the work varied with the aim of establishing a focus prior to mapping the occurrence of the disturbed zone.

8.3.1 Ultrasonics

Q-tunnel

For the Q-tunnel a measurement was made on slab BC using a ½-sensor length between the measurements, see Figures 8-15 and 8-16 below. For further information, see Appendix 1.

The P-wave velocity shows an increasing trend the further away one measures into the rock and away from the tunnel wall. The velocity varies from approximately 5,700 m/s to approximately 6,000 m/s.

In total, it can be said that the measurements indicate that there are more micro cracks at the beginning of the scan line than in the latter part. The results thus indicate a disruption in the microporosity at a distance of approximately 25–35 cm from the tunnel wall.

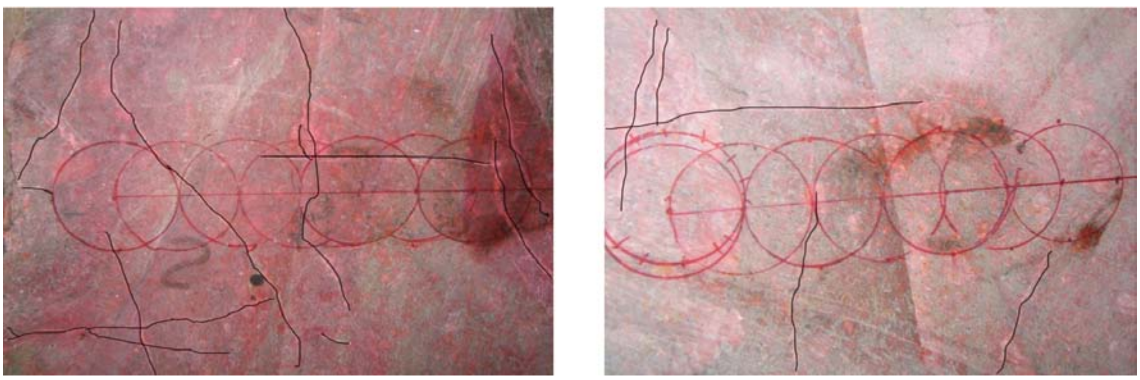

Figure 8-15. Ultrasonic scan line on slab BC. The beginning of the scan line is to the left in both images. The fractures are marked with black lines.

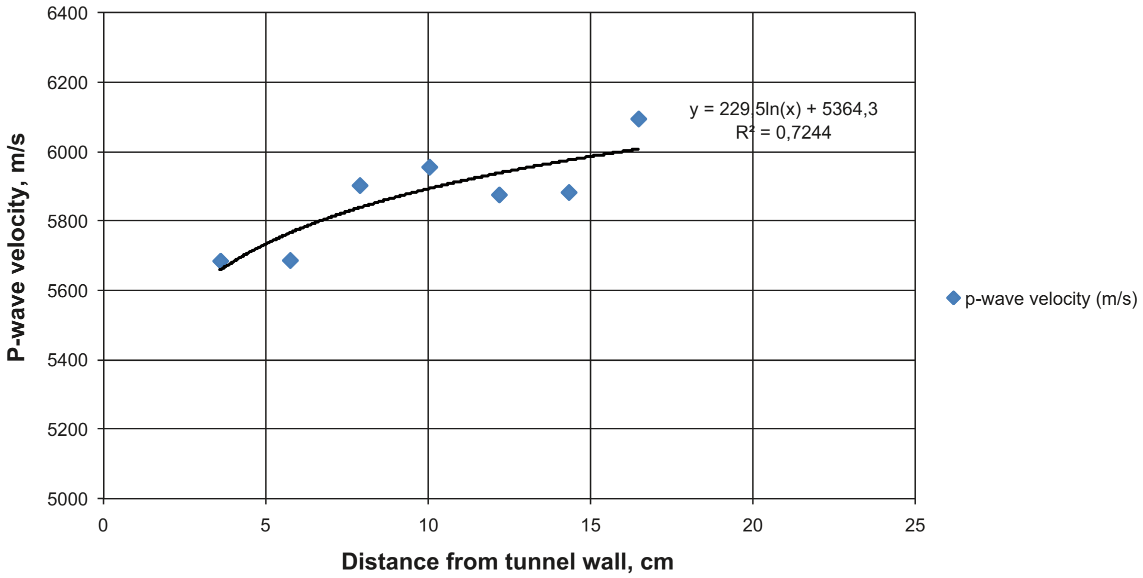

Figure 8-16. *P-wave velocity vs distance from the tunnel wall and into the rock for slab BC in the Q-tunnel.*

S-tunnel

Six measurements were performed for the S-tunnel on five slabs, see Table 5-4 for the scan line designations. The distance between the values varies in length from ½- 1 sensor, i.e. 2.05 cm to 4.1 cm. There are measurements both from the tunnel wall and into the rock as well as parallel to the tunnel wall. For further information, see Appendix 2. Figures 8-17 to 8-22 below show the ultrasonic results for each scan line.

The starting point for *LS0036041* is a short distance from the tunnel wall and the end-point is in the rock. The P-wave velocity increases for the first three values and then remains relatively stable. The velocity varies from approximately 4,600 m/s to approximately 5,700 m/s. The slab also shows a larger number of fractures at the beginning of the scan line, see Appendix 2.

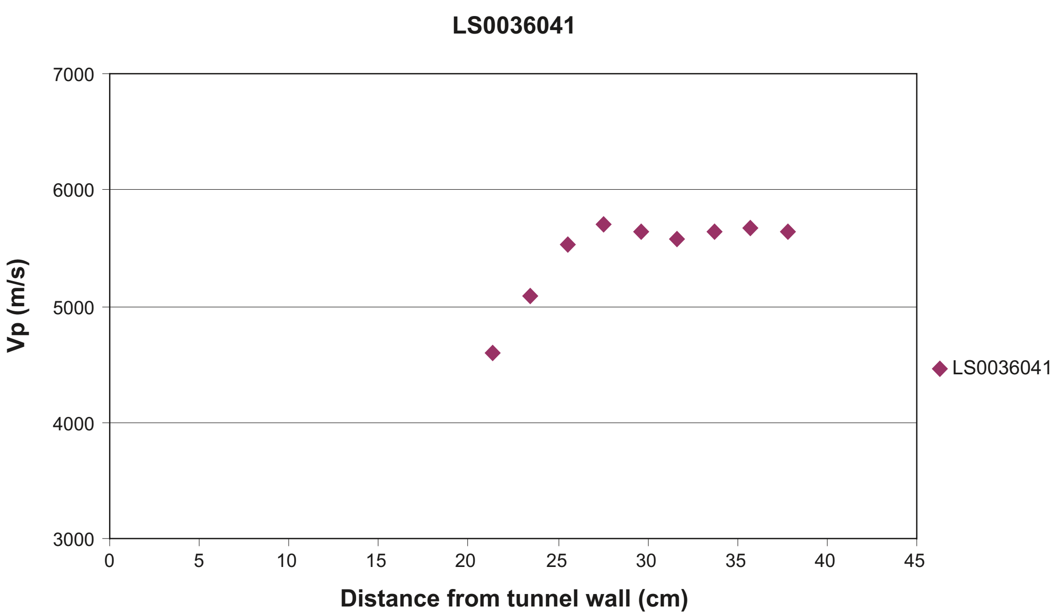

Figure 8-17. *P-wave velocity as a function of the distance from the tunnel wall for line LS0036041.*

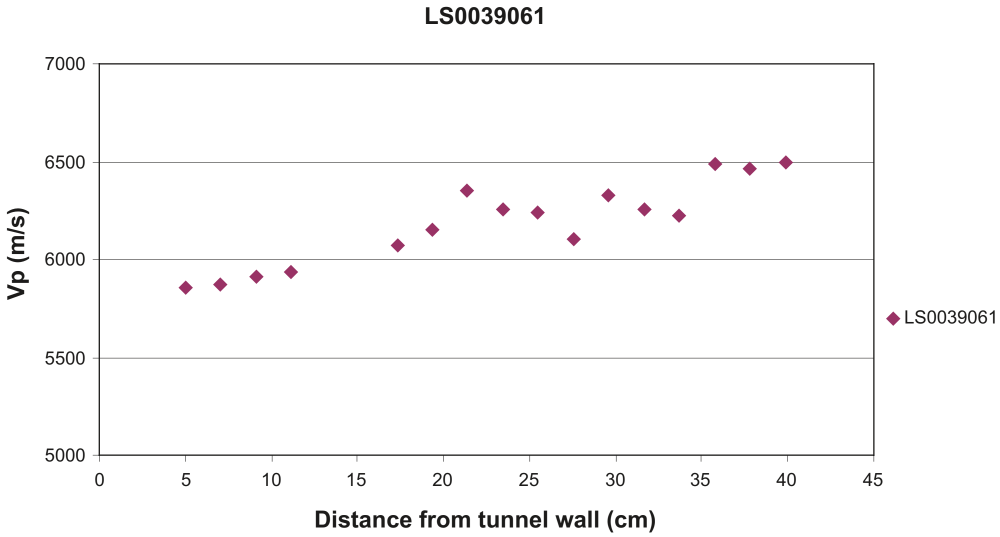

Figure 8-18. The P-wave distance as a function of the distance from the tunnel wall for line LS0039061.

The P-wave distance for line *LS0039061* shows a tendency towards an increase in velocity the farther one moves from the tunnel wall into the rock. The velocity varies from approximately 5,800 m/s to approximately 6,500 m/s. The slab also reveals greater fracturing at the beginning of the scan line, see Appendix 2.

The P-wave velocity for line *LS0039062* varies from approximately 5,400 m/s to 5,900 m/s. The graph does not show any tendency towards an increase in velocity the farther one moves from the starting point for the measurement. The scan line follows the length of the tunnel wall. The fracturing in the slab, along the scan line, also varies, see Appendix 2. The velocity is generally even.

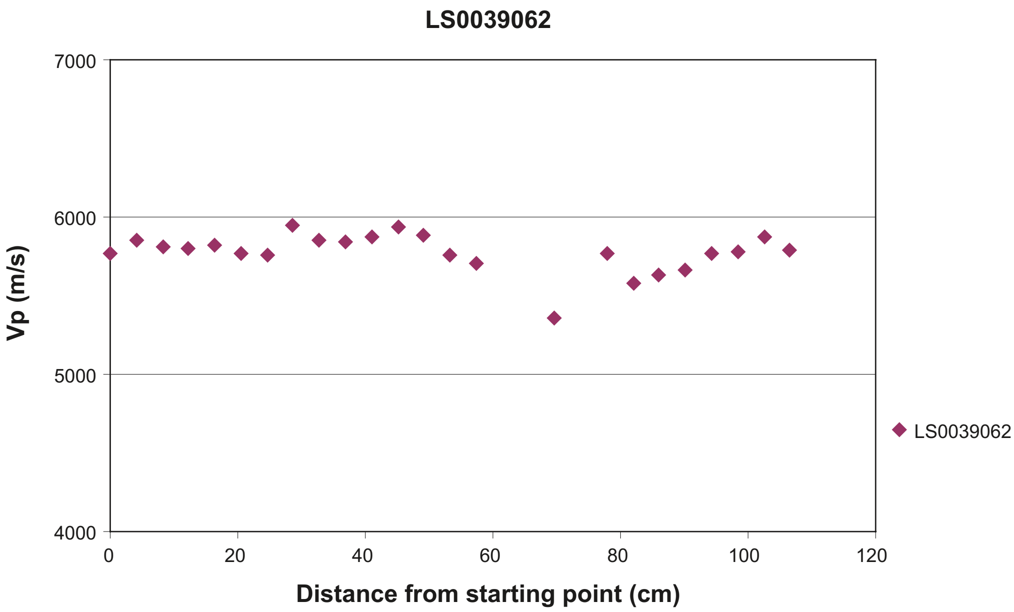

Figure 8-19. P-wave velocity vs distance from the measurement starting point for line LS0039062.

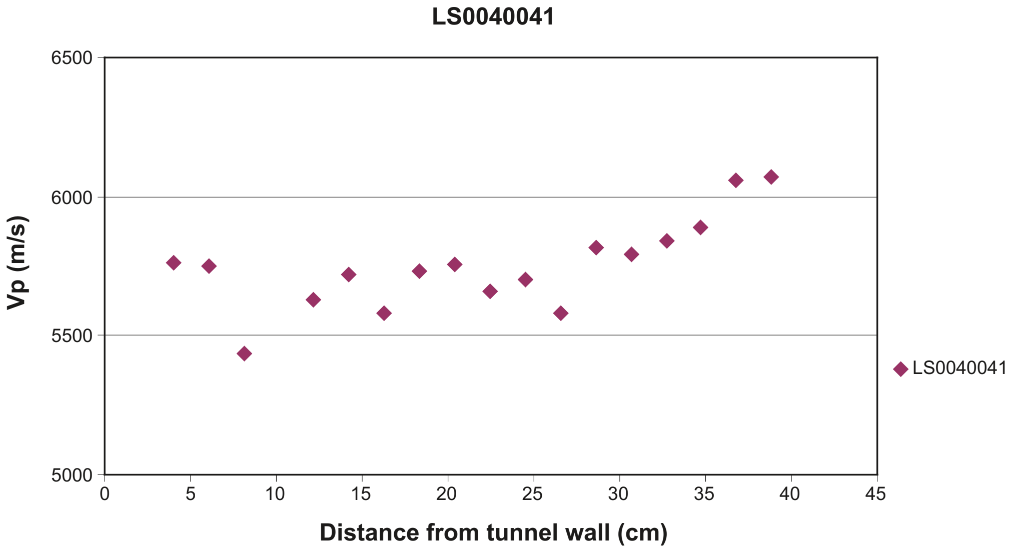

Figure 8-20. P-wave velocity as a function of the distance from the tunnel wall for line LS0040041.

The P-wave velocity for line *LS0040041* varies from approximately 5,400 m/s to 6,000 m/s. A weak tendency towards an increase in velocity can be seen in the graph from the starting point of the measuring line at the tunnel wall and into the rock. Two measuring values are distinctly lower than the values around them, at 4.1 cm and 22.55 cm from the starting point of the scan line. These concur with two fractures that traverse the scan line, see Appendix 2.

The p-wave velocity for line *LS0040061* varies from approximately 5,500 m/s to 5,900 m/s. There is no visible increase in velocity from the starting point at the tunnel wall and into the rock due to several natural open fractures in parallel with the scanline.

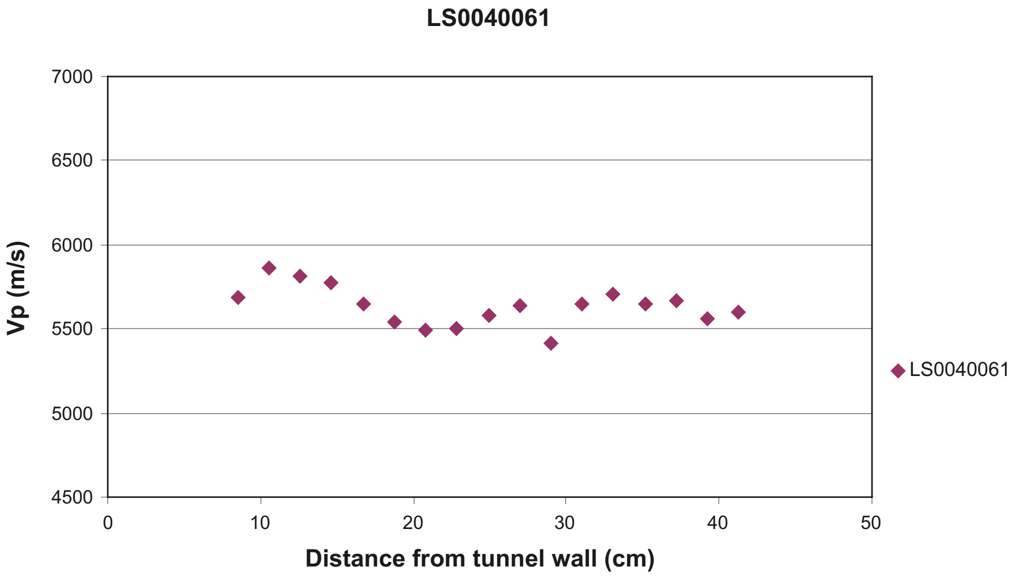

Figure 8-21. The p-wave velocity as a function of the distance from the tunnel wall for line LS0040061.

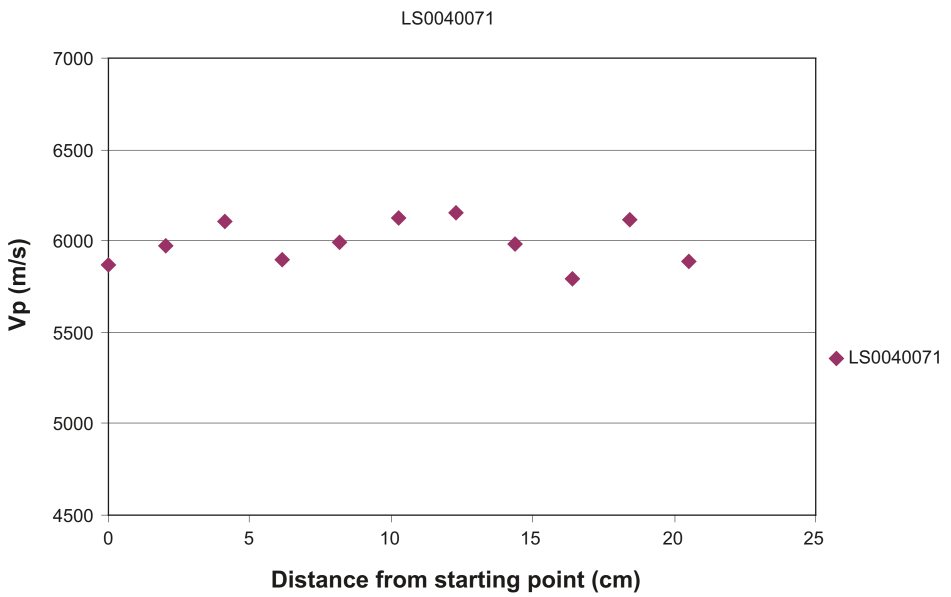

***Figure 8-22.** The P-wave velocity vs the distance from the measurement starting point for line LS0040071.*

The P-wave velocity for line *LS0040071* varies from approximately 5,900 m/s to 6,150 m/s from the starting point to the end. The scan line extends some way into the rock and follows the line of the tunnel wall. The velocity is generally high and even.

In summary, the ultrasonic measurement of slabs from the S-tunnel indicates that a minor change in microporosity has taken place up to a distance of approximately 25–35 cm from the tunnel wall.

8.3.2 Matrix porosity, Q-tunnel

The matrix porosity has been calculated for the smaller samples h1a to h1e from slab BC, taken from the Q-tunnel. The samples extend from the tunnel wall into the rock. The porosity decreases from the charge borehole and into the rock with the exception of one value, see Figure 8-23. The results for the porosity change are thus comparable with the results from the ultrasonic investigation, which is shown in Figure 8-16. For further information, reference can be made to Appendix 1.

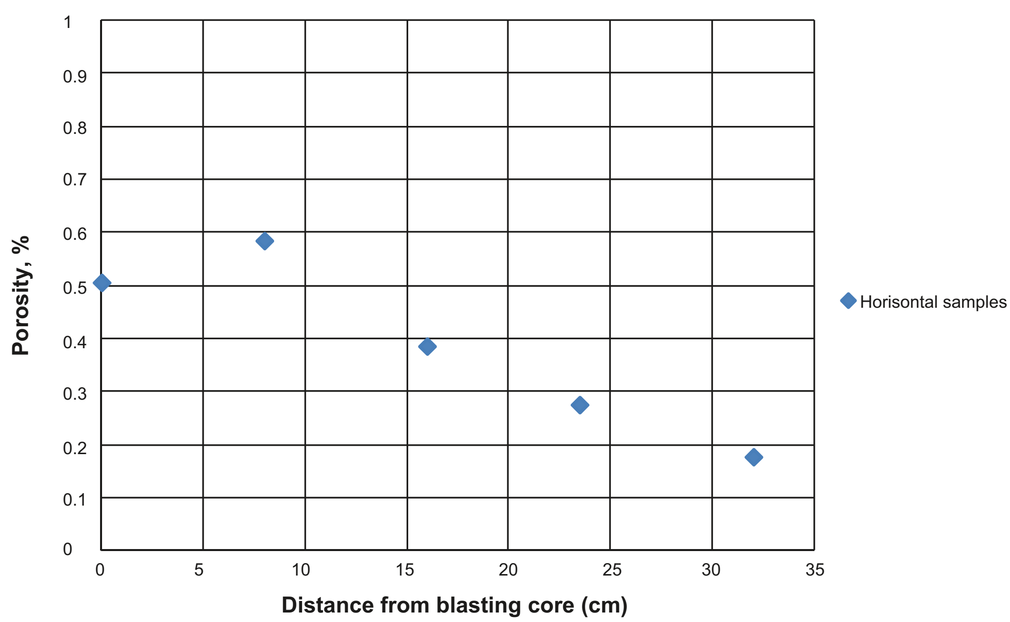

***Figure 8-23.** Porosity vs distance in a core from the tunnel wall into the rock. The samples are taken from the Q-tunnel, slab BC, h1a–h1e.*

8.3.3 Microscoping

Thin section analysis in a microscope shows that the rock that was analysed had very few natural micro cracks. Samples were analysed from the Q-tunnel and one example is showed in Figure 8-24. An alteration of feldspars and the relatively low quartz content are considered to be the primary reasons for the scarcity of micro cracks. Normally, micro cracks appear in grain borders and as intragranular fractures along a plane of weakness in the middle.

The very few blast-induced micro cracks were found in the thin section from all samples apart from sample v1b although they were so few in number that no quantitative measurement could be made. This observation indicates a local influence of disturbance in the Q-tunnel equivalent to 30–35 cm. The majority of the micro cracks that were discovered were mainly old, healed cracks that had been reopened. In a small number of samples, new micro cracks had been formed as transgranular cracks (cutting through several mineral grains). For further information, reference can be made to Appendix 4.

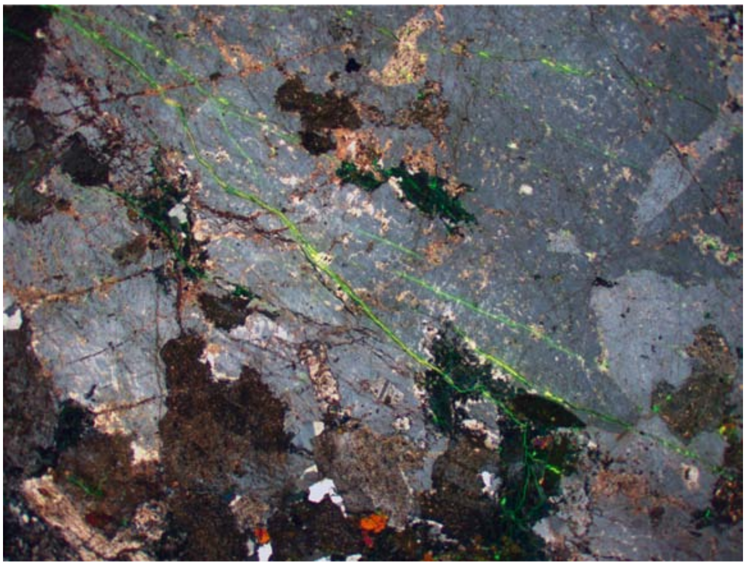

Figure 8-24. *The figure shows a feldspar crystal in the specimen h1c from the Q-tunnel in a combined fluorescent and polarised image. The image size is 5.5×4.2 mm. The open micro cracks in green are mainly related to old sealed micro cracks and only a few new micro cracks have been created.*

9 Discussion and conclusions

The overall aim of this work has been to examine hydraulic conditions and possible effects of blasting on the transmissive features closest to a tunnel in a post-closure phase of a nuclear waste repository. Schematically, the issues can be seen in Figure 9-1.

In /Bäckblom 2008/ it is stated and assumed that site-specific relations are created between damage and density of explosive charge as the basic parameter for estimation of damage extent and properties. Such relations need to be established for different rock types and fracturing. Thus large-scale sampling and geometrical modelling of the fractured rock in the disturbed zone in the S-tunnel at Äspö HRL was carried out by /Olsson et al. 2009/. Careful blasting was found to create a discontinuous distribution of blast-induced fractures. Current data of direct blast-induced fractures and induced fractures indicate that the axial fracture connectivity is estimated to be insignificant due to the sparse distribution of these visible fractures, see Figure 9-2. This conclusion is supported by the results from the detailed fracture mapping of the slabs respectively. Figure 9-3 shows the length distribution with natural fractures (separated into open, tight and healed), direct blast-induced fractures and induced fractures. Natural open fractures are more elongated compared to direct blast-induced and induced fractures in the slabs.

Even though careful blasting was used there is an indication of sparsely distributed micro fracturing up to a distance of 250–350 mm from the tunnel wall. The microfracturing has been determined by means of ultrasonic measurements and microscopic analyses. Furthermore, a small matrix porosity increase, from approximately 0.2% to 0.5%, has been observed close to the wall. As regards micro cracking, similar results have been observed in a previous ultrasonic borehole measurement study in the Q-tunnel at Äspö /Schuster 2007/.

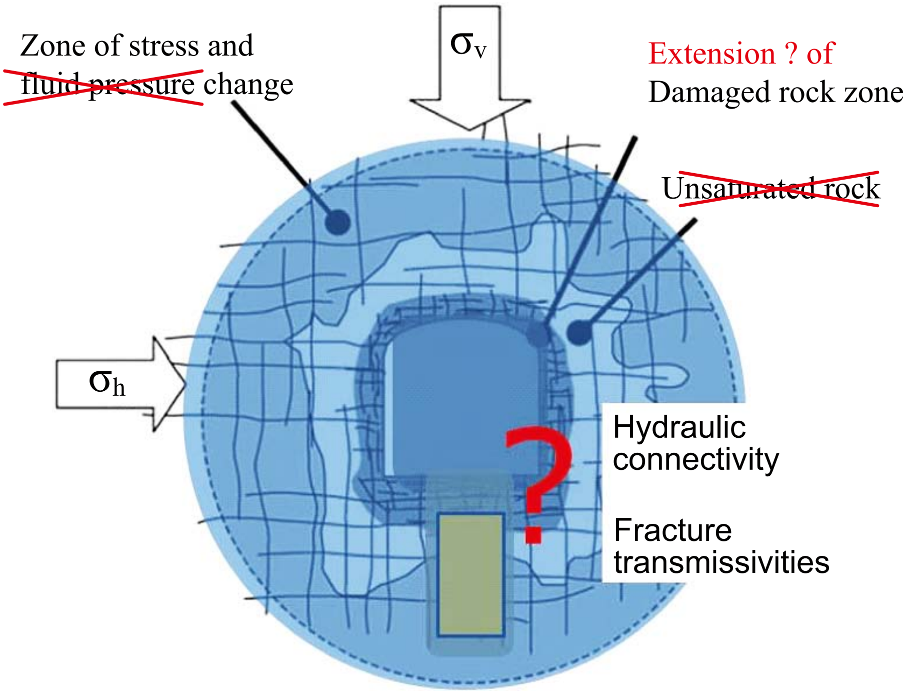

Figure 9-1. *Post-closure condition of a nuclear waste repository. The host rock is saturated with no pressure change compared to undisturbed conditions. Rock stresses may be different due to excavation and we may also consider a disturbed and a damaged rock zone with a certain extension which surrounds the tunnel. Hydraulic issues mainly concern the connectivity of the flow paths and the fracture transmissivities (figure modified from /Rutqvist and Stephansson 2003/).*

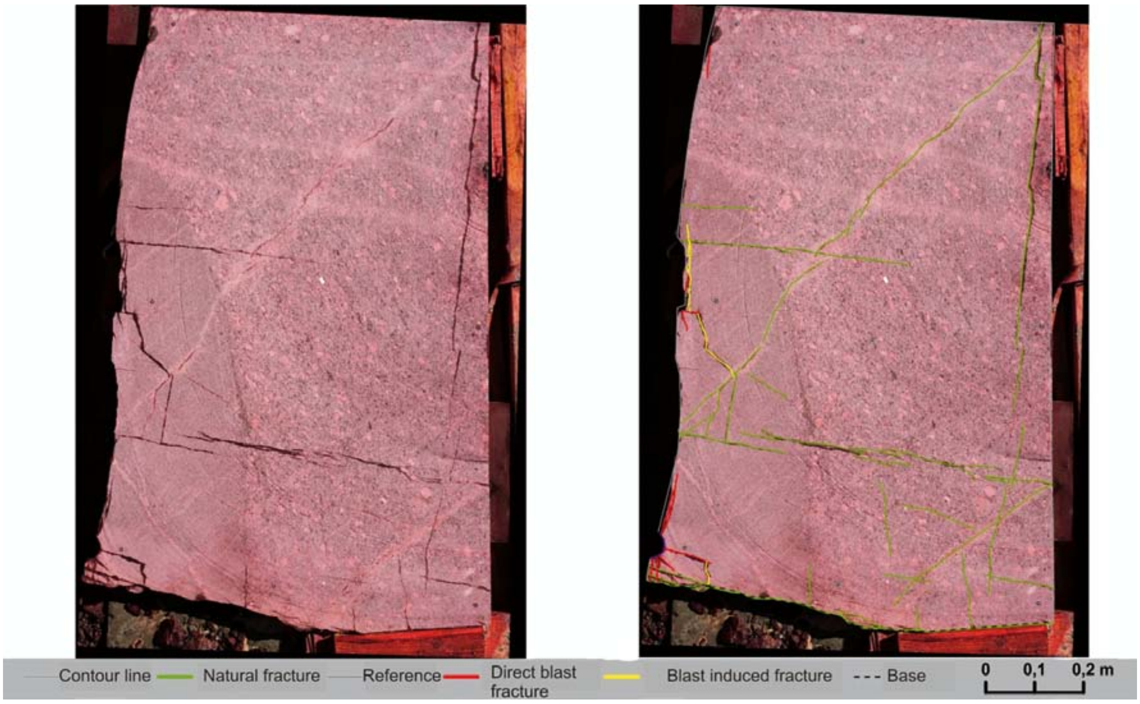

Figure 9-2. The picture exemplifies a conceptual 2D image of the occurrence of fractures perpendicular to the wall in a tunnel with careful blasting. The distribution of blast fractures is discontinuous and connected to the charge boreholes. There are secondary blast-induced fractures which terminate against natural fractures. An increased axial fracture connectivity due to blast and blast-induced fractures is estimated to be insignificant due to the sparse distribution of these visible fractures. Natural fractures may be effected at the tunnel perimeter. Even when careful blasting is used there may be sparsely distributed micro cracking at a distance of 250–350 mm from the tunnel wall. The micro cracking most probably have insignificant influence on the major hydraulic conditions.

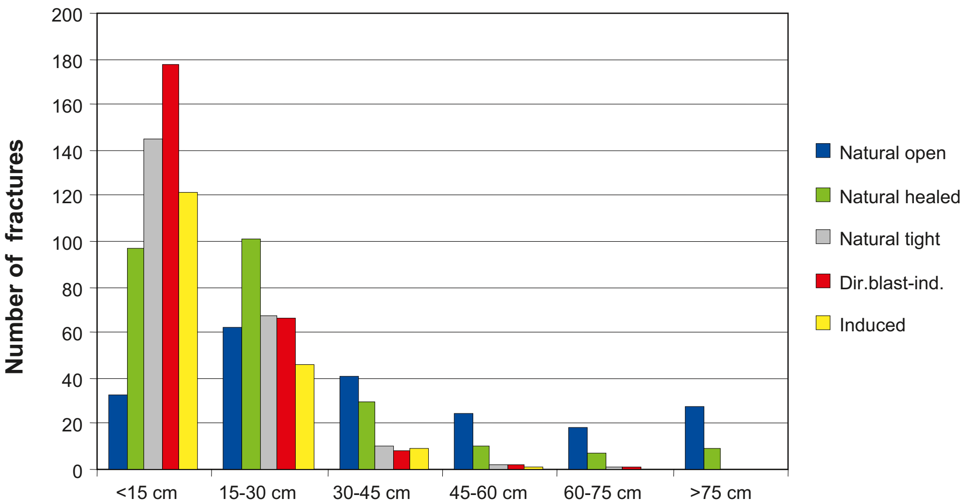

Figure 9-3. Length distribution with natural fractures (separated into open, tight and healed), direct blast-induced fractures and induced fractures as mapped on all the 75 slabs from S-tunnel.

In /Bäckblom 2008/ typical EDZ assessing tests are suggested within the area of the deposition holes. These tests are: ultrasonic measurements, testing of hydraulic transmissivity by multipackers and laboratory permeameter tests on rock cores. The present project has comprised these types of investigations.

A triaxial cell permeameter was developed in order to determine saturated fracture transmissivities in relatively large samples with a diameter of 200 mm and a height of 100 mm. The equipment has been found to be a robust method for fracture transmissivity determination. However, proper sampling is crucial for the reliability of the results. For the testing procedures the fracture normal stress levels were set at 0.5 MPa and 1.0 MPa and equal to the axial stress. The stress levels were chosen according to scoping numerical calculations of the stress regimes that surround the tunnels at a depth of 450 m at Äspö.

The methodology for hydraulic testing with the permeameter equipment was first developed using samples from the Q-tunnel. Then 19 samples from a sampling campaign on slabs from the S-tunnel were analysed. In order to improve the understanding of the hydraulic regime surrounding a tunnel there was a need for a reclassification of the fractures in the geometrical model. Together with the direct blast and blast-induced fractures the so-called natural fractures were subdivided into natural open, natural closed/tight and natural healed fractures.

In summary, the permeameter results show the following:

- Generally, the normal stress of 0.5 MPa generates transmissivity values half an order of magnitude higher compared to the 1.0 MPa stress level.
- Conspicuous, single-induced fractures show low transmissivity values $T < 5 \cdot 10^{-9}$ m^2/s although the sample is small: only three specimens.
- Natural tight/closed and natural healed fractures have low transmissivity values, approximately $T < 5 \cdot 10^{-9}$ m^2/s.
- Considering the natural open fractures from a statistical population, the confining pressure of 0.5 MPa will give a mean value $T = 3.7 \cdot 10^{-6}$ m^2/s and a standard deviation STD[log] = 0.31. At a confining pressure of 1.0 MPa the mean value is $T = 2.1 \cdot 10^{-6}$ m^2/s and STD[log] = 0.34.
- During the methodology development of the triaxial cell permeameter it is obvious that there are uncertainties regarding representative normal stress levels when running the equipment. The *in situ* results indicate a normal stress level in the laboratory determinations that was slightly too low. Figure 8-10 shows that the stress level ought to be approximately 2.0–3.0 MPa in order to simulate similar *in situ* open natural fractures (preliminary interpretation based on 32 mm drill cores from test holes) experienced from the single hole testings in the tunnel wall.

Using additional single-hole testing equipment (Diameter 32 mm, hole depth ~ 0.5 m) it has been possible to compare the laboratory data with *in situ* results. Eleven water injection tests were performed in the S-tunnel below the block excavation site and at the opposite wall in the S-tunnel. In summary the *in situ* results show:

- The single-hole hydraulic test close to the tunnel contour is a robust method to determine the range of transmissivity values, although there is a need for improvement regarding initial pressure conditions since half of the tests indicated zero or negative initial water pressures (unsaturated). These circumstances may imply transmissivity determinations that were slightly too low.
- Based on the water injection tests the median value considered as a characteristic transmissivity value of the disturbed zone around the S-tunnel was determined at $T = 9.2 \cdot 10^{-9}$ m^2/s and the distribution interval covers approximately three orders of magnitude.
- Sections sealed off with packers were chosen according to the occurrence of fractures in the drilling cores. Considering all sealed-off sections as representative for single fractures the fracture transmissivity median was determined to be $T = 2.9 \cdot 10^{-9}$ m^2/s. The distribution interval covers approximately four orders of magnitude.

A generalised conclusion from the field study at Äspö and the laboratory tests at Chalmers indicates the following:

- Natural open fractures are the dominating hydraulic features that surround the tunnel if the excavation has been carefully blasted similar to what was done in the S-tunnel at Äspö HRL.
- The excavation disturbed zone as indicated by micro cracks has an extension of 250–350 mm into the tunnel wall.
- There is no significant axial hydraulic connectivity due to few blast-induced fractures.
- A typical in situ mean transmissivity determined from slim boreholes in the excavation disturbed zone is $T = 10^{-8}\ m^2/s$ and the values may be distributed over three orders of magnitude. If fracture transmissivities in the zone are considered, typical values equal $T = 3 \cdot 10^{-9}\ m^2/s$ and the range interval may be even larger.
- If the features in the tunnel wall are classified into induced, natural open, natural closed and healed fractures and combined with representative T-values determined in permeameters, the DFN-modelling in the engineered barrier may be improved.

References

Andersson C, 2007. Äspö Pillar Stability Experiment, Final Report. Rock mass response to coupled mechanical thermal loading. SKB TR-07-01, Svensk Kärnbränslehantering AB.

Bäckblom G, 2008. Excavation damage and disturbance in crystalline rock – results from experiments and analyses. SKB TR-08-08, Svensk Kärnbränslehantering AB.

Christiansson R, Ericsson L O, Gustafson G, 2009. Hydraulic characterisation and conceptual modelling of the Excavation Disturbed Zone (EDZ). Proceedings from SINOROCK 2009, International Symposium on Rock Mechanics "Rock Characterization, Modelling and Engineering Design Methods" 19–22 May 2009, Hong Kong.

Fransson Å, 2009. Literature survey: Relations between stress change, deformation and transmissivity for fractures and deformation zones based on *in situ* investigations. SKB R-09-13, Svensk Kärnbränslehantering AB.

Funehag J, 2008. Injekteringen av TASS-tunneln. Delresultat t o m september 2008. SKB R-08-123, Svensk Kärnbränslehantering AB.

Gustafson G, 2009. Hydrogeologi för bergbyggare. Formas. Stockholm.

Hernqvist L, Fransson Å, Gustafson G, Emmelin A, Eriksson M, Stille H, 2009. Analyses of the grouting results for a section of the APSE tunnel at Äspö Hard Rock Laboratory. International Journal of Rock Mechanics & Mining Sciences 46, 2009. 439–449.

Hudson JA, Backstrom A, Rutqvist J, Jing L, Backers T, Chijimatsu M, Christiansson R, Feng XT, Kobayashi A, Koyama T, Lee HS, Neretnieks I, Pan PZ, Rinne M, Shen BT, 2009. Characterising and modelling the excavation damaged zone in crystalline rock in the context of radioactive waste disposal, Environmental Geology, 57 (6), 1275–1297.

Laaksoharju M, Gimeno M, Auqué L, Gómez J, Acero P, Pedersen K, 2009. Hydrogeochemical and microbiological effects on fractures in the Excavation Damaged Zone (EDZ). SKB R-09-05, Svensk Kärnbränslehantering AB.

Larsson E, 1997. Groundwater flow through a natural fracture. Flow experiments and numerical modelling. Licentiate degree thesis, Report A 82, Dep. of Geology, Chalmers University of Technology. Göteborg.

Olsson M, Niklasson B, Wilson L, Andersson C, Christiansson R, 2004. Experience of blasting of the TASQ tunnel. SKB R-04-73, Svensk Kärnbränslehantering AB.

Olsson M, Markström I, Pettersson A, 2008. Methodology study for documentation and 3D modelling of blast induced fractures. SKB Rapport R-08-90, Svensk Kärnbränslehantering AB.

Olsson M, Markström I, Pettersson A, Sträng M, 2009. Examination of the Excavation Damaged Zone in the TASS tunnel, Äspö HRL. SKB R-09-39, Svensk Kärnbränslehantering AB.

Rutqvist J, Stephansson O ,2003. The role of hydromechanical coupling in fractured rock engineering. Hydrogeology Journal, Vol 11 (1), 7–40.

Schuster, 2007. Äspö Hard Rock Laboratory-DECOVALEX-Ultrasonic borehole measurements in the TASQ tunnel (450 m level) at Äspö HRL performed by BGR in November 2006.

Appendix 1

Investigations in the Q-tunnel Äspö HRL. Database

Sample-ID	BB1	BB2	BB3
Air temp (°C)	20	21.1	20
Water temp (°C)	14	Room temperature	14
Sample height (m)	0.112	0.115	0.117
Dh (mvp)	0.64	0.64	0.64
a) Trace length of fractures, upper side (m) *o – open* *1/2-o: half-open* *c – closed* *h – healed*	1a) 0.134 m *(o)*. 2a) 0.173 m *(o)*. 3a) 0.08 m *(o)*. 4a) 0.05 m *(o)*	1a) 0.195 *(o)*. 2a) 0.135 *(o)*. 3a) 0.07 *(o)*	No visible fracture
b) Trace length of fractures, bottom side (m) *o – open* *1/2-o: half-open* *c – closed* *h – healed*	1b) 0.125 *(o)*. 2b) 0.17 *(c)*. 3b) 0.06 *(c)*	1b) 0.185 *(o)* 2b) 0.10 *(o)* 3b) 0.185 *(c)*	No visible fracture
Combination of fractures	1a and 1b is the same fracture.	1a and 1b is the same fracture.3a and 2b is the same fracture.	–
Interpr. mean trace length for flow (m)	0.216 m	0.2 m	0.2 m
Fracture type	–	–	–
Flow path length (m)	–	–	–
Flow path length, calc. (m)	0.114 (h = 0.112)	0.116 (h = 0.115)	–

Sample-ID BB1

Pressure (bar)	**5**						
Time (c)	1,242	1,457	1,690	1,916	2,070	2,250	2,400
Q (m³/s)	8.052E-07	6.863E-07	5.917E-07	5.219E-07	4.831E-07	4.444E-07	4.167E-07
Pressure (bar)	**10**						
Time (c)	2,610	2,648	2,772	2,852	3,064	3,260	
Q (m³/s)	3.831E-07	3.776E-07	3.608E-07	3.506E-07	3.264E-07	3.067E-07	

Sample-ID BB2

Pressure (bar)	**5**			**7.5**		
Time (c)	560	560	550	950	920	930
Q (m³/s)	1.786E-06	1.786E-06	1.818E-06	1.053E-06	1.087E-06	1.075E-06
Pressure (bar)	**10**			**7.5**		
Time (c)	1,560	1,570	1,570	1,620	1,620	1,620
Q (m³/s)	6.410E-07	6.369E-07	6.369E-07	6.173E-07	6.173E-07	6.173E-07

Pressure (bar)	**5**			
Time (c)	1,500	1,530	1,550	1,530
Q (m³/s)	6.667E-07	6.536E-07	6.452E-07	6.536E-07

Sample-ID BB3

Pressure (bar)	**5**
Time (c)	59,400
Q (m³/s)	0.00E+00

Sample-ID	BC
Air temp (°C)	**1)** 20.7 (2008-09-03) **2)** 19.8 (2008-09-04) **3)** 19.5 (2008-09-16) **4)** 20.3 (2008-09-18) **5)** 15.5 (2008-09-19)
Water temp (°C)	**1)** 18 (2008-09-03) **2)** 18 (2008-09-04) **3)** 16 (2008-09-16) **4)** 15 (2008-09-18) **5)** 20 (2008-09-19)
Sample height (m)	0.091
Dh (mvp) **(mvp)**	0.64
a) Trace length of fractures, upper side (m)	1a) 0.18 m *(o)* 2a) 0.195 *(c)*
o – open *1/2-o: half-open* *c – closed* *h – healed*	3a) 0.255 (h)
b) Trace length of fractures, bottom side (m)	1b) 0.135 *(o)* 2 b) 0.03 *(1/2-ö)*
o – open *1/2-o: half-open* *c – closed* *h – healed*	3b–7b varying length of closed fractures
Combination of fractures	1a and 1b is the same fracture.
Interpr. mean trace length for flow (m)	0.115 m
Fracture type	–
Flow path length (m)	–
Flow path length, calc. (m)	0.102 (h = 0.091)

Sample-ID BC

Pressure (bar)	1) 0										
Time (c)	40.69	40.34	39.5	39.22	39.03	38.57	38.28	38.07	38	37.62	37.75
Q (m³/s)	2.458E-05	2.479E-05	2.532E-05	2.550E-05	2.562E-05	2.593E-05	2.612E-05	2.627E-05	2.632E-05	2.658E-05	2.649E-05
Pressure (bar)	1) 2					1) 4					
Time (c)	380	373	373	373	373	421	426	427	427	429	
Q (m³/s)	2.632E-06	2.681E-06	2.681E-06	2.681E-06	2.681E-06	2.375E-06	2.347E-06	2.342E-06	2.342E-06	2.331E-06	
Pressure (bar)	2) 6							2) 8			
Time (c)	524	534	523	526	532	544	544	621	634	642	647
Q (m³/s)	1.908E-06	1.873E-06	1.912E-06	1.901E-06	1.880E-06	1.838E-06	1.838E-06	1.610E-06	1.577E-06	1.558E-06	1.546E-06
Pressure (bar)	3) 10			4) 10							
Time (c)	876	877	883	1,050	1,083	1,119	1,136	1,160			
Q (m³/s)	1.142E-06	1.140E-06	1.133E-06	9.524E-07	9.234E-07	8.937E-07	8.803E-07	8.621E-07			
Pressure (bar)	5) 6					5) 2					
Time (c)	1,294	1,306	1,366	1,420	1,484	1,502	1,348	1,362	1,360	1,352	
Q (m³/s)	7.728E-07	7.657E-07	7.321E-07	7.042E-07	6.739E-07	6.658E-07	7.418E-07	7.342E-07	7.353E-07	7.396E-07	

Sample-ID	No.	Midpoint. ½ transmitter length (cm)	Mean diameter	Time (μs)	V_p (m/s)
Slab BC	1	3.6	93.18	16.393	5,684
	2	5.75	93.18	16.386	5,686
	3	7.9	93.18	15.788	5,902
	4	10.05	93.18	15.648	5,955
	5	12.2	93.18	15.86	5,875
	6	14.35	93.18	15.84	5,882
	7	16.5	93.18	15.289	6,094

Slab BC	Sample-ID	Distance from contour hole in cm	Length (cm)	Time (μs)	V_p (m/s)
	v1a	20	8.552	15.149	5,645
	v1b	34.5	8.528	14.361	5,938
	h1c	16	5.853	10.659	5,491
	h1d	23.5	8.553	15.845	5,398
	h1e	32.05	6.771	11.803	5,737

Slab BC	Sample-ID	Length (cm)	Initial weight (g)	Porosity %	Density (g/cm^3)	Weight in water (g)	Final weight (g)	Radius (cm)
	v1a	8.552	339.27	0.157229	2.69409	–	339.468	2.165
	v1b	8.528	342.894	0.170578	2.720469	–	343.109	2.169
	h1a	–	254.223	0.504762	–	161.308	254.692	–
	h1b	–	277.137	0.583995	–	175.595	277.730	–
	h1c	5.853	233.907	0.384046	2.715325	–	234.238	2.165
	h1d	8.553	339.771	0.273169	2.691393	–	340.116	2.168
	h1e	6.771	257.854	0.174353	2.585075	–	258.028	2.166

Slab BC	Sample-ID	Density (kg/m^3)	Vp (m/s)	E-modulus (GPa)
	v1a	2,694	5,645	86
	v1b	2,720	5,938	96
	h1c	2,715	5,491	82
	h1d	2,691	5,398	78
	h1e	2,585	5,737	85

Sample-ID	BD1–BD2
Air temp (°C)	20.6
Water temp (°C)	Room temperature
Sample height (m)	0.110
Dh (mvp) **(mvp)**	0.64
a) Trace length of fractures, upper side (m) *o – open* *1/2-o: half-open* *c – closed* *h – healed*	1a) 0.066 *(o)* 2a) 0.102 *(o)* 3a) 0.045 *(c)* 4a) 0.11 *(c)* 5a) 0.09 *(c)* + a number of smaller closed fractures
b) Trace length of fractures, bottom side (m) *o – open* *1/2-o: half-open* *c – closed* *h – healed*	1b) 0.107 *(o)* 2b) 0.097 *(1/2-o)* 3b) 0.12 *(1/2-o)* 4b) 0.095 *(1/2-o)* 5b) 0.175 *(1/2-o)*
Combination of fractures	Complex system. **1)** 1a and 3b is the same fracture. **2)** 2a and 1b is the same fracture.
Interpr. mean trace length for flow (m)	0.404 m
Fracture type	–
Flow path length (m)	–
Flow path length, calc. (m)	**1)** 0.121 (h = 0.11) **2)** 0.124 (h = 0.11)

Sample-ID BD1–BD2

Pressure (bar)	5					
Time (c)	8,090	9,795	11,570	12,950	13,740	14,260
Q (m³/s)	1.236E-07	1.021E-07	8.643E-08	7.722E-08	7.278E-08	7.013E-08

Pressure (bar)	10				
Time (c)	17,480	18,120	19,540	22,000	23,930
Q (m³/s)	5.721E-08	5.519E-08	5.118E-08	4.545E-08	4.179E-08

Sample-ID	2. AB1-AB2
Air temp (°C)	20.1
Water temp (°C)	Room temperature
Sample height (m)	0.101
Dh (mvp) **(mvp)**	0.64
a) Trace length of fractures, upper side (m) *o – open* *1/2-o: half-open* *c – closed* *h – healed*	0.195 *(o)*
b) Trace length of fractures, bottom side (m) *o – open* *1/2-o: half-open* *c – closed* *h – healed*	0.197 *(o)*
Combination of fractures	1a and 1b is the same fracture.
Interpr. mean trace length for flow (m)	0,196 m
Fracture type	–
Flow path length (m)	Sample height
Flow path length, calc. (m)	–

Sample-ID 2.AB1–AB2

Pressure (bar)	5					
Time (c)	4,170	4,240	4,470	4,570	4,560	4,560
Q (m^3/s)	2.398E-07	2.358E-07	2.237E-07	2.188E-07	2.193E-07	2.193E-07
Pressure (bar)	**10**			
Time (c)	8,370	8,400	8,420	8,450
Q (m^3/s)	1.195E-07	1.190E-07	1.188E-07	1.183E-07

Sample-ID	3.AC1–AC2
Air temp (°C)	20.4
Water temp (°C)	Room temperature
Sample height (m)	0.099
Dh (mvp) **(mvp)**	0.64
a) Trace length of fractures, upper side (m) *o – open* *1/2-o: half-open* *c – closed* *h – healed*	1a) 0.187 *(o)* 2a) 0.12 *(o)*
b) Trace length of fractures, bottom side (m) *o – open* *1/2-o: half-open* *c – closed* *h – healed*	1b) 0.185 *(o)* 2b) 0.08 *(1/2-o)*
Combination of fractures	1a and 1b is the same fracture. 2a and 2b is the same fracture
Interpr. mean trace length for flow (m)	0.226 m
Fracture type	–
Flow path length (m)	Sample height
Flow path length, calc. (m)	–

Sample-ID 2.AB1–AB2

Pressure (bar)	5			10		
Time (c)	1,890	1,880	1,870	2,600	2,660	2,660
Q (m^3/s)	5.291E-07	5.319E-07	5.348E-07	3.846E-07	3.759E-07	3.759E-07

Sample-ID	1.4 övre
Air temp (°C)	20.1
Water temp (°C)	Room temperature
Sample height (m)	0.076
Dh (mvp) **(mvp)**	0.64
a) Trace length of fractures, upper side (m) *o – open* *1/2-o: half-open* *c – closed* *h – healed*	1a) 0.187 *(o)* 2a) 0.032 (1/2-o)
b) Trace length of fractures, bottom side (m) *o – open* *1/2-o: half-open* *c – closed* *h – healed*	1b) 0.12 *(o)* There is a cavity in the fracture from the bottom side and up into the rock sample. The cavity is 0.067 m long and elongated in the fracture direction, with a widening in the middle.
Combination of fractures	1a and 1b is the same fracture.
Interpr. mean trace length for flow (m)	0.17 m
Fracture type	–
Flow path length (m)	Sample height
Flow path length, calc. (m)	–

Sample-ID 1.4 övre

Pressure (bar)	5			10		
Time (c)	400	405	405	655	665	665
Q (m^3/s)	0.0000025	2.469E-06	2.469E-06	1.527E-06	1.504E-06	1.504E-06

Sample-ID	4.1 undre
Air temp (°C)	20.8
Water temp (°C)	Room temperature
Sample height (m)	0.083
Dh (mvp) **(mvp)**	0.64
a) Trace length of fractures, upper side (m) *o – open* *1/2-o: half-open* *c – closed* *h – healed*	1a) 0.134 *(1/2-o)* 2a) 0.067 *(c)*
b) Trace length of fractures, bottom side (m) *o – open* *1/2-o: half-open* *c – closed* *h – healed*	–
Combination of fractures	–
Interpr. mean trace length for flow (m)	0.070 m
Fracture type	–
Flow path length (m)	–
Flow path length, calc. (m)	–

Sample-ID 4.1 undre

Pressure (bar)	5
Time (c)	1,800
Q (m^3/s)	0.000E+00

Sample-ID	2.2.2
Air temp (°C)	21.1
Water temp (°C)	Room temperature
Sample height (m)	0.108–0.117
Dh (mvp) **(mvp)**	0.64
a) Trace length of fractures, upper side (m) *o – open* *1/2-o: half-open* *c – closed* *h – healed*	1a) 0.177 *(c)* 2a) 0.13 *(o)* 3a) 0.144 *(o)* 4a) 0.044 *(1/2-o)* 5a) 0.027 *(o)*
b) Trace length of fractures, bottom side (m) *o – open* *1/2-o: half-open* *c – closed* *h – healed*	1b) 0.186 *(o)* 2b) 0.13 *(c)* 3b) 0.077 *(c)*
Combination of fractures	1b och 2a is the same fracture. It crosses through the whole rock sample only on one edge. 5a looks like it crosses through the whole sample but there is no fracture on the b-side corresponding to 5a. Complex system.
Interpr. mean trace length for flow (m)	0.458 m
Fracture type	–
Flow path length (m)	–
Flow path length, calc. (m)	–

Sample-ID 2.2.2

Pressure (bar)	5			10		
Time (c)	2,980	2,960	2,980	4,070	4,180	4,190
Q (m³/s)	3.356E-07	3.378E-07	3.356E-07	2.457E-07	2.392E-07	2.387E-07

Sample-ID	XX
Air temp (°C)	21.2
Water temp (°C)	Room temperature
Sample height (m)	0.102
Dh (mvp) **(mvp)**	0.64
a) Trace length of fractures, upper side (m) *o – open* *1/2-o: half-open* *c – closed* *h – healed*	1a) 0.195 *(o)*
b) Trace length of fractures, bottom side (m) *o – open* *1/2-o: half-open* *c – closed* *h – healed*	1b) 0.186 *(o)* 2b) 0.15 (o) 3b) 0.095 *(o)* 4b) 0.06 *(o)*
Combination of fractures	1a and 1b–3b is the same fracture.
Interpr. mean trace length for flow (m)	0.19 m
Fracture type	–
Flow path length (m)	Sample height
Flow path length, calc. (m)	–

Sample-ID XX

Pressure (bar)	5			7.5		
Time (c)	2,090	2,150	2,160	3,110	3,210	3,510
Q (m³/s)	3.356E-07	3.378E-07	3.356E-07	2.457E-07	2.392E-07	2.387E-07

Pressure (bar)	10			7.5		5		
Time (c)	4,730	5,080	5,230	5,400	5,440	5,390	5,880	5,970
Q (m³/s)	2.114E-07	1.969E-07	1.912E-07	1.852E-07	1.838E-07	1.855E-07	1.701E-07	1.675E-07

Appendix 2

Investigations in the S-tunnel Äspö HRL, Database

VS0036B04

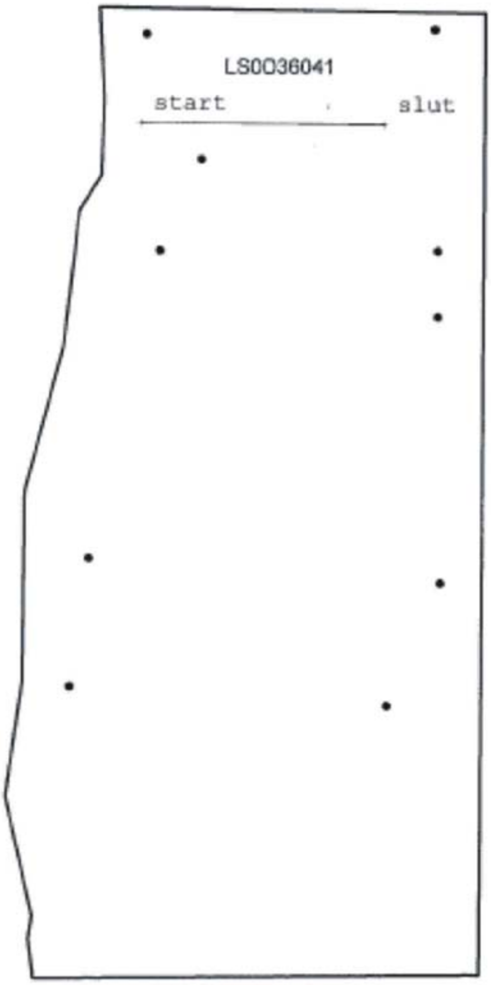

VS0036B04

Scanline-ID	No.	Distance from start (mm)	Diameter (mm)	Time (μs)	V_p (m/s)	Comments
LS0036041	0	0	90	–	–	No signal
	1	2.05	90.2	–	–	No signal
	2	4.1	90.3	–	–	No signal
	3	6.15	90.5	–	–	No signal
	4	8.2	90.6	–	–	No signal
	5	10.25	90.8	–	–	No signal
	6	12.3	90.9	–	–	No signal
	7	14.35	91.1	–	–	No signal
	8	16.4	91.3	19.818	4,604	Weak signal
	9	18.45	91.4	17.979	5,084	Weak signal
	10	20.5	91.6	16.582	5,522	
	11	22.55	91.7	16.096	5,698	Good signal
	12	24.6	91.9	16.295	5,638	Good signal
	13	26.65	92.0	16.497	5,579	
	14	28.7	92.2	16.346	5,640	
	15	30.75	92.3	16.283	5,671	
	16	32.8	92.5	16.4	5,640	
	17	34.85	92.7	–	–	No signal

VS0036B09

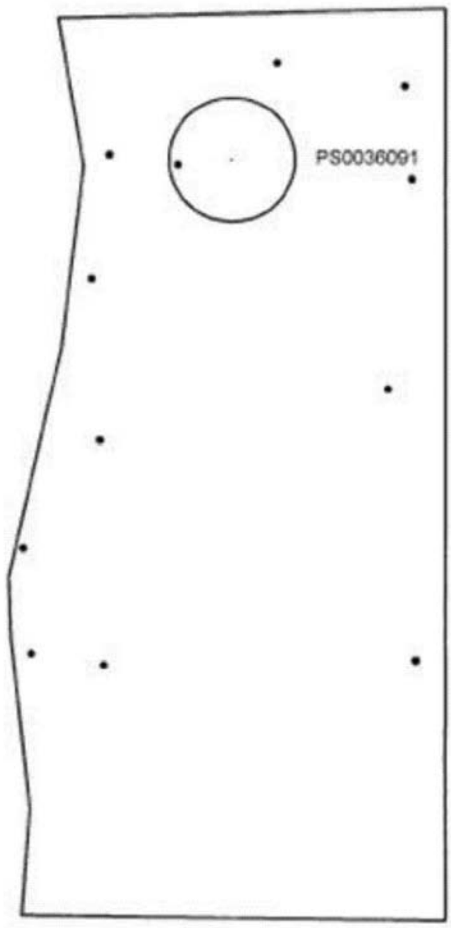

VS0036B09

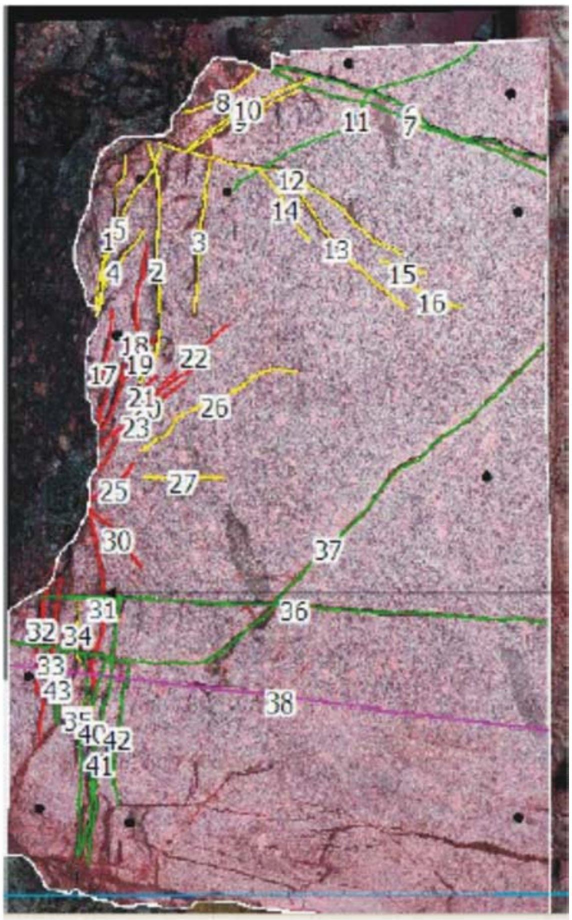

Sample-ID	PS0036091
Air temp (°C)	20
Water temp (°C)	Room temperature
Sample height (m)	0.13–0.135
Dh (mvp) **(mvp)**	35.1
a) Trace length of fractures, upper side (m) *o – open* *1/2-o: half-open* *c – closed* *h – healed*	1a) 0.145 *(1/2-o)* 2a) 0.175 *(h)*
b) Trace length of fractures, bottom side (m) *o – open* *1/2-o: half-open* *c – closed* *h – healed*	1b) 0.15 *(1/2-o)* 2b) 0.107 3b) 0.07 4b) 0.055 5b) 0.075 6b) 0.07 7b) 0.12 8b) 0.06 9b) 0.03 2b–9b *(h)*
Combination of fractures	1b and 2b meet at side and emerge in 1a. 1b is same fracture as 2a. Complex system.
Interpr. mean trace length for flow (m)	0,1475
Fracture type	induced
Flow path length (m)	–
Flow path length, calc. (m)	–

Sample-ID PS0036091

Pressure (bar)	5			10	10*	
Time (s)	4,200	5,250	5,390	15,950	161	163
Q (m³/s)	2.381E-07	1.905E-07	1.855E-07	6.270E-08	2.44E-08	2.41E-08

* Method of measurement with 5 cm rubber hose. Volume 3.93E-06 m^3.

VS0037B05

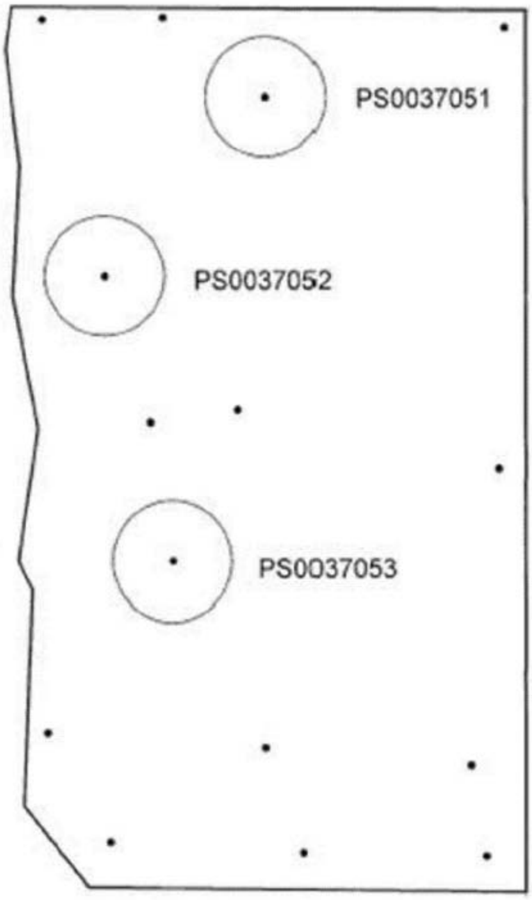

VS0037B05

Sample-ID	PS0037051	PS0037052	PS0037053
Air temp (°C)	20.6 20.6 20.6	20	20.6
Water temp (°C)	Room temperature	Room temperature	Room temperature
Sample height (m)	0.091–0.093	0.094	0.093
Dh (mvp) **(mvp)**	0.64	35.1	0.64
a) Trace length of fractures, upper side (m) *o – open* *1/2-o: half-open* *c – closed* *h – healed*	1a) 0.19 *(h)*	1a) 0.19 *(h)*	1a) 0.195 *(o)* 2a) 0.18 *(1/2-o)* 3 a) 0.18 *(h)*
b) Trace length of fractures, bottom side (m) *o – open* *1/2-o: half-open* *c – closed* *h – healed*	1b) 0.135 *(h)* 2 b) 0.05 *(h)* 3 b) 0.05 *(h)*	1b) 0.13 *(h)*	1b) 0.19 *(o)* 2b) 0.18 *(h)* 3b) 0.1 *(h)* 4 b) 0.07 *(h)*
Combination of fractures	–	1a and 1b is the same fracture. 1 b is located further to the side than 1a which crosses at the centre of the upper side of the rock sample The fracture is in an oblique angle.	1a and 1b is the same fracture. 3a and 3b is the same fracture
Interpr. mean trace length for flow (m)	0,1625	0,16	0,1925
Fracture type	natural	natural	natural
Flow path length (m)	–	–	Sample height
Flow path length, calc. (m)	–	0.110 (h = 0.094)	

Sample-ID PS0037051

Pressure (bar)	5	10
Time (s)	780	600
Q (m^3/s)	0.00E+00	0.000E+00

Sample-ID PS0037052

Pressure (bar)	5	10*
Time (s)	–	3,600
Q (m^3/s)	–	0.000E+00

* Method of measurement with 5 cm rubber hose. Volume 3.93E-06 m^3.

Sample-ID PS0037053

Pressure (bar)	5		10		
Time (s)	216	218	440	450	455
Q (m^3/s)	4.630E-06	4.587E-06	2.273E-06	2.222E-06	2.198E-06

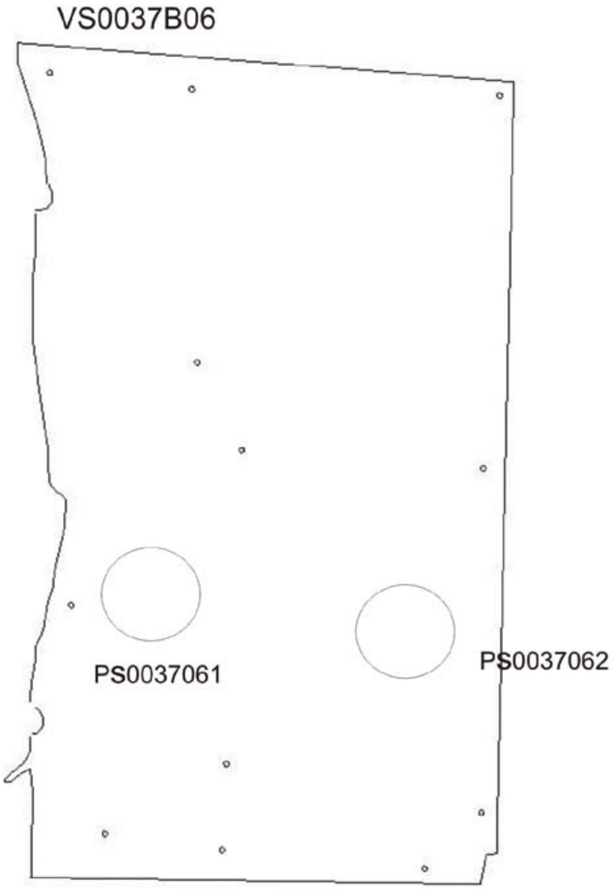

Sample-ID	PS0037061	PS0037062
Air temp (°C)	20.6 20.6 20.6	20
Water temp (°C)	Room temperature	Room temperature
Sample height (m)	0.1 is the thickest point and 0.09 is the thinnest. sprickans utgång och 0.09 m på det tunnaste stället	0.09–0.099
Dh (mvp) **(mvp)**	0.64	35.3–35.8
a) Trace length of fractures, upper side (m) *o – open* *1/2-o: half-open* *c – closed* *h – healed*	1a) 0.19 *(o)* 2a) 0.185 *(h)* 3a) 0.145 *(h)*	1a) 0.185 *(c)* 2a) 0.13 *(c)*
b) Trace length of fractures, bottom side (m) *o – open* *1/2-o: half-open* *c – closed* *h – healed*	1b) 0.19 *(o)* 2 b) 0.102 m *(1/2-o)*	1b) 0.165 *(c)* 2b) 0.14 *(c)*
Combination of fractures	1a and 1b is the same fracture. 2a and 2b is the same fracture.	1a and 1b is the same fracture. 2a and 2b is the same fracture.
Interpr. mean trace length for flow (m)	0,19	0,31
Fracture type	natural	natural
Flow path length (m)	–	Sample height
Flow path length, calc. (m)	0.091 (h = 0.09) 0.096 (h = 0.095) 0.101 (h = 0.1)	–

Sample-ID PS0037061

Pressure (bar)	2		4			6	
Time (s)	84	84	120	125	125	180	180
Q (m^3/s)	1.190E-05	1.190E-05	8.333E-06	8.000E-06	8.000E-06	5.556E-06	5.556E-06

Pressure (bar)	8		10			8		
Time (s)	235	235	290	300	300	295	295	300
Q (m^3/s)	4.255E-06	4.255E-06	3.448E-06	3.333E-06	3.333E-06	3.390E-06	3.390E-06	3.333E-06

Pressure (bar)	6		4		2	
Time (s)	290	290	285	290	265	270
Q (m^3/s)	3.448E-06	3.448E-06	3.509E-06	3.448E-06	3.774E-06	3.704E-06

Pressure (bar)	4		6		8		
Time (s)	285	285	300	295	320	325	325
Q (m^3/s)	3.509E-06	3.509E-06	3.333E-06	3.390E-06	3.125E-06	3.077E-06	3.077E-06

Pressure (bar)	10			20		18	
Time (s)	345	350	345	1,000	1,010	950	950
Q (m^3/s)	2.899E-06	2.857E-06	2.899E-06	1.000E-06	9.901E-07	1.053E-06	1.053E-06

Pressure (bar)	16		14		12	
Time (s)	950	960	1,000	1,010	990	1,000
Q (m^3/s)	1.053E-06	1.000E-06	1.000E-06	9.901E-07	1.010E-06	1.000E-06

Pressure (bar)	10				8		6		
Time (s)	990	970	940	950	1,000	960	960	890	870
Q (m^3/s)	1.010E-06	1.031E-06	1.064E-06	1.053E-06	1.000E-06	1.000E-06	1.042E-06	1.124E-06	1.149E-06

Pressure (bar)	4		2	
Time (s)	790	800	660	660
Q (m^3/s)	1.266E-06	1.250E-06	1.515E-06	1.515E-06

Sample-ID PS0037062

Pressure (bar)	5*		10*	
Time (s)	102.59	102.13	126.25	126.78
Q (m^3/s)	3.828E-08	3.845E-08	3.110E-08	3.097E-08

* Method of measurement with 5 cm rubber hose. Volume 3.93E-06 m^3.

VS0039B01

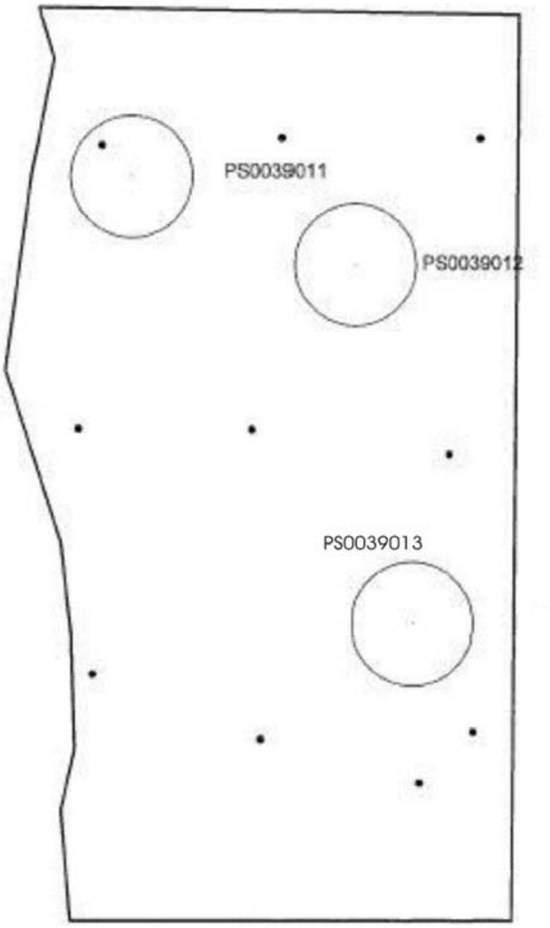

VS0039B01

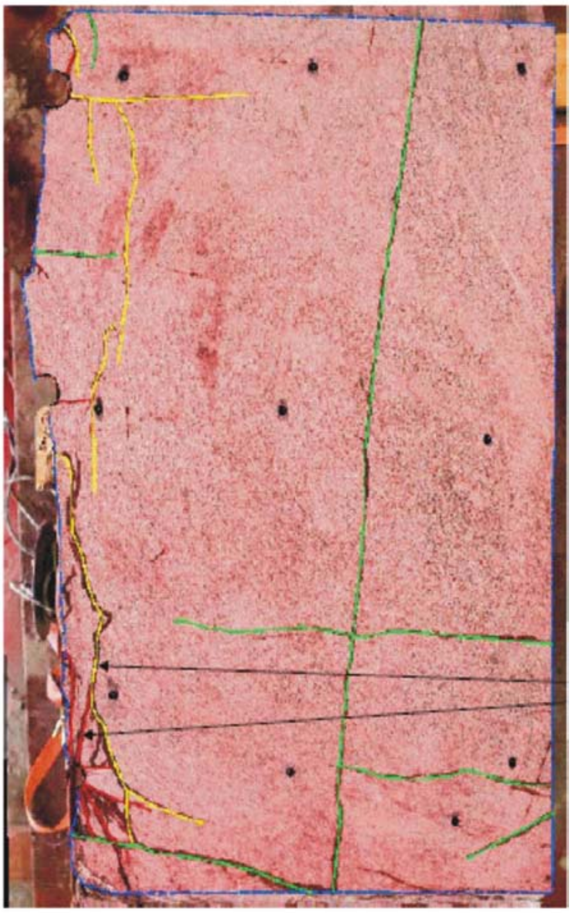

Sample-ID	PS0039011	PS0039012	PS0039013
Air temp (°C)	20 20.6 20.6	20.6	20
Water temp (°C)	Room temperature	Room temperature	
Sample height (m)	0.061–0.073 sprickans utgång och 0.09 m på det tunnaste stället	0.085–0.079	0.096–0.099
Dh (mvp) (mvp)	35.1	0.64	34.8
a) Trace length of fractures, upper side (m) *o – open* *1/2-o: half-open* *c – closed* *h – healed*	1a) 0.17 *(c)*	1a) 0.19 *(o)*	1a) 0.195 *(1/2-o)*. 0.07 m of 1a is *(h)*
b) Trace length of fractures, bottom side (m) *o – open* *1/2-o: half-open* *c – closed* *h – healed*	1 b) 0.19 *(c)*	1b) 0.165 *(o)*	1b) 0.1 *(c–h)* 2b) 0.19 *(c–h)* a very weak indication of a fracture.
Combination of fractures	1a and 1b is the same fracture	1a and 1b is the same fracture.	1a and 1b is the same fracture but 1a has also contact with the very weakly indicated 2b.
Interpr. mean trace length for flow (m)	0,18 *(c)*	0,18	0,19
Fracture type	induced	natural	–
Flow path length (m)	–	–	–
Flow path length, calc. (m)	0.061 (h = 0.061) 0.067 (h = 0.067) 0.073 (h = 0.073)	0.099 (h = 0.085) 0.096 (h = 0.082) 0.093 (h = 0.079)	0.113 (h = 0.096) 0.116 (h = 0.099)

Sample-ID PS0039011

Pressure (bar)	5*
Time (s)	3,600
Q (m^3/s)	0.00E+00

* Method of measurement with 5 cm rubber hose. Volume 3.93E-06 m^3.

Sample-ID PS0039012

Pressure (bar)	5				10	
Time (s)	580	590	610	615	1,130	1,140
Q (m^3/s)	1.72E-06	1.70E-06	1.64E-06	1.63E-06	8.85E-07	8.77E-07

Sample-ID PS0039013

Pressure (bar)	5		10	10*
Time (s)	7,700	8,700	26,580	120
Q (m^3/s)	1.299E-07	1.149E-07	3.762E-08	3.27E-08

* Method of measurement with 5 cm rubber hose. Volume 3.93E-06 m^3.

VS0039B02

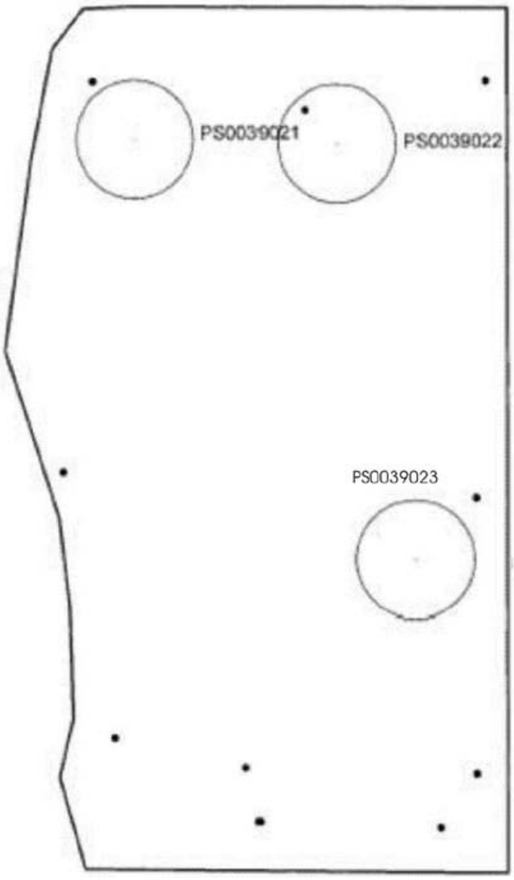

VS0039B02

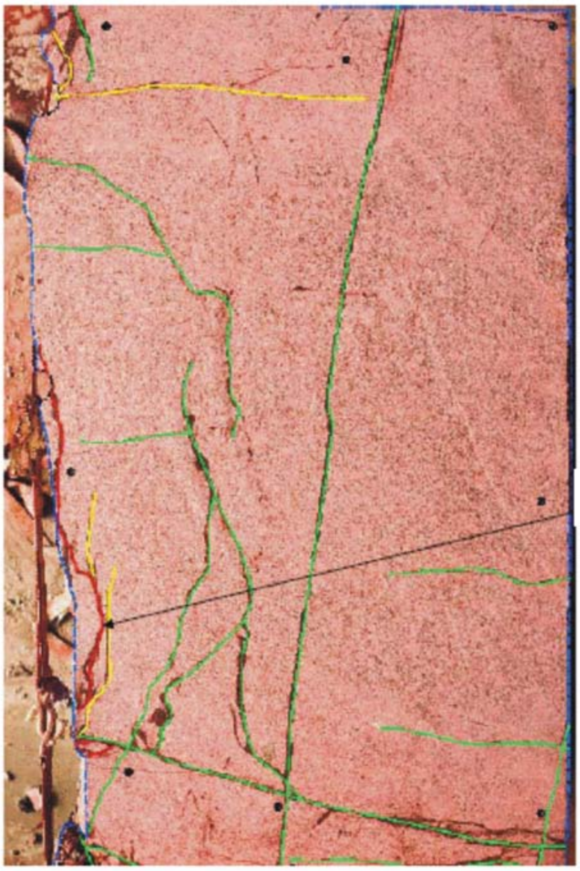

Sample-ID	PS0039021	PS0039022	PS0039023
Air temp (°C)	20 20.6 20.6	20.6	20.6
Water temp (°C)	Room temperature	Room temperature	Room temperature
Sample height (m)	0.090–0.096	0.094	0.09
Dh (mvp) (mvp)	35.1	0.64	35.1
a) Trace length of fractures, upper side (m) *o – open* *1/2-o: half-open* *c – closed* *h – healed*	1 a) 0.19 m (1/2-o) 2a) 0.106 m *(h)*	1 a) 0.19.5 m (o) 2a) 0.095 (1/2-o)	1a) 0.19 *(h)*
b) Trace length of fractures, bottom side (m) *o – open* *1/2-o: half-open* *c – closed* *h – healed*	1 b) 0.185 *(1/2-o)* 2 b) 0.19 *(h)* 3b) 0.16 *(h)* 4b) 0.045 *(h)* 5b) 0.095 *(h)*	1 b) 0.135 m *(o)* 2 b) 0.03 *(1/2- o)* 3b–7b varying sizes of healed fractures.	1b) 0.165 *(h)*
Combination of fractures	1a and 1b is the same fracture.	1a and 1b is the same fracture. 2a and 2b is the same fracture. It starts at 1 a and 1b and runs vertically to the edge of the sample.	1a and 1b is the same fracture
Interpr. mean trace length for flow (m)	0,19	0,165	0,18 *(h)*
Fracture type	induced	natural	natural
Flow path length (m)	–	–	–
Flow path length, calc. (m)	0.093 (h = 0.09) 0.096 (h = 0.093) 0.099 (h = 0.96)	0.112 (h = 0.094) 0.091 (h = 0.082) 0.089 (h = 0.079)	0.096 (h = 0.09)

Sample-ID PS0039021

Pressure (bar)	5*			10*		
Time (s)	863	771	776	967	1,067	1,118
Q (m^3/s)	4.550E-09	5.093E-09	5.061E-09	4.061E-09	3.680E-09	3.513E-09

* Method of measurement with 5 cm rubber hose. Volume 3.93E-06 m^3.

Sample-ID PS0039022

Pressure (bar)	5			10			
Time (s)	435	460	455	700	750	770	800
Q (m^3/s)	2.299E-06	2.174E-06	2.198E-06	1.429E-06	1.333E-06	1.299E-06	1.250E-06

Sample-ID PS0039023

Pressure (bar)	5				10		
Time (s)	90	94	106	105	210	250	237
Q (m^3/s)	4.36E-08	4.18E-08	3.70E-08	3.74E-08	1.87E-08	1.57E-08	1.66E-08

VS0039B05

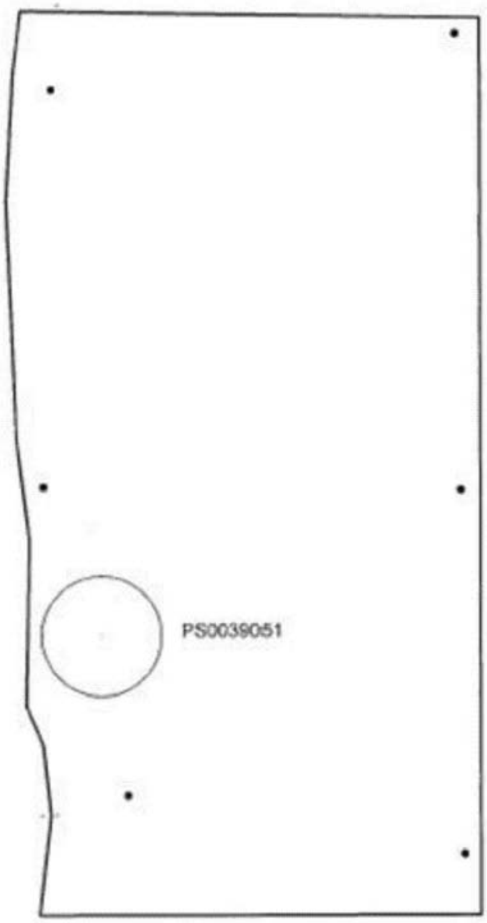

VS0039B05

Sample-ID	PS0039051
Air temp (°C)	20
Water temp (°C)	Room temperature
Sample height (m)	0.093
Dh (mvp) **(mvp)**	0.64
a) Trace length of fractures, upper side (m) *o – open* *1/2-o: half-open* *c – closed* *h – healed*	1a) 0.195 *(o)* 2a) 0.093 *(o)* 3a) 0.098 *(1/2-o)*
b) Trace length of fractures, bottom side (m) *o – open* *1/2-o: half-open* *c – closed* *h – healed*	1b) 0.198 *(o)* 2b) 0.057 *(o)* 3b) 0.1 *(1/2-o)*
Combination of fractures	1a and 1b is the same fracture. 2a and 2b is the same fracture. It starts at 1a and 1b and runs vertically to the edge of the sample. 3a and 3b is the same fracture.
Interpr. mean trace length for flow (m)	0,37
Fracture type	–
Flow path length (m)	–
Flow path length, calc. (m)	0.102 (h = 0.093)

Sample-ID PS0039051

Pressure (bar)	5		10	
Time (s)	39.8	38.3	56.7	56.85
Q (m^3/s)	2.513E-05	2.611E-05	1.764E-05	1.759E-05

VS0039B06

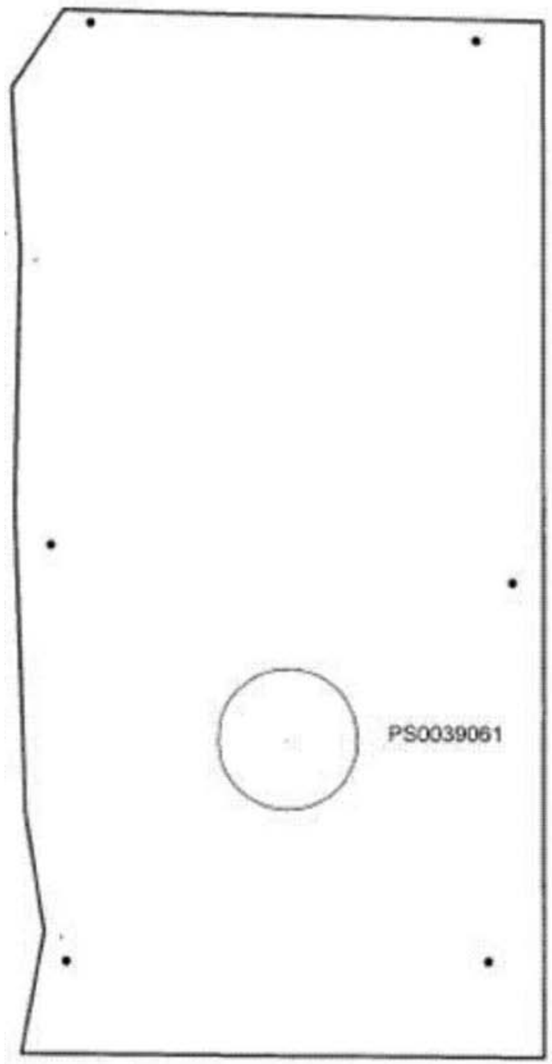

VS0039B06

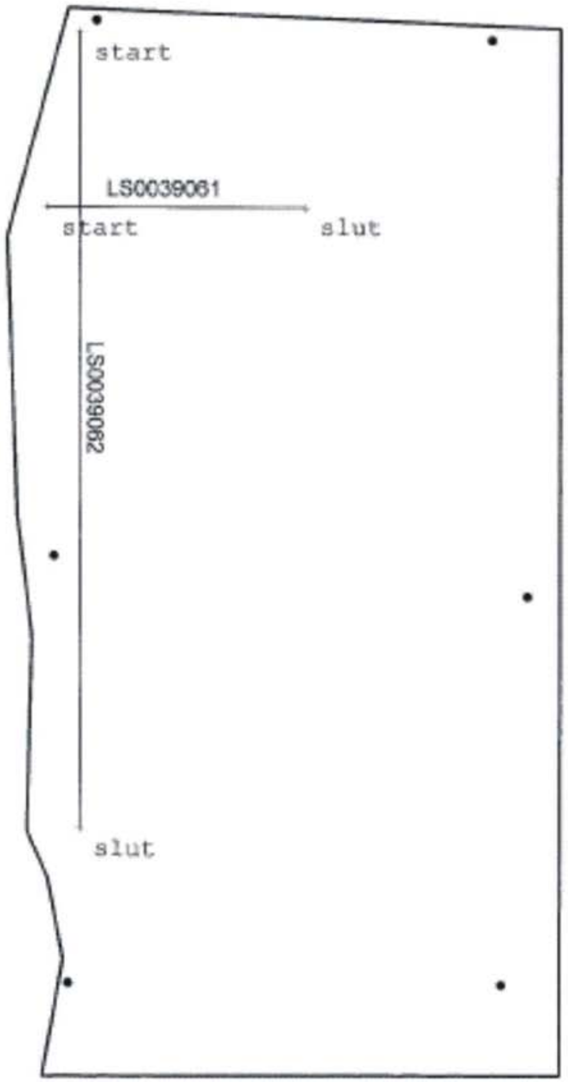

VS0039B06

Sample-ID	PS0039061
Air temp (°C)	20
Water temp (°C)	Room temperature
Sample height (m)	0.09
Dh (mvp) **(mvp)**	0.64
a) Trace length of fractures, upper side (m)	1a) 0.19 *(o)*
o – open *1/2-o: half-open* *c – closed* *h – healed*	
b) Trace length of fractures, bottom side (m)	1b) 0.18 *(o)*
o – open *1/2-o: half-open* *c – closed* *h – healed*	
Combination of fractures	1a and 1b is the same fracture.
Interpr. mean trace length for flow (m)	0,19
Fracture type	natural
Flow path length (m)	–
Flow path length, calc. (m)	0.100 (h = 0.09)

Sample-ID PS0039061

Pressure (bar)	**5**			**10**			**7.5**		
Time (s)	205.3	202.2		370	368.8		371.3	362.8	375
Q (m³/s)	4.871E-06	4.946E-06		2.703E-06	2.711E-06		2.693E-06	2.756E-06	2.667E-06
Pressure (bar)	**5**			**2.5**			**5**		
Time (s)	352.8	345.7	354.7	326.6	310	314.7	351.6	350	
Q (m³/s)	2.834E-06	2.893E-06	2.819E-06	3.062E-06	3.226E-06	3.178E-06	2.844E-06	2.857E-06	
Pressure (bar)	**7.5**			**10**			**20**		
Time (s)	378.5	370.6	373.7	404.4	405.5		924.4	920.3	
Q (m³/s)	2.642E-06	2.698E-06	2.676E-06	2.473E-06	2.466E-06		1.082E-06	1.087E-06	
Pressure (bar)	**15**			**10**			**5**		
Time (s)	884.4	881		793.2	783		688.5	664.7	668.7
Q (m³/s)	1.131E-06	1.135E-06		1.261E-06	1.277E-06		1.452E-06	1.504E-06	1.495E-06
Pressure (bar)	**10**			**15**			**20**		
Time (s)	772.1	777.1		859.3	866.5		992.5	1,039.4	1,040.6
Q (m³/s)	1.295E-06	1.287E-06		1.164E-06	1.154E-06		1.008E-06	9.621E-07	9.610E-07
Pressure (bar)	**25**			**20**			**15**		
Time (s)	1,247.2	1,299.1	1,285	1,344.6	1,296.3	1,320	1,214	1,210.3	
Q (m³/s)	8.018E-07	7.698E-07	7.782E-07	7.624E-07	7.714E-07	7.576E-07	8.237E-07	8.262E-07	
Pressure (bar)	**10**			**7.5**			**5**		
Time (s)	1,093.4	1,099.7		1,001.9	996.9		856.9	865.4	
Q (m³/s)	9.146E-07	9.093E-07		9.981E-07	1.003E-06		1.167E-06	1.156E-06	
Pressure (bar)	**2.5**								
Time (s)	717.2	721.9							
Q (m³/s)	1.394E-06	1.385E-06							

Scanline-ID	No.	Distance from start (mm)	Diameter (mm)	Time (µs)	V_p (m/s)	Comments
LS0039061	0	0	93.5	15.965	5,857	
	1	2.05	93.9	15.985	5,873	
	2	4.1	94.3	15.934	5,916	
	3	6.15	94.6	15.952	5,933	
	4	8.2	95.0	–	–	No contact
	5	10.25	95.4	–	–	No contact
	6	12.3	95.8	15.775	6,073	
	7	14.35	96.2	15.642	6,149	
	8	16.4	96.6	15.197	6,354	
	9	18.45	96.9	15.49	6,258	
	10	20.5	97.3	15.593	6,241	
	11	22.55	97.7	16.001	6,106	
	12	24.6	98.1	15.497	6,329	
	13	26.65	98.5	15.746	6,254	
	14	28.7	98.9	15.881	6,225	
	15	30.75	99.2	15.301	6,486	
	16	32.8	99.6	15.402	6,468	
	17	34.85	100.0	15.399	6,494	

Value with half length of transmitter, 2.05 cm.

Scanline-ID	No.	Distance from start (mm)	Diameter (mm)	Time (µs)	V_p (m/s)	Comments
LS0039062	0	0	93	16.132	5,765	
	1	4.1	93	15.893	5,852	
2	8.2	92.6	15.936	5,811		
3	12.3	92.6	15.968	5,799		
4	16.4	93	15.98	5,820		
5	20.5	93	16.134	5,764		
6	24.6	93.3	16.207	5,757		
7	28.7	93.5	15.718	5,949		
8	32.8	93	15.9	5,849		
9	36.9	93	15.933	5,837		
10	41	93	15.847	5,869		
11	45.1	92.6	15.597	5,937		
12	49.2	92.2	15.675	5,882		
13	53.3	92	15.97	5,761		
14	57.4	91	15.95	5,705		
15	61.5	90.6	–	–		Fracture in middle of line
16	65.6	90.9	–	–		No contact
17	69.7	90.3	16.848	5,360		
18	73.8	90.2	–	–		No contact
19	77.9	90.1	15.632	5,764		One transmitter of line away from wall.
20	82	90.1	16.157	5,577		One transmitter of line away from wall.
21	86.1	90	15.987	5,630		
22	90.2	89.9	15.879	5,662		
23	94.3	89.7	15.542	5,771		
24	98.4	89.2	15.444	5,776		No good contact
25	102.5	88.8	15.113	5,876		1/2 transmitter of line against tunnel wall
26	106.6	88.6	15.302	5,790		

Value with one length of transmitter, 4.1 cm.

VS0039B07

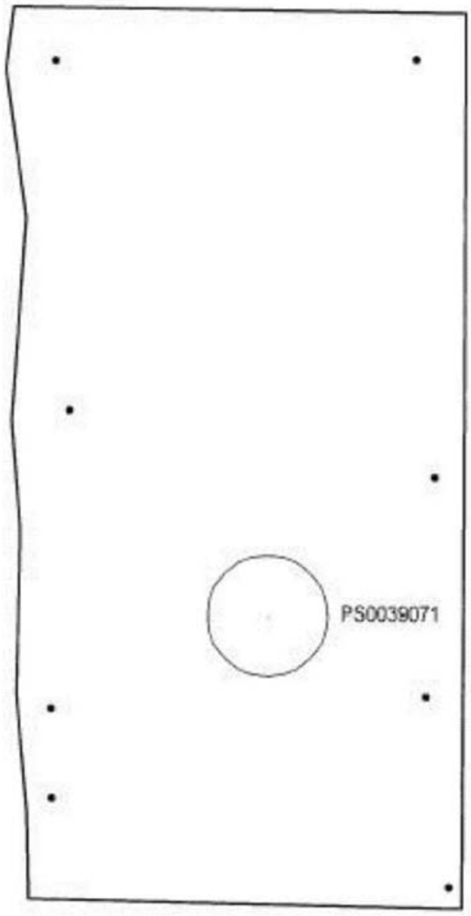

VS0039B07

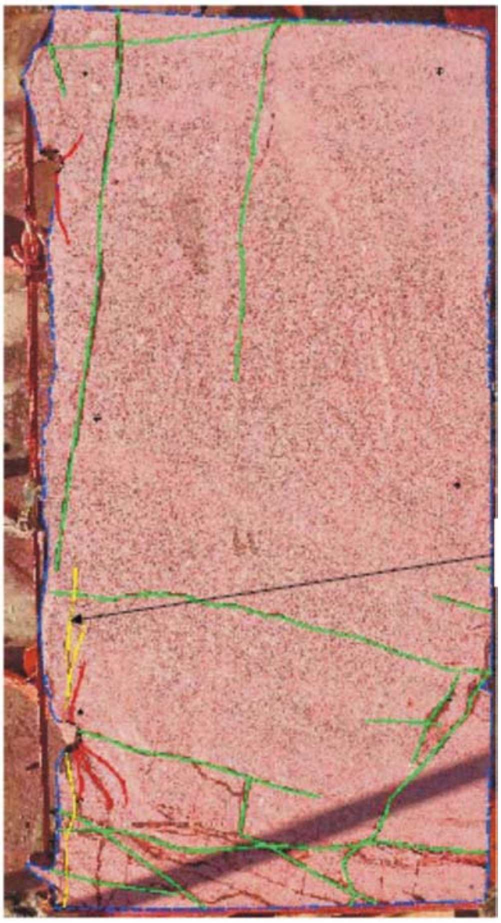

Sample-ID	PS0039071
Air temp (°C)	20
Water temp (°C)	Room temperature
Sample height (m)	0.098
Dh (mvp) **(mvp)**	35.1
a) Trace length of fractures, upper side (m)	1a) 0.19 *(c)*
o – open *1/2-o: half-open* *c – closed* *h – healed*	
b) Trace length of fractures, bottom side (m)	1b) 0.19 *(c)*
o – open *1/2-o: half-open* *c – closed* *h – healed*	
Combination of fractures	1a and 1b is the same fracture.
Interpr. mean trace length for flow (m)	0,19
Fracture type	Natural
Flow path length (m)	Sample height
Flow path length, calc. (m)	–

Sample-ID PS0039071

Pressure (bar)	5	10*	
Time (s)	31,385	258	263
Q (m^3/s)	3.19E-08	1.52E-08	1.49E-08

* Method of measurement with 5 cm rubber hose. Volume 3.93E-06 m^3.

VS0040B04

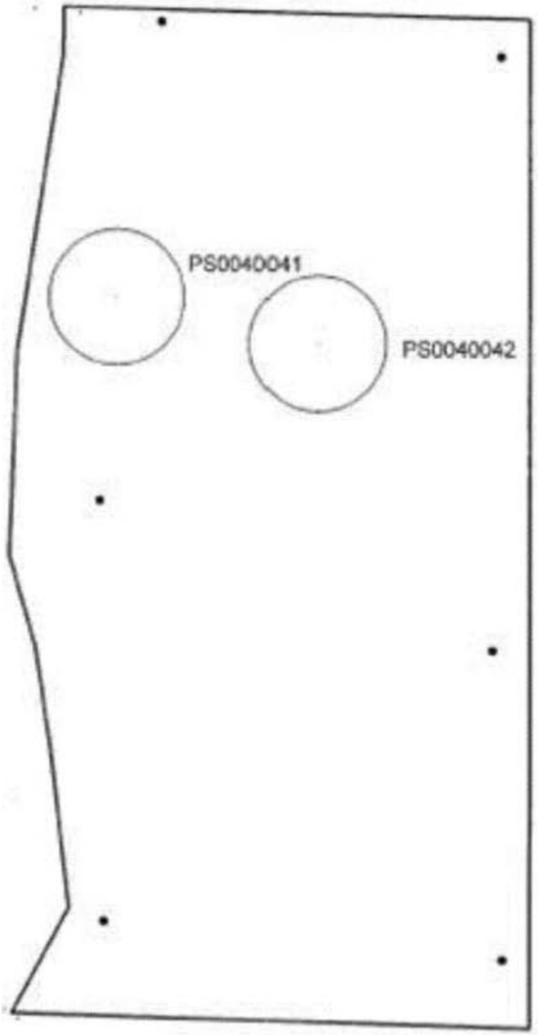

VS0040B04

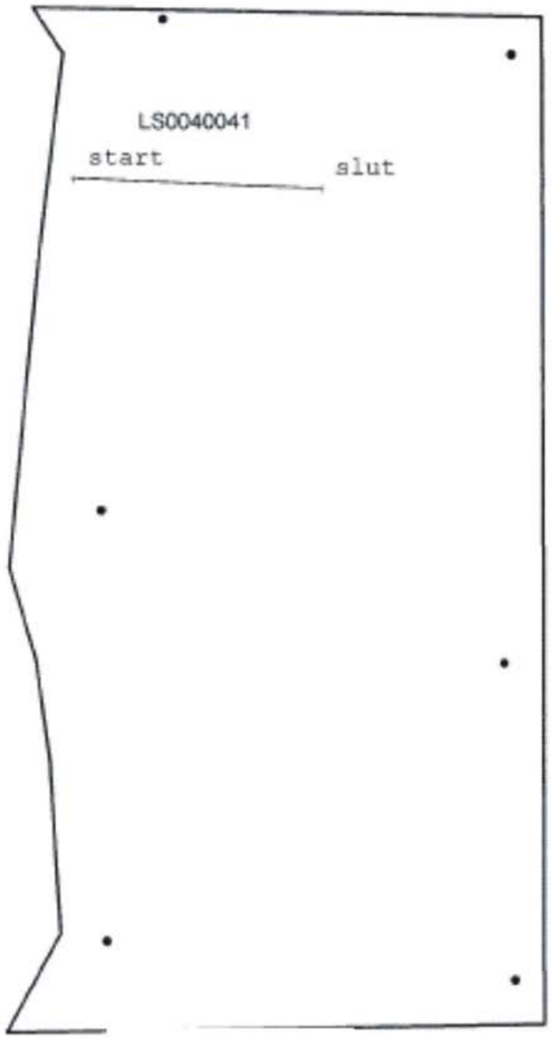

VS0040B04

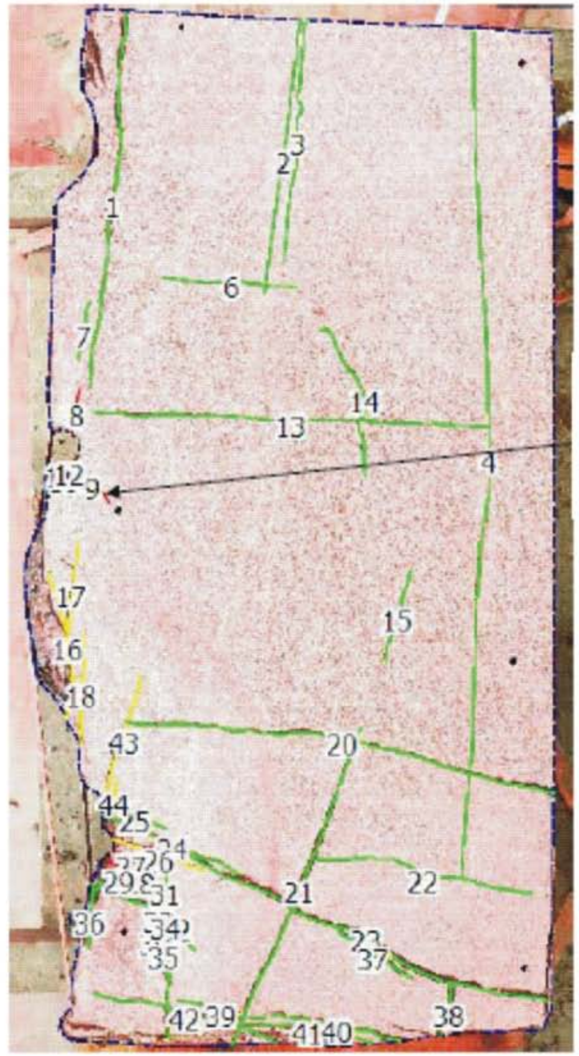

Sample-ID	PS0040041	PS0040042
Air temp (°C)	20 20.6 20.6	20
Water temp (°C)	Room temperature	Room temperature
Sample height (m)	0.09	0.091
Dh (mvp) **(mvp)**	35.1	35.1
a) Trace length of fractures, upper side (m) *o – open* *1/2-o: half-open* *c – closed* *h – healed*	1a) 0.145 *(h)*	1a) 0.135 *(c)*
b) Trace length of fractures, bottom side (m) *o – open* *1/2-o: half-open* *c – closed* *h – healed*	1b) 0.19 *(h)*	–
Combination of fractures	1a and 1b is the same fracture. 1b is located further to the edge than 1a which, on the upper side, runs through the centre of the sample. The fracture is in an oblique angle.	No fracture on the bottom side
Interpr. mean trace length for flow (m)	0,17	0,091
Fracture type	natural	natural
Flow path length (m)	–	–
Flow path length, calc. (m)	0.104 (h = 0.09)	–

Sample-ID PS0040041

Pressure (bar)	5		10	10*
Time (s)	3,620	3,640	5,645	23
Q (m³/s)	2.762E-07	2.747E-07	1.771E-07	1.71E-07

* Method of measurement with 5 cm rubber hose. Volume 3.93E-06 m³.

Sample-ID PS0040042

Pressure (bar)	5
Time (s)	3,360
Q (m³/s)	0.00E+00

Scanline-ID	No.	Distance from start (mm)	Diameter (mm)	Time (μs)	V_p (m/s)	Comments
LS0040041	0	0	92	15.961	5,764	
	1	2.05	92	15.998	5,751	
	2	4.1	92	16.929	5,434	
	3	6.15	92	–	–	No contact
	4	8.2	92	16.344	5,629	
	5	10.25	92	16.092	5,717	
	6	12.3	92	16.477	5,584	
	7	14.35	92	16.046	5,734	
	8	16.4	92	15.99	5,754	
	9	18.45	92	16.255	5,660	
	10	20.5	92	16.132	5,703	
	11	22.55	92	16.477	5,584	
	12	24.6	92	15.817	5,817	
	13	26.65	92	15.887	5,791	
	14	28.7	93	15.929	5,838	
	15	30.75	94	15.965	5,888	
	16	32.8	95	15.683	6,058	
	17	34.85	96	15.817	6,069	

Value with half length of transmitter, 2.05 cm.

VS0040B06

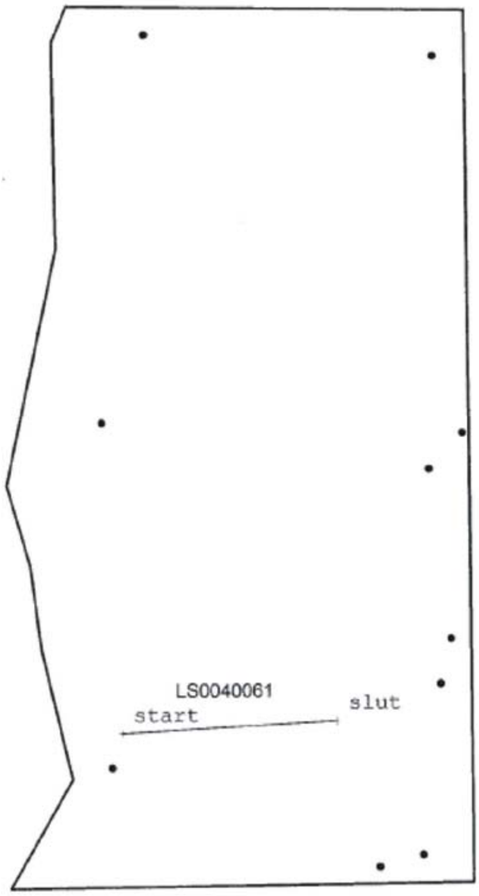

VS0040B06

Scanline-ID LS0040061	No.	Distance from start (mm)	Diameter (mm)	Time (µs)	V_p (m/s)	Comments
	0	0	94.8	16.684	5,682	
	1	2.05	94.8	16.159	5,867	
	2	4.1	92.8	15.952	5,817	
	3	6.15	92.8	16.059	5,779	
	4	8.2	90.5	16.014	5,651	
	5	10.25	90.5	16.346	5,537	
	6	12.3	90.5	16.482	5,491	
	7	14.35	90.5	16.463	5,497	
	8	16.4	90.5	16.225	5,578	
	9	18.45	90.5	16.049	5,639	
	10	20.5	90.5	16.723	5,412	
	11	22.55	90.5	16.013	5,652	
	12	24.6	90.5	15.871	5,702	
	13	26.65	90.5	16.013	5,652	
	14	28.7	90.5	15.956	5,672	
	15	30.75	90.5	16.269	5,563	
	16	32.8	92.5	16.511	5,602	

Value with half length of transmitter, 2.05 cm.

VS0040B07

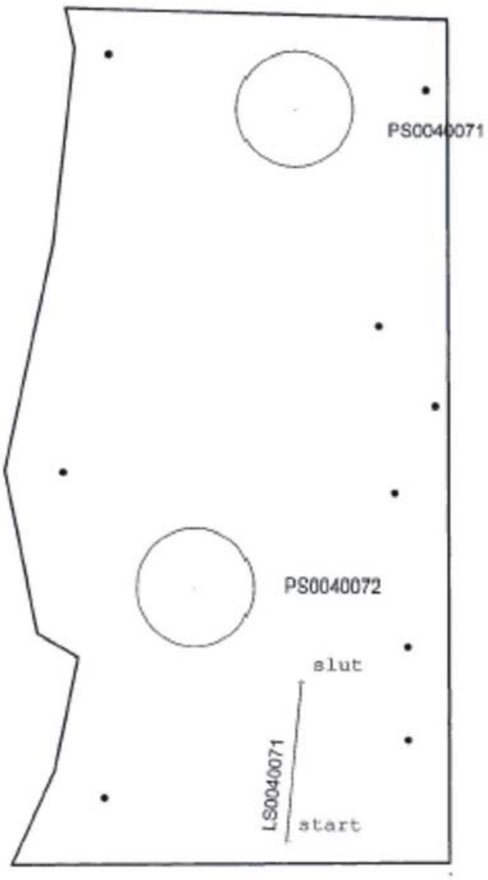

VS0040B07

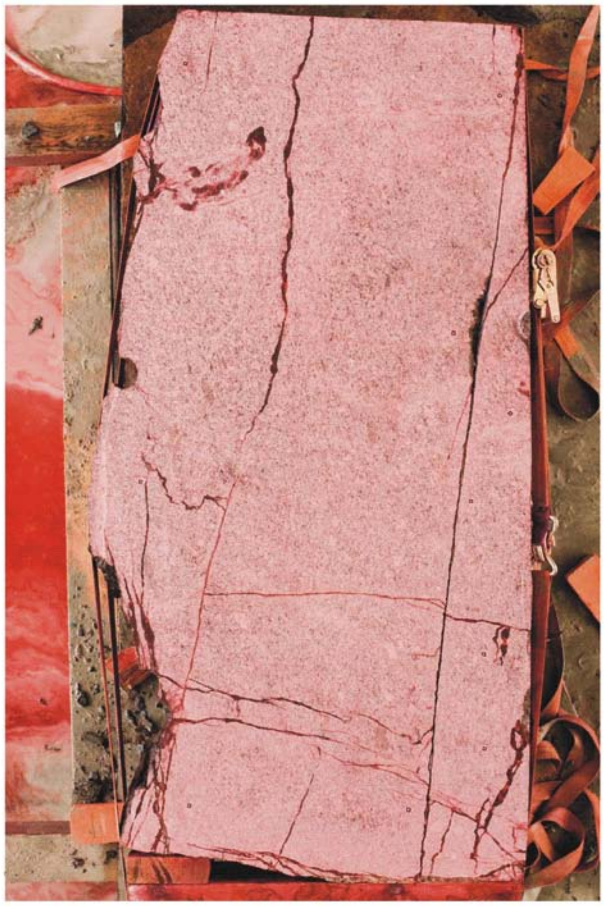

Sample-ID	PS0040071	PS0040072
Air temp (°C)	20 20.6 20.6	20
Water temp (°C)	Room temperature	Room temperature
Sample height (m)	0.09	0.085 m
Dh (mvp) (mvp)	35.1	**1)** 6.5 **2)** 35.1
a) Trace length of fractures, upper side (m) *o – open* *1/2-o: half-open* *c – closed* *h – healed*	1a) 0.195 *(h)*	1a) 0.194 *(1/2-o to c)*
b) Trace length of fractures, bottom side (m) *o – open* *1/2-o: half-open* *c – closed* *h – healed*	1b) 0.115 *(h)* 2 b) 0.15 *(o)* 3b) 0.07 *(h)*	1b) 0.164 *(1/2-o to c)*
Combination of fractures	1a and 1b is the same fracture. 3b is an off-shoot from 1b. 2b does not cross through the sample. It ends on one edge of the sample.	1a and 1b is the same fracture
Interpr. mean trace length for flow (m)	0,155	0,18
Fracture type	–	–
Flow path length (m)	–	–
Flow path length, calc. (m)	–	0.098 (h = 0.085)

Sample-ID PS0040071

Pressure (bar)	5
Time (s)	7,200
Q (m³/s)	0.00E+00

Sample-ID PS0040072

Pressure (bar)	1) 5	2) 5*	2) 10**
Time (s)	4,200	1,075	2,771
Q (m³/s)	0.00E+00	3.6530E-09	4.2515E-10

* Method of measurement with 5 cm rubber hose. Volume 3.93E-06 m^3.

* *Method of measurement with 1.5 cm rubber hose. Volume 1.18E-06 m^3.

Scanline-ID	No.	Distance from start (mm)	Diameter (mm)	Time (µs)	V_p (m/s)	Comments
LS0040071	0	0	91	15.497	5,872	
	1	2.05	91.55	15.322	5,975	
	2	4.1	92.1	15.082	6,107	
	3	6.15	92.65	15.711	5,897	
	4	8.2	93.2	15.548	5,994	
	5	10.25	93.75	15.31	6,123	
	6	12.3	94.3	15.33	6,151	
	7	14.35	94.85	15.858	5,981	
	8	16.4	95.4	16.467	5,793	
	9	18.45	95.95	15.692	6,115	
	10	20.5	96.5	16.387	5,889	
	11	22.55	96.5	–	–	No contact
	12	24.6	96.5	–	–	No contact
	13	26.65	96.5	–	–	No contact

Field investigations in the S-tunnel Äspö HRL. Database

Data and interpreted transmissivities (**Q/Dh**) for all Single Hole Tests in EDZ in TASS-tunnel. Äspö HRL.

Test id	Packer-depth (cm)	Borehole-depth (cm)	Sealed off-interval (m)	Dh (m)	Injected volume (ml)	Duration of test (min)	Q (m^3/s)	Q/Dh (m^2/s)
1_1	7.3	59	0.517	91.9197	116.84	5.0	3.89E-07	4.24E-09
1_2	21.2	59	0.378	89.4672	11.04	40.0	4.6E-09	5.14E-11
2_2	1.9	53	0.511	31.4901	131.1	8.2	2.68E-07	8.51E-09
2_3	14.7	53	0.383	47.3823	1.84	30.0	1.02E-09	2.16E-11
2_4	14.7	53	0.383	96.2361	2.3	15.0	2.56E-09	2.66E-11
3_1	2.3	54	0.517	48.8538	131.1	28.3	7.71E-08	1.58E-09
3_2	2.3	54	0.517	95.0589	123.74	11.4	1.81E-07	1.9E-09
4_1	3.4	53	0.496	19.4238	125.12	0.4	5.44E-06	2.8E-07
4_2	24.5	53	0.285	18.9333	127.88	0.5	4.74E-06	2.5E-07
4_4	30.5	53	0.225	1.7658	33.81	30.0	1.88E-08	1.06E-08
4_5	30.5	53	0.225	31.392	124.2	3.0	6.9E-07	2.2E-08
5_1	2.6	58	0.554	22.563	128.34	2.0	1.07E-06	4.74E-08
5_2	11.2	58	0.468	22.563	124.2	2.0	1.04E-06	4.59E-08
5_3	20.8	58	0.372	22.563	128.3	9.0	2.38E-07	1.05E-08
5_4	31.1	58	0.269	27.7623	0	5.0	0	0
5_5	31.1	58	0.269	13.5378	5.28	10.0	8.8E-09	6.5E-10
5_6	31.1	58	0.269	100.062	1.38	10.0	2.3E-09	2.3E-11
6_2	21.4	52	0.306	24.1326	6.44	10.0	1.07E-08	4.45E-10
6_3	21.4	52	0.306	50.031	35.88	30.0	1.99E-08	3.98E-10
7_1	3.6	60	0.564	22.1706	121.9	10.0	2.03E-07	9.16E-09
8_1	4	60	0.56	14.8131	52.9	4.5	1.96E-07	1.32E-08
8_2	4	60	0.56	20.2086	129.26	17.5	1.23E-07	6.09E-09
9_1	2.3	60	0.577	25.1136	111.78	0.5	3.73E-06	1.48E-07
9_2	10	60	0.5	20.0124	128.8	0.5	4.67E-06	2.33E-07
9_3	24.5	60	0.355	17.1675	131.1	0.4	5.7E-06	3.32E-07
9_4	42.7	60	0.173	21.0915	5.06	10.0	8.43E-09	4E-10
9_5	42.7	60	0.173	51.6987	10.58	10.0	1.76E-08	3.41E-10
10_1	4	52	0.48	21.7782	117.3	2.5	7.82E-07	3.59E-08
10_2	23.7	52	0.283	21.4839	6.9	17.0	6.76E-09	3.15E-10
10_3	23.7	52	0.283	48.6576	34.96	40.0	1.46E-08	2.99E-10
10_4	23.7	52	0.283	99.3753	7.36	3.0	4.09E-08	4.11E-10
11_2	13.8	53	0.392	19.0314	2.76	5.0	9.2E-09	4.83E-10
11_3	13.8	53	0.392	47.8728	32.66	35.0	1.56E-08	3.25E-10
11_4	13.8	53	0.392	92.6064	7.36	3.0	4.09E-08	4.42E-10

Characterisation of micro cracks in EDZ

TEST REPORT

Date	Reference	Page
2009-09-03	P803489	2 (8)

CBI Betonginstitutet

Handled by
Urban Åkesson
Material, Borås
010-516 51 48, Urban.Akesson@cbi.se

Chalmers Tekniska Högskola
Lars O Ericsson
412 96 GÖTEBORG

Characterisation of micro cracks in EDZ

Commission

The commission include characterisation of micro cracks on drill cores drilled from rock slabs, taken from EDZ.

Specimen data and sample preparation

Five specimens have been analysed, three specimens are oriented perpendicular to the tunnel wall (H-specimen) and the other two are oriented parallel to the tunnel wall (V-specimen).

Specimen	Relation to the tunnel wall
H1 C	Far
H1 D	Middle
H1 E	Far
V1 A	Close
V1 B	Far

The specimens were cut into two half and one thin section, oriented parallel to the drill-core axis was made from each specimen. To detect the micro cracks, the specimen was vacuum impregnated with epoxy containing fluorescent dye.

Results

The thin sections show that the analysed rock type is extremely few existing micro cracks. This is mainly due to the extensive alteration of feldspars and the relatively low content of quartz. Normally, existing micro cracks appears in grain boundaries and as intragranular cracks in the crystal planes within the minerals.

Blast induced micro cracks appears in all specimens except V1 B, but they very few so no quantitative analyses have been possible to do. Most of the micro cracks are old sealed cracks that have been reopened after the blast. Just in a few specimens have new micro cracks formed, and these cracks are transgranular (cutting several minerals).

Specimen H1 C

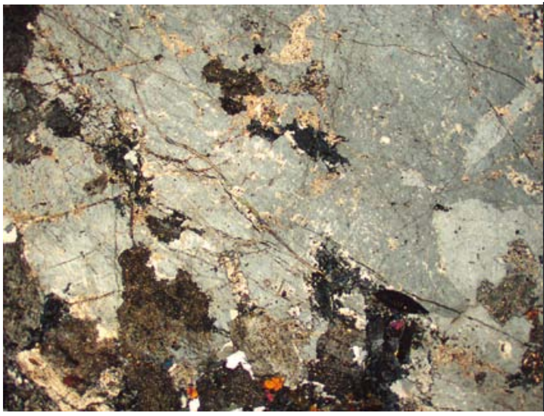

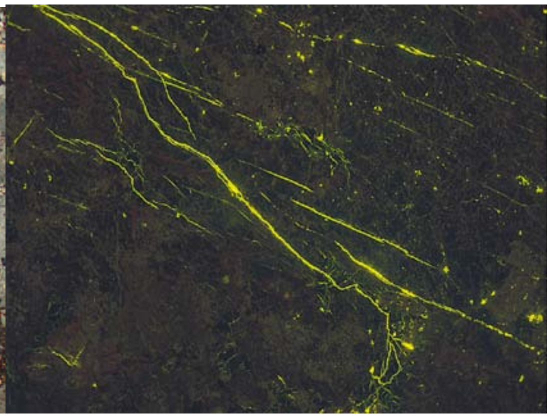

The figures show a feldspar crystal from specimen H1 C in polarised and fluorescent light, the image size is 5.5 x 4.2 mm. Here it is possible to see that the open micro cracks mainly are related to old sealed micro cracks, a few new micro cracks have also been formed. The image below is a combined fluorescent and polarised image.

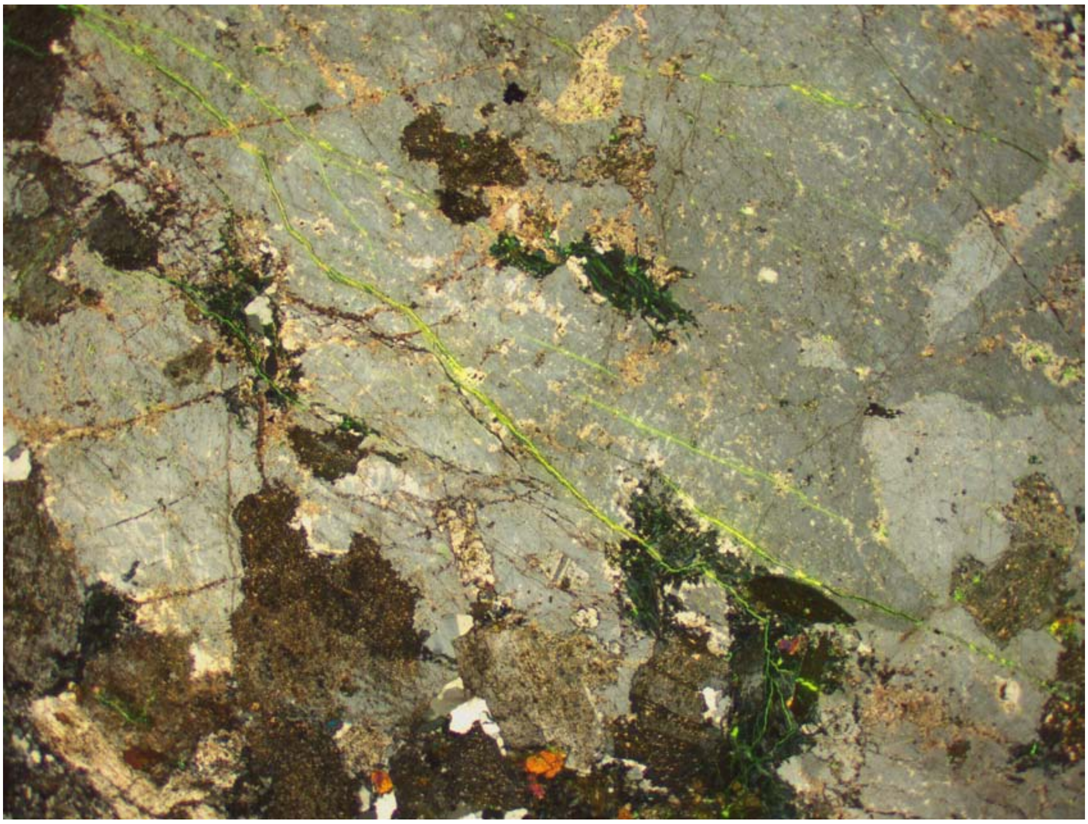

Specimen H1 D

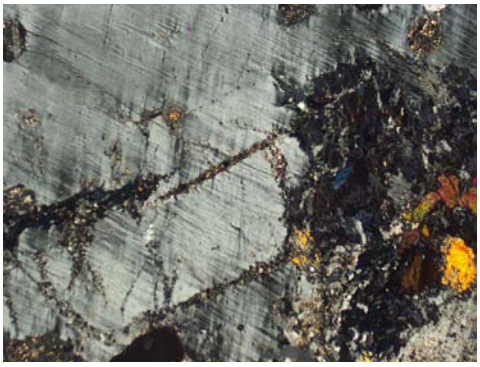 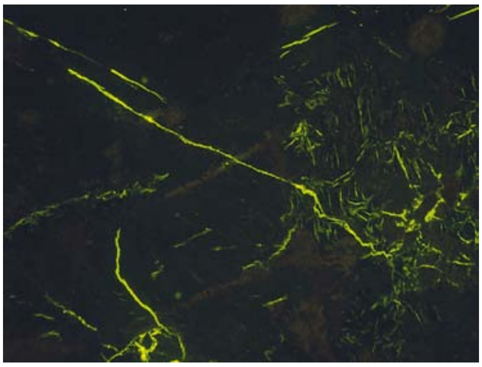

The figures of specimen H1 D also shows a feldspar crystal in polarised and fluorescent light. The image size is 2.8 x 2.1 mm. The combined image below shows that it is an old crack who has reopened and propagate into a matrix of iotite and epidote.

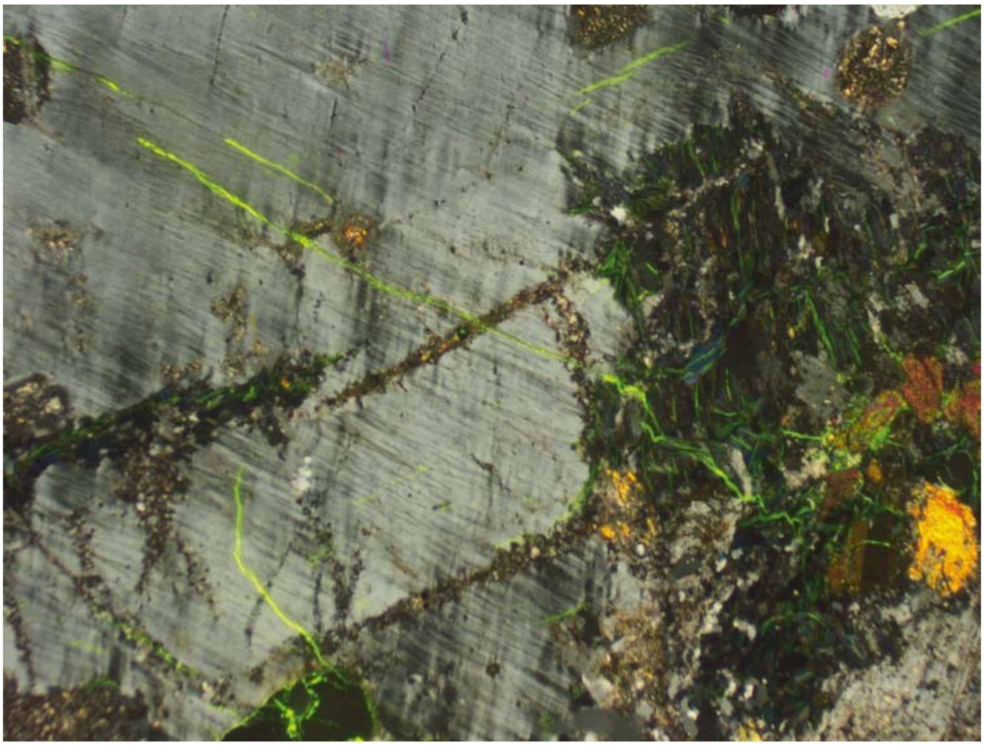

Specimen H1 E

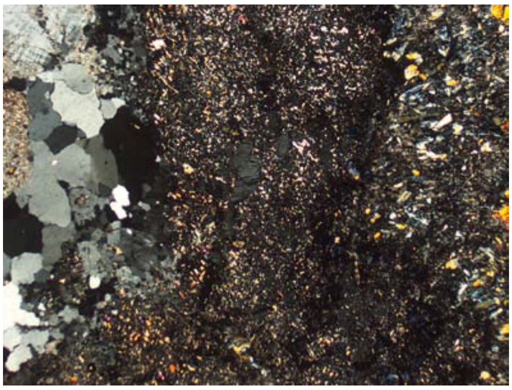 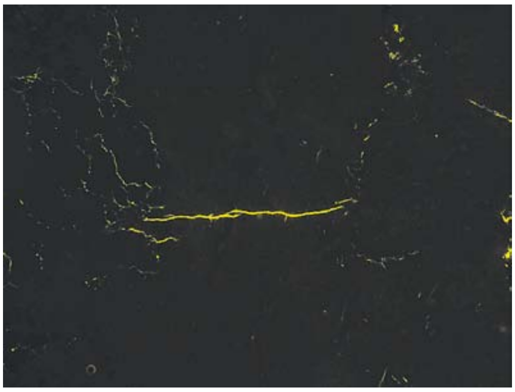

The figures show specimen H1 E in polarised and fluorescent light. The image size is 2.8 x 2.1 mm. The combined image below show a newly formed transgranular crack.

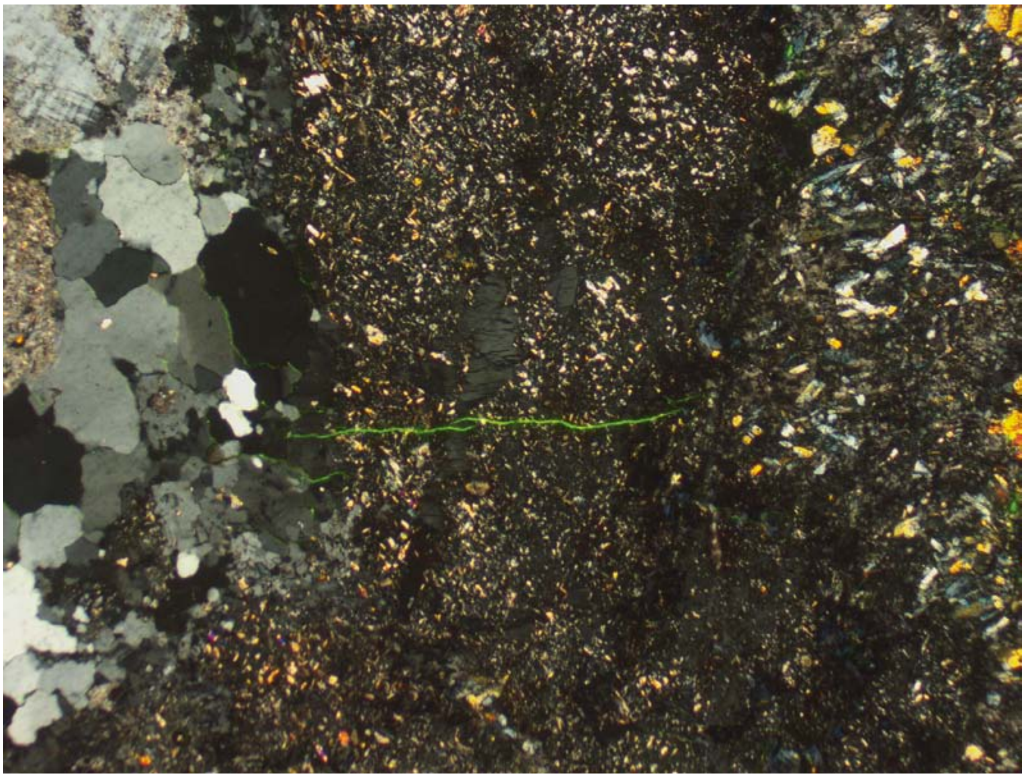

Specimen V1 A

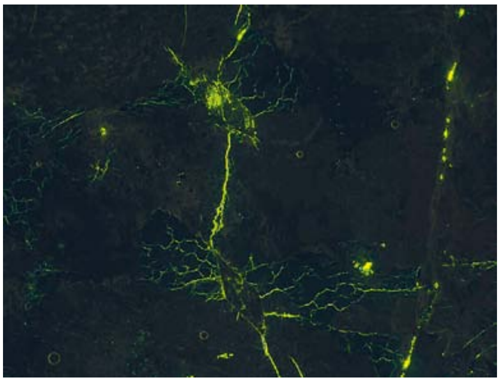

The figures show specimen V1 A in polarised and fluorescent light, and a combined image below. The image size is 5.4 x 4.2 mm. The images show an example how a transgranular crack have formed between two titanite grains who has a higher e-modulus compared to the surrounding minerals.

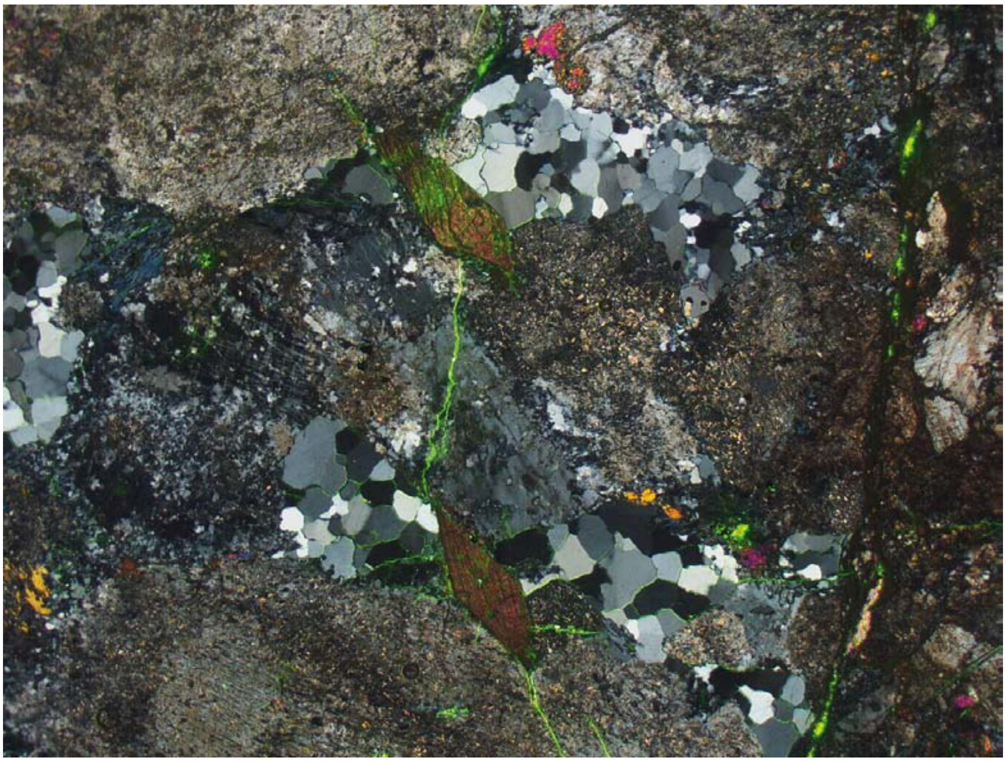

Specimen V1 B

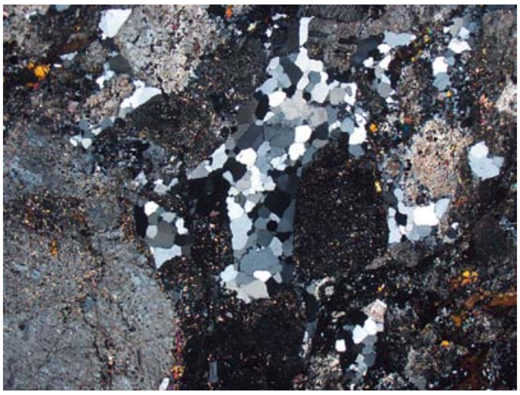

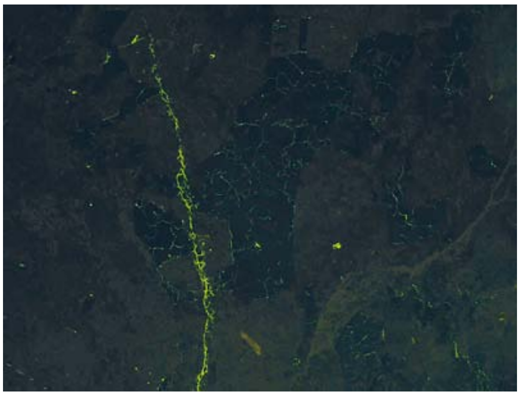

The figures show specimen V1 B in polarised and fluorescent light, and a combined image below. The image size is 5.4 x 4.2 mm. This open system of grain boundary micros cracks are probably existing micro cracks. If it had been blast induced crack it should occur as transgranular crack cutting all the crack-filled minerals.

CBI Swedish Cement and Concrete Research Institute
Material - Materials, Borås

Urban Åkesson
Technical Manager/Officer

Appendix 5

Investigation of natural fracture traces used in EDZ 3D-model

Sara Kvartsberg, Chalmers University of Technology, October 2009

A5.1 Introduction

A5.1.1 Background

To increase the understanding of Excavation Damage Zone (EDZ) in tunnels, a project was initiated to examine a section of the wall in the TASS-tunnel and create a 3D-model of the fractures in this section. The examination was performed by cutting slabs from a section of the wall, spray a dye penetrant on the surfaces to make the fractures appear clearly, digitize the fractures appearing on the photographs and create a 3D-model of those fractures.

The test section was 8 m long, 1.5 m high and 0.7 m deep. Eight blocks were excavated, and from these a total of 75 slabs were wire sawed. The penetrant fluid was able to detect fractures down to 20 µm and the visible fractures were vectorized, generating 2D DWG-files as output. The vectorized fractures were then moved to MicroStation®/RVS where a 3D-model was made and the fracture traces were connected into undulating fracture planes. A number of fracture traces were only found once in the slabs and in order to get a complete model regarding the number of fractures, these single fracture traces were modelled simplified as rectangular planes /Olsson et al. 2009/.

All modelled fractures were classified into three different types of fractures: direct blast induced fractures, induced fractures and natural fractures. Direct blast-induced fractures are fractures formed by the blasting process and these fractures originate from the borehole. Induced fractures are also caused by the blasting although they do not originate from the borehole itself. Natural fractures are fractures that existed in the rock before the blasting /Olsson et al. 2008/. In the 3D-model, created for this section of the TASS-tunnel, there are a total of 1,223 modelled fractures. Of these, 777 are modelled natural fractures, 261 direct blast-induced fractures and 185 induced fractures.

A5.1.2 Scope of the study

The purpose of this project "Investigation of natural fracture traces used in EDZ 3D- model" was to perform a more detailed study of the condition of the natural fracture traces used in the 3D-model mentioned above. In this investigation, the EDZ slabs excavated from the TASS-tunnel in 2008 were surveyed with the intention to classify these natural fractures into **open** fractures, **healed** fractures and **tight/closed** fractures. Other fracture characteristics, such as mineral fillings, were investigated to some extent.

Information concerning the length of the all the fracture traces in the 2D DWG-files has also been used in this project to obtain length distributions of the natural-, induced- and direct blast-induced fractures modelled in the 3D-model.

A5.2 Method

The methodology used in this investigation comprised the following steps: use the 2D DWG-files for the identification of natural fractures, survey these fractures on the slabs, update information of the natural fractures in the 3D model and compile this information with together with the fracture length statistics.

A total of 75 slabs were examined. These slabs are labelled with a number from which of the eight blocks they originated (named 36 to 43) and a number describing their position in the block (1 to 10). The slabs are about 1.5 m high, 0.7 m wide and 0.1 m deep and are stored in a machine hall near the entrance to the Äspö underground laboratory. In order to identify the natural fractures used in the 3D-model on the surface of the slabs, 2D DWG-files with vectorized fractures were used; see an example of these DWG-files in Figure A5-1. A total of 1,801 natural fractures were, if possible, to be examined with the purpose to classify these into one of the following categories: open fractures (partly or wide open fractures), healed fractures (closed with mineral fillings) and tight fractures (closed with no visible mineral filling). Also fracture properties such as mineral fillings and oxidation were studied to some extent.

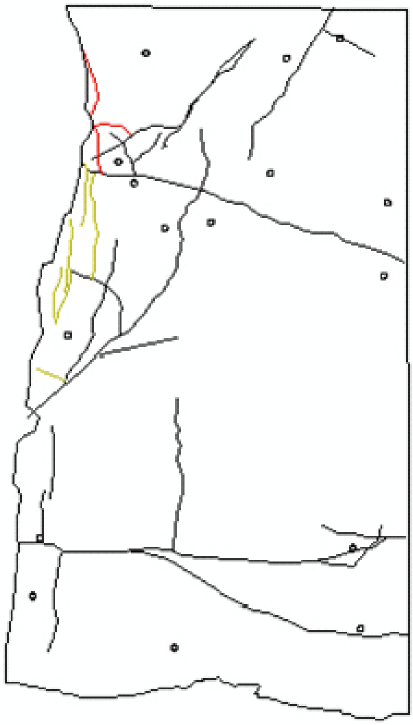

Figure A5-1. *Digitized slab surface with fractures, 36B-05. Natural fractures are black.*

The information obtained from the survey was then incorporated into the 3D model. The 1,801 natural fracture traces from the slab surfaces corresponds to 777 natural fractures in the 3D model, since many traces were connected into undulating fracture planes. Natural fractures modelled from fractures traces found in several slabs have the prefix **N** followed by a serial number starting from 001 and running upwards in the order they were modelled. Fractures found in several slabs are also called "large" fractures. Natural fractures modelled from single fracture traces have the prefix **n** followed by a serial number starting from 501 and running upwards in the order they were modelled /Olsson et al. 2009/. These single trace fractures are also called "small".

The classification of n-fractures came from a single observation, but in the classification of N-fractures, several observations were combined into one resulting description. The result from the survey can be found in appendix 6. In the cases when the survey gave contradictive observations about the N-fractures, the most frequent observation, or a combination of them, were used. An example of this could be an N-fracture surveyed as open in two slabs, and healed in a third. The combined picture gives an open fracture and this is how it is modelled, although it could be healed in some parts. The fractures surveyed as open were coloured blue in the 3D model, the healed were coloured green and the tight fractures grey.

The length of all the fracture traces identified in slabs was measured when creating the 2D DWG-files in the investigation performed by /Olsson et al. 2009/. This length information has been used in this project to compile length distributions for the natural fractures (open, healed or tight) but also to compare the distribution for direct blast-induced, induced- and natural fractures. Since the length information was given for the 2,509 fracture traces on the slabs, the lengths had to be converted to somehow match the 1,223 modelled fractures. The length of each modelled fracture is therefore described by the longest fracture trace from which the fracture plane originates.

A5.3 Result

The result from this project is separated into two parts; in the first part the classification of natural fractures originating from the survey of the slabs is presented. This includes distributions of open, healed and tight fractures and a revising of the natural fractures in the 3D-model. In the second part, results from the length distribution of the fractures are presented.

A5.3.1 Classification of natural fractures

A total number of 777 natural fractures are modelled as planes in the 3D model. After the survey, 713 of these could be classified into *open*, *healed* or *tight* fractures; see Table A5-1. Information was missing for 64 fractures due to broken slabs or other difficulties in finding them. As can be seen in Figure A5-2, most of the unknown fractures are n-fractures.

Table A5-1. Classification of natural fractures.

Classification	All fractures	N-fractures	n-fractures
Open	214 (28%)	176 (41%)	38 (11%)
Healed	261 (34%)	158 (37%)	103 (29%)
Tight	238 (31%)	79 (19%)	159 (45%)
Unknown	64 (8%)	13 (3%)	51 (15%)
Total	777 (100%)	426 (100%)	351 (100%)

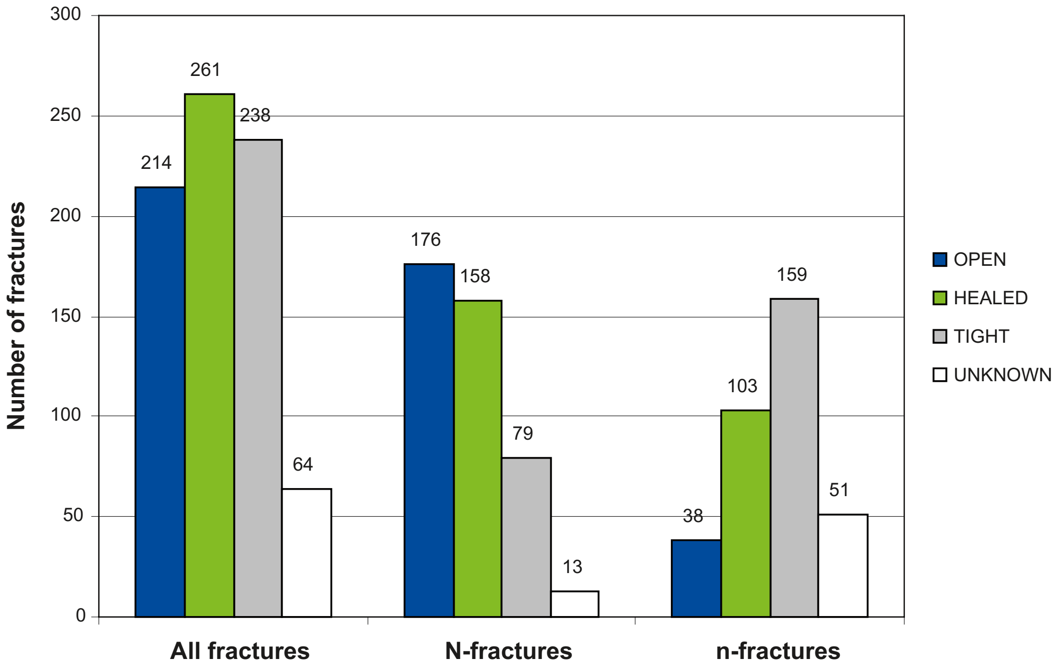

Figure A5-2. *Classification of all natural fractures, and with a separation into N-fractures and n-fractures.*

The natural fractures were reclassified in the MicroStation®/RVS 3D-model, a model which describes the fractures in an 8 m long section of the TASS-tunnel wall. In Figure A5-3 to A5-5, fracture planes are shown together with the blast holes and the 75 slab outlines. In Figure A5-3 all 1,223 modelled fractures are shown, with open fractures coloured in blue, healed fractures in green and tight fractures in grey. Direct blast-induced fractures are shown in red and induced fractures in yellow. In Figure A5-4 only the natural fractures are shown and in Figure A5-5, only "large" fractures are displayed.

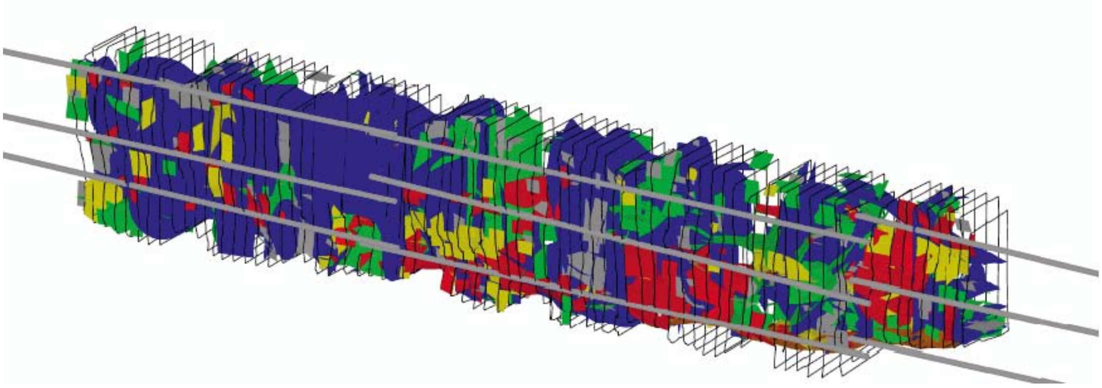

Figure A5-3. *All modelled fractures, slab outlines and blast holes. Natural fractures are either open (blue) healed (green) or tight (grey). Direct blast-induced fractures are displayed in red and induced fractures in yellow.*

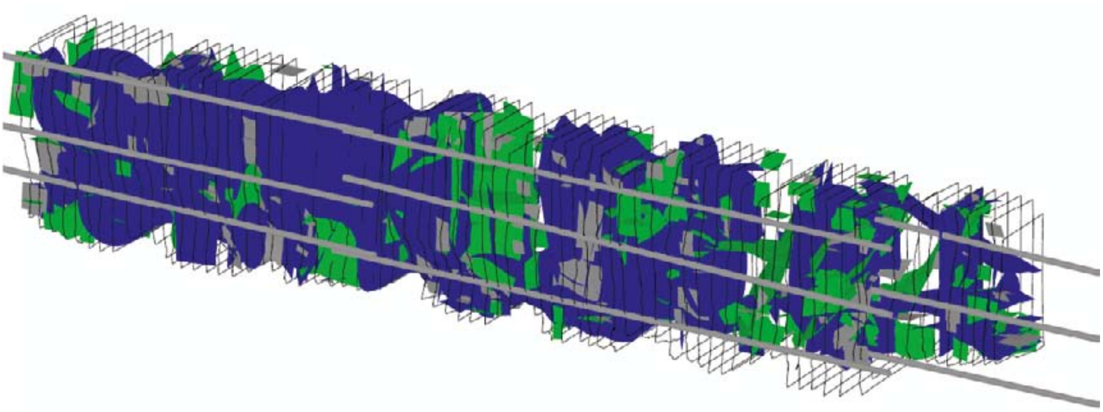

Figure A5-4. *Open (blue), healed (green) and tight (grey) fractures.*

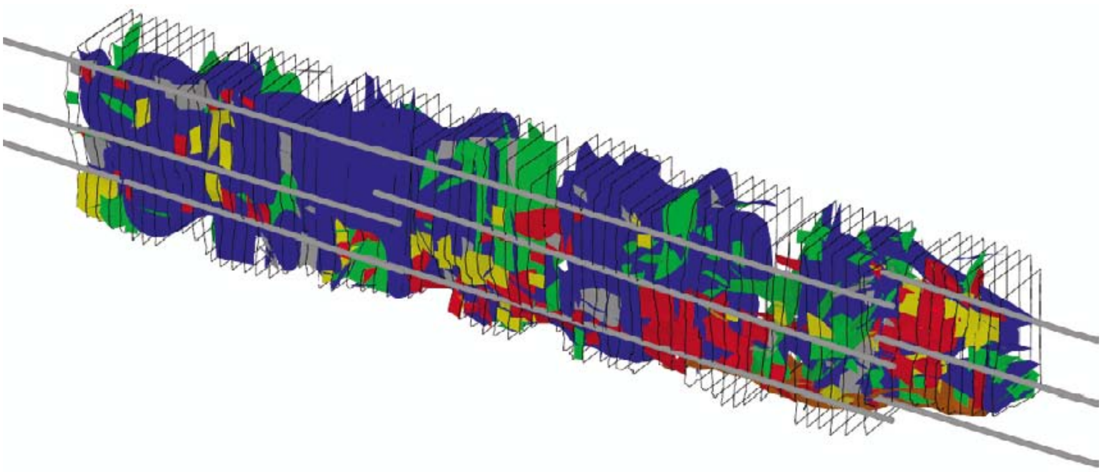

Figure A5-5. *Only "large" fractures.*

A5.3.2 Length distribution of fractures in the 3D-model

The length information of the fractures traces have been used to create length distributions for the fractures in the 3D-model. The length of each modelled fracture is described by the longest fracture trace that describes the fracture plane. In the first part of this section, the fractures are only described as natural, direct blast-induced or induced. In the second part, the natural fractures are also described by the classification into open, healed or tight fractures.

Distribution of natural-, direct blast-induced and induced fractures

There are a total of 1,223 fractures in the 3D-model. Length information is found for 1,187 of these, see Table A5-2.

The fractures with length information have been divided into six length categories; < 15 cm, 15–30 cm, 30–45 cm, 45–60 cm, 60–75 cm and < 75 cm. The upper limit is set because the slabs are around 70–80 cm wide. The length data can be found in Appendix 7. As can be seen in Figure A5-6, which displays the fractures divided into the above mentioned length categories; most fractures have a maximum fracture length of less than 15 cm.

If the fractures are separated in "large" and "small" fractures, as in Figure A5-7, it can be seen that almost all of the small fractures are less than 30 cm.

Table A5-2. Fractures in 3D-model with length information assigned, separated in large and small fractures for natural-, direct blast-induced and induced fractures.

Description	Natural fractures	Direct blast-induced fractures	Induced fractures
Large fractures	417 (54%)	163 (62%)	97(53%)
Small fractures	338 (43%)	92 (35%)	80 (43%)
No information	21 (3%)	6 (3%)	8 (4%)
Total	777	261	185

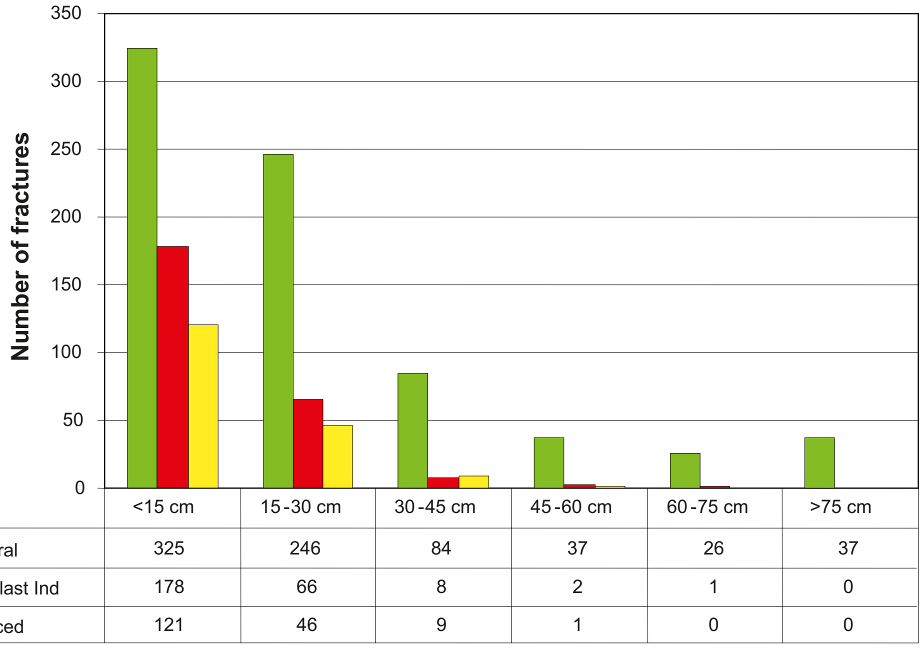

Figure A5-6. Length distribution of natural (green), direct blast-induced (red) and induced (yellow) fractures in the 3D-model.

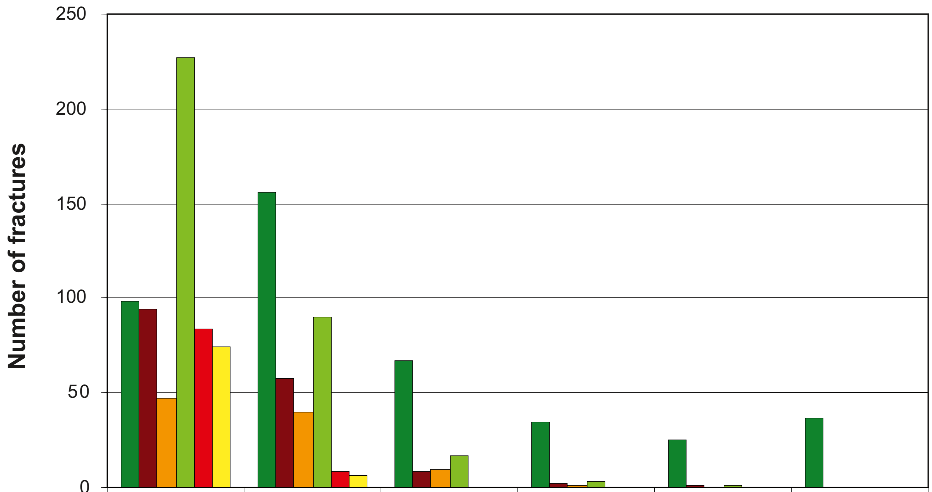

	<15 cm	15-30 cm	30-45 cm	45-60 cm	60-75 cm	>75 cm
Natural "large"	98	156	67	34	25	37
Dir Blast "large"	94	58	8	2	1	0
Ind. "large"	47	40	9	1	0	0
Natural "small"	227	90	17	3	1	0
Dir Blast "small"	84	8	0	0	0	0
Ind. "small"	74	6	0	0	0	0

***Figure A5-7.** Length distribution of natural, direct blast-induced and induced fractures, separated in large and small fractures.*

Distribution of natural fractures classified into open, healed and tight

Of the 777 natural fractures in the model, 713 of them were possible to classify into open, healed and tight. Fracture traces with length information given from the previous investigation was found for 685 of these, see Table A5-3. Figure A5-8 shows the length distribution of these natural fractures with respect to their classification, and in Figure A5-9, direct blast-induced and induced fractures have been included. The length data for the sorted natural fractures can be found in Appendix 8.

Table A5-3. Natural fractures in the 3D-model with length information, separated into open, healed and tight fractures.

Description	Open fractures	Healed fractures	Tight fractures
Large fractures	169 (79%)	154 (59%)	74 (31%)
Small fractures	37 (17%)	100 (38%)	151 (63%)
No information	8 (4%)	7 (3%)	13 (5%)
Total	214	261	238

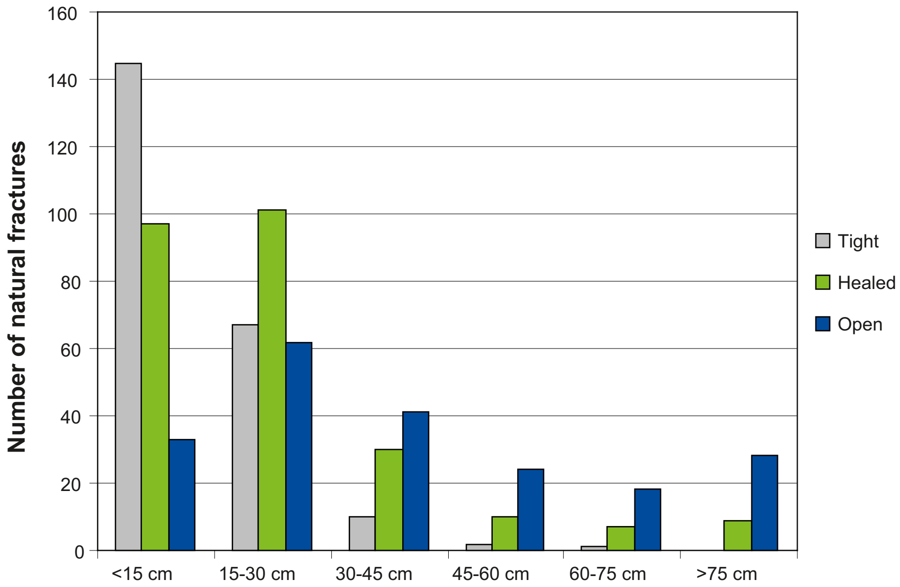

Figure A5-8. *Length distribution of natural fractures, separated into tight, healed and open fractures.*

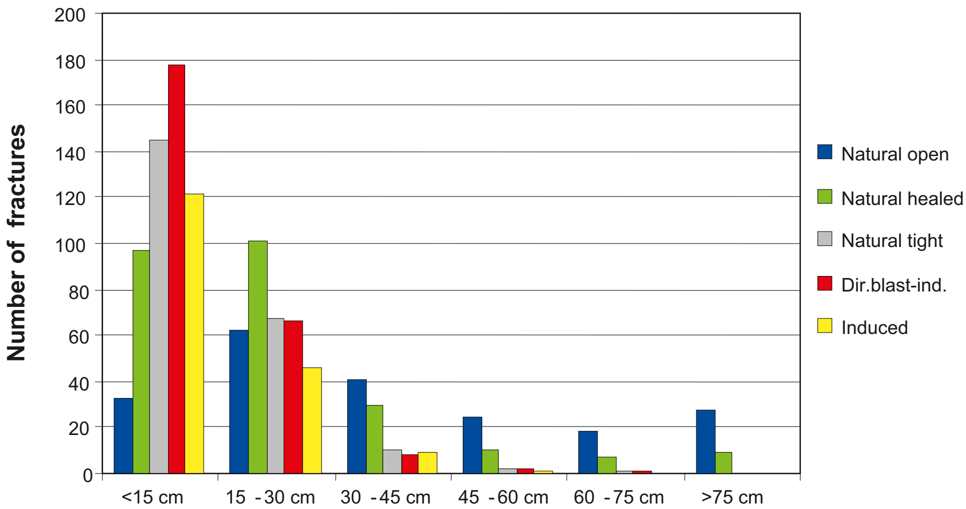

Figure A5-9. *Length distribution with natural fractures (separated into open, tight and healed), direct blast-induced fractures and induced fractures.*

A5.4 Discussion

It was possible to find the natural fractures in the slabs by using the 2D DWG-files and then convert the results of the survey into a classification of the natural fractures in the 3D-model. Describing a natural fracture as either open, healed or tight can give useful information about the fracture and this property can be determined quite easily.

The conditions for the survey were somewhat restricted because the slabs used in this study were over one year old, and in some cases damaged with pieces missing. About eight percent of the fractures used in the model were not found in the survey of the slabs. Some slabs were heavily coloured from the earlier use of penetrant, making it hard to survey mineral fillings, which means that some of fractures classified as tight fractures could have had small amounts of mineral fillings and should therefore have been classified as healed. Some of the "large" fractures (existing in several slabs) were surveyed with contradictive observations; the fracture could be described as open in one slab and healed in another. An interpretation of the results had to be made, which introduced even more uncertainty to the final classification result.

Another aspect mentioned in earlier investigations is the fact that the tight and healed natural fractures only were modelled to some extent because of shortcomings in the penetration and vectorization. Fractures visible on the slabs were not included in the 3D-model because they were not penetrated and visible on the photographs or they were lost in the vectorization process. As a result, the proportion of open fractures in this study can be expected to be larger than the actual proportion. The fractures could also have been influenced by the transportation process, which could have open up old fractures that were healed *in situ*.

References

Olsson M, Markström I, Pettersson A, 2008. Methodology study for documentation and 3D modelling of blast induced fractures. SKB R-08-90, Svensk Kärnbränslehantering AB.

Olsson M, Markström I, Pettersson A, Sträng M, 2009. Examination of the Excavation Damaged Zone in the TASS tunnel, Äspö HRL. SKB R-09-39. Svensk Kärnbränslehantering AB.

Appendix 6

Survey of natural fractures in EDZ slabs

HEALED	158	37%
TIGHT	79	19%
UNKNOWN	13	3%

n-fractures

TOTAL	351	
OPEN	38	11%
HEALED	103	29%
TIGHT	159	45%
UNKNOWN	51	15%

Mapping form

Mapping form is influenced by the *Tunnel Mapping System TMS*

Descriptions:

Open - Truly open natural fracture
Healed - Closed natural fracture with fracture filling

Tight - Closed natural fracture without fracture filling

Classification confidence:

A - Certain
B - Probable

Fracture filling:

CL - Chlorite
PR - Prehnite
QZ - Quartz
RF - Red feldspar
EP - Epidote
CA - Calcite
OX- Oxidation around fracture
XX - Unidentified filling

FRACTURE-ID RVS-MODEL	LENGTH OF FRACTURE[m]	OPEN	HEALED	TIGHT	MINERAL FILL	MINERAL1	MINERAL2	MINERAL3	MINERAL4	MINERAL5	REMARK
N001	0.6306	B			Y	CL	PR	EP	CA	OX	
N002	0.5063	B			Y	EP	CA				
N003	0.8116	B			Y	CL	CA	PR			
N004	0.6234	B			Y	PR	CA	CL	EP		
N005	0.6577	B			Y	CL	PR	CA	EP	OX	
N006	0.6473	B			Y	PR	CL	CA			
N007	0.0689	B			Y	PR	EP	OX			
N008	0.2059	B			Y	PR	EP	CL			
N009	0.1195		A		Y	CL					
N010	0.2489		A		Y	EP	CL				
N011	0.3625		A		Y	EP	CA	CL	PR	OX	
N012	0.0716		A		Y	CL					
N013	0.2998		A		Y	CA	CL	OX			
N014	0.2409	B			Y	PR	CL	CA			
N015	0.241	B			Y	CA	CL	RF			
N016	0.2481		B		Y	CL	CA	OX			
N017	0.6038		A		Y	EP	CL	OX			
N018	0.2516		A		Y	PR	QZ				
N019	0.8175	B			Y	CL					

FRACTURE-ID RVS-MODEL	LENGTH OF FRACTURE[m]	OPEN	HEALED	TIGHT	MINERAL FILL	MINERAL1	MINERAL2	MINERAL3	MINERAL4	MINERAL5	REMARK
N020											No information
N021											No information
N022											No information
N023	0.6258		A		Y	EP	CL	OX			
N024	0.9106		A		Y	CL	EP	OX			
N025	0.941		A		Y	CL	EP	PR	CA	OX	
N026	0.6829		A		Y	EP	CL	OX	CA		
N027	0.2885			A	N						
N028	0.2726	B			Y	CL					
N028b	0.1859	B			Y	CL	PR				
N029	0.2544		B		Y	CL					
N030	0.3316			A	N						
N031	0.5179	B			Y	CL	PR				
N032	0.3806		A		Y	CL	PR				
N033	0.308	B			Y	CL					
N034		B			Y	CL	PR				
N035	0.2165		A		Y	CA	RF	OX			
N036	0.3488		A		Y	CL	PR	EP	CA	OX	
N037	0.2695		A		Y	CL					
N038	0.2195	B			Y	CL	PR				
N039	0.258		A		Y	PR					
N040	0.3964		A		Y	EP	CL	CA			
N041	0.2446		A		Y	CL	OX				
N042	0.0908		A		Y	CL	PR	EP	OX	CA	
N043	0.1633	B			Y	CL					
N045	0.344		A		Y	CL					
N046	0.1819		A		Y	CL	PR				
N048	0.1881		A		Y	CA					
N049				B	N						
N050	0.1284			A	N						
N052	0.0859		A		Y	CL					
N053	0.3015	B			Y	CL	CA	PR			
N055	0.1023		A		Y	EP					
N056	0.1084			A	N						
N057	0.296			A	N						
N058	0.2009	B			Y	CL					
N059a	0.7342	B			Y	CL	CA				
N059b	0.1371			A	N						
N060	0.2356		A		Y	CL					
N061	0.223		A		Y	RF	OX				
N062a	0.2233		B		Y	EP	CL				
N062b	0.3559	B			Y	EP	OX	CL			
N063a			A		Y	CL					
N063b	0.2189		A		Y	CL	PR				
N064	0.2825			A	N						
N065	0.1612			A	N						
N066	0.082		B		Y	CL					
N067			B		Y	CL	PR				
N068		B			Y	CL					
N069			B		Y	CA	PR				
N070		B			Y	CL	PR				
N071				A	N						
N072	0.0959		A		Y	CA	CL				
N073	0.2061			A	N						
N074	0.0925		A		Y	EP					
N075l	0.2195	B			Y	CL					
N075u	0.2892		A		Y	CL					
N076	0.544		A		Y	EP	CL	OX			
N077	0.4062		A		Y	EP					
N078				A	N						
N079			A		Y	CL	PR				
N080	0.231		A		Y	PR	CL	CA			
N081	0.1153		A		Y	CL	EP				
N082	0.4841		A		Y	PR	CL	OX			

FRACTURE-ID RVS-MODEL	LENGTH OF FRACTURE[m]	OPEN	HEALED	TIGHT	MINERAL FILL	MINERAL1	MINERAL2	MINERAL3	MINERAL4	MINERAL5	REMARK
N083	0.1574			A	N						
N084	0.0294		A		Y	EP					
N085	0.2066		A		Y	RF	OX				
N086	0.0811			A	N						
N087	0.527	B			Y	CL					
N088a											No information
N088b											No information
N089	0.1741	B			Y	CL	PR	EP			
N090	0.0549			A	N						
N091	0.1316			A	N						
N092	0.2171		B		Y	CL	CA				
N093	0.1269		A		Y	PR	CL				
N094	0.0691		A		Y	CL					
N095	0.2274	B			Y	EP	PR	CA	CL	OX	
N096	0.2645		A		Y	PR	CL				
N097	0.1677		A		Y	PR	CL				
N098	0.37	B			Y	CA	CL				
N099	0.2191		B		Y	CL	EP				
N100	0.2218		A		Y	OX					
N101	0.1683			A	N						
N102	0.1033		A		Y	OX					
N103	0.8208		A		Y	EP	CA				
N104	0.2358	B			Y	CL					
N105	0.2738	B			Y	CL					
N106	0.1545		A		Y	CL					
N107	0.2793		A		Y	EP					
N108	0.1472		A		Y	EP	OX				
N109	0.3196		A		Y	CL	PR				
N110	0.1707			A	N						
N111	0.2191		B		Y	EP					
N112	0.0872		A		Y	CL	PR				
N113l	0.5102	B			Y	CL	PR	CA			
N113u	0.6514	B			Y	PR	CL	EP			
N114l	0.3122		A		Y	CA					
N114u	0.339			A	N						
N115	0.4063			A	N						
N116	0.5656		A		Y	RF	CA	OX			
N117	1.5241	B			Y	CL	PR	OX			
N118	1.566	B			Y	PR	CL	CA			
N119	0.3422		A		Y	CA	CL	RF	OX		
N120	0.405	B			Y	CA					
N120b	0.1098		A		Y	CA					
N121	0.7836	B			Y	CL	PR	CA			
N122	0.3146		A		Y	CL	EP	OX			
N123	0.6666		A		Y	CA					
N124	0.4406		B		Y	CA					
N125	0.2925			A	N						
N126	0.117	B			Y	CA	OX				
N127	0.1677		A		Y	CL					
N128	0.1213		B		Y	CL	OX				
N129	0.2623	B			Y	CL	PR				
N130	0.2751		A		Y	PR					
N131	0.1373		B		Y	CL					
N132	0.3422		B		Y	EP					
N133	0.6954	B			Y	CL	PR	CA			
N134	0.7835	B			Y	CL	PR				
N135	1.7463	B			Y	CA	PR				
N136	0.4915	B			Y	CL	PR				
N137	0.4207		A		Y	PR	CL	CA			
N138	0.5374	B			Y	CL	PR	CA			
N139	0.0577		A		Y	CL					
N140	0.0468			A	N						
N141	0.1581		A		Y	RF					
N142				A	N						

FRACTURE-ID RVS-MODEL	LENGTH OF FRACTURE[m]	OPEN	HEALED	TIGHT	MINERAL FILL	MINERAL1	MINERAL2	MINERAL3	MINERAL4	MINERAL5	REMARK
N143	0.2792		A		Y	EP					
N144	0.1278	B			Y	CL					
N145	0.1054		A		Y	EP	CL				
N146	0.1038	B			Y	CL	PR				
N147	0.0839		B		Y	PR					
N148	0.1959	B			Y	CL					
N149	0.118		A		Y	CL	CA				
N150	0.3815		A		Y	CL					
N151	0.2963		A		Y	CA	PR				
N152	0.3826		A		Y	RF	CA	OX			
N153	0.2667			A	N						
N154	0.2451	B			Y	PR	CL				
N155	0.1979		A		Y	CA					
N156	0.2823	B			Y	CL					
N157	0.2951		A		Y	CL					
N158	0.1866		B		Y	PR					
N159	0.2409	B			Y	PR	CL				
N160	0.2206		A		Y	PR					
N161	0.2769	B			Y	CA	CL	OX			
N162	0.1486	B			Y	PR					
N163	0.1407			B	N						
N164		B			Y	CA	CL				
N165	0.3431	B			Y	PR	CL	CA			
N166	0.7602		A		Y	RF	CA	OX			
N167	0.411		A		Y	CL	CA				
N168	0.4415	B			Y	KL					
N169	0.7335	B			Y	CL	PR	CA			
N170	0.3706	B			Y	CL					
N171	0.8552	B			Y	CL	EP				
N172	0.4669	B			Y	CL	PR	CA			
N173	0.8609	B			Y	CL	EP	PR	CA		
N174	0.6435	B			Y	CL	PR	EP	CA	OX	
N175	0.7801	B			Y	CL	CA	OX			
N176	0.2323	B			Y	EP	PR	OX	CL		
N177	0.4016	B			Y	CL	PR				
N178	0.6651	B			Y	CA	CL				
N179	0.2127			A	N						
N180	0.0671	B			Y	PR					
N181	0.2827			A	N						
N182	0.3993		B		Y	PR	CA				
N183	0.1443			A	N						
N184	0.1241			A	N						
N185	0.4297	B			Y	CL	PR	CA			
N186	0.2201			A	N						
N187	0.1751		A		Y	CA					
N188	0.1227			A	N						
N189	0.4383	B			Y	CL	PR	OX			
N190	0.5887		A		Y	CL					
N191l	0.62	B			Y	CL	PR	EP	CA		
N191u	0.764	B			Y	CL	CA				
N192	1.4828	B			Y	CL	PR	EP	CA		
N193	1.4508		A		Y	EP	CL	PR			
N194	1.2449		A		Y	EP	PR	CL			
N195	0.4034			A	N						
N196	0.2864	B			Y	CL	OX	FE			
N197	0.6557		A		Y	CL	EP	PR	OX		
N198	0.08		A		Y	CL					
N199	0.5858	B			Y	CL	OX				
N200	0.1855		B		Y	CL	EP				
N201	0.1918		A		Y	CL	OX				
N202	0.2517	B			Y	CL					
N203	0.1129		B		Y	EP					
N204a	0.1433			A	N						
N204b	0.2164		A		Y	CL	RF	OX			

FRACTURE-ID RVS-MODEL	LENGTH OF FRACTURE[m]	OPEN	HEALED	TIGHT	MINERAL FILL	MINERAL1	MINERAL2	MINERAL3	MINERAL4	MINERAL5	REMARK
N205				A	N						
N206	0.2964	B			Y	CL					
N207	0.2809		A		Y	PR					
N208											No information
N209	0.0993			A	N						
N210											No information
N211	0.199		A		Y	CL	PR				
N212	0.2565	B			Y	PR					
N213	0.0808		A		Y	PR					
N214		B			Y	CL					
N215	0.1198	B			Y	CL	CA				
N216	0.2208		A		Y	CL	PR				
N217	0.5068	B			Y	CL	PR	EP	CA		
N218	0.1564			A	N						
N219	0.1297			B	N						
N220	0.2953		A		Y	KL	OX	PR	KA		
N221	0.3517	B			Y	CL					
N222	0.2248	B			Y	CL	EP				
N223	0.5554	B			Y	CL	PR				
N224	0.4058	B			Y	CL	EP				
N225	0.1577			A	N						
N226	0.0817		A		Y	CL	EP	OX			
N227	0.3142	B			Y	CL					
N228	0.2004		B		Y	PR					
N229	0.1104			A	N						
N230	0.3223		A		Y	EP					
N231	1.0112	B			Y	CA	CL				
N232											No information
N233	0.5874	B			Y	CL					
N234	0.1912	B			Y	CL	PR	CA	EP		
N235	0.0959			A	N						
N236	0.3897		A		Y	CL	PR	OX	EP	CA	
N237	1.0176		B		Y	PR					
N238	1.0306	B			Y	PR	CA	CL			
N238b	0.5882	B			Y	CL					
N238u		B			Y	CL					
N239	0.9916	B			Y	EP	PR	CL			
N240	0.3164	B			Y	CA	CL				
N241	0.1349			A	N						
N242	0.3697	B			Y	CL					
N243	0.4846	B			Y	CL	OX				
N244		B			Y	CA	CL				
N245	1.043	A			Y	CL	CA				
N246	0.4728	B			Y	CL	CA				
N247	0.5174	B			Y	OX	CA				
N248	0.2295		A		Y	OX					
N249	0.185			A	N						
N250	0.5877		A		Y	XX					
N251	0.4223		B		Y	CL					
N252	0.3529	B			Y	CL	CA				
N253	0.9675	B			Y	CL	CA	PR			
N254	0.9063	B			Y	CL					
N255	0.3387	B			Y	CL	OX	PR	EP		
N256	0.3332	B			Y	CA	CL				
N257											No information
N258	0.3183			A	N						
N259	0.3093	B			Y	CA	CL				
N260	0.4294	B			Y	CL	PR				
N261	0.2017			B	N						
N262	0.2461		A		Y	PR	OX				
N263	0.2301			A	N						
N264	0.6471	B			Y	PR	CL	EP	CA		
N265	0.3298	B			Y	CL					
N266	0.1531	B			Y	CL					

FRACTURE-ID RVS-MODEL	LENGTH OF FRACTURE[m]	OPEN	HEALED	TIGHT	MINERAL FILL	MINERAL1	MINERAL2	MINERAL3	MINERAL4	MINERAL5	REMARK
N267	0.5315	B			Y	EP	PR				
N268	0.5279	B			Y	EP	PR	CL			
N269	0.7583	A			Y	PR	CL				
N270	1.2009	B			Y	CL					
N271u	0.9922		A		Y	EP	PR	KL	OX		
N271n	0.4701		A		Y	EP	CL	OX	PR		
N272	1.023	B			Y	CL					
N273	0.6292	B			Y	CL					
N274	0.703	B			Y	CL					
N275	0.1652	B			Y	CL	CA				
N276	0.7818	B			Y	CL	CA	PR			
N277	0.2883	B			Y	CA					
N278	0.0989			A	N						
N279	0.3256	B			Y	CL					
N280	0.4089	B			Y	CL					
N281	0.5215			B	N						
N282	0.2223			A	N						
N283	0.1491			A	N						
N284	0.1265		A		Y	XX					
N285	0.1694			A	N						
N286	0.1695			A	N						
N287	0.1065			A	N						
N288	0.1172	B			Y	CL	PR				
N289	0.7094	B			Y	CA	CL				
N290	0.1109			A	N						
N291	0.1536			A	N						
N292	0.4043	B			Y	CL					
N293	0.2655			A	N						
N294	0.3747	B			Y	CL					
N295	0.1861	B			Y	CL					
N296	0.1391	B			Y	CL					
N297	0.1813	B			Y	CL					
N298a	0.176			A	N						
N298b	0.086			A	N						
N298c	0.1533			A	N						
N298d	0.148		A		Y	CL	OX				
N299	1.0981	B			Y	CL	EP	CA			
N299b	0.1349	B			Y	CL	PR				
N299c	0.1189	B			Y	CL					
N300	0.1279			A	N						
N301	1.1566	B			Y	CL	EP				
N302	0.2338		A		Y	CA	PR	EP	OX		
N303	0.4776	B			Y	CL	PR				
N304	0.3046	B			Y	CL					
N305	0.1762			A	N						
N306	0.4208	B			Y	CA	PR	EP			
N307	0.1685		A		Y	PR					
N308	0.3396	B			Y	EP	OX				
N309a	0.151		A		Y	CA					
N309b											No information
N310	0.6625		B		Y	CA	CL	PR			
N311	0.1934		A		Y	CA					
N312	0.2414		A		Y	CL					
N313	0.1385			A	N						
N314	0.1193		A		Y	EP	PR				
N315	0.2333		A		Y	EP					
N316	0.1799	B			Y	CL	PR				
N317	0.2729	B			Y	CL					
N318	1.2287	B			Y	CL					
N319	0.3251	B			Y	KL					
N320	0.243	B			Y	CL					
N321	0.09			A	N						
N322	0.1119	B			Y	CL					
N323	0.347	B			Y	CL	OX	PR			

FRACTURE-ID RVS-MODEL	LENGTH OF FRACTURE[m]	OPEN	HEALED	TIGHT	MINERAL FILL	MINERAL1	MINERAL2	MINERAL3	MINERAL4	MINERAL5	REMARK
N324	0.5495	B			Y	CL	PR				
N325	0.4232	B			Y	CL	PR				
N326	0.1605	B			Y	PR					
N327	0.1641	B			Y	CL					
N328	0.8647	B			Y	CL	CA	OX			
N329	0.5443		A		Y	EP	CL	OX			
N330	0.1279		A		Y	CL					
N331	0.0882		A		Y	CA					
N332	0.1068	B			Y	EP	CL				
N333	1.0378	B			Y	CL	CA				
N333b	0.2709	B			Y	XX					
N334	0.6998		A		Y	EP	OX	CA			
N335	0.5157	B			Y	EP	OX	PR			
N336	0.2353	B			Y	CL					
N337	0.1203			A	N						
N338	0.1816		B		Y	PR	CL				
N339	0.2067		A		Y	CL	PR				
N340	0.0861	B			Y	CL					
N341	0.1635	B			Y	PR	CL				
N342	0.1066	B			Y	CL					
N343	0.1501			A	N						
N344	0.0574	B			Y	CA					
N345	0.3566			A	N						
N346	0.2597			A	N						
N347	0.2038	B			Y	CL					
N348	0.5915	B			Y	CL	OX	PR			
N349	0.2134		A		Y	CL	QZ	CA	EP		
N350	1.2317		A		Y	CL	EP	OX			
N351	0.7415	B			Y	CL	PR				
N352	0.6071	B			Y	CL	PR				
N353	0.6012			A	N						
N354	0.7766	B			Y	EP	CL				
N355	0.3358			A	N						
N356	0.4619		B		Y	PR	OX				
N358	0.2728	B			Y	CL					
N359	0.5257	B			Y	PR					
N360	0.5934		A		Y	CL	EP	OX			
N361	0.241	B			Y	CL					
N362	0.1179		B		Y	PR					
N363	0.1512		A		Y	PR					
N364	0.1606		B		Y	EP	PR				
N365	0.3893		A		Y	CL	PR				
N366	0.2652		A		Y	EP					
N367	0.1889			A	N						
N368	0.3064		A		Y	PR					
N369	0.3518		A		Y	CL	PR				
N370	0.19		A		Y	CL	EP	OX			
N371	0.1625			A	N						
N372	0.2181			A	N						
N373	0.1123	B			Y	KL					
N374	0.2204		B		Y	CL					
N375	0.3734	B			Y	PR	CL	CA			
N376	0.1953			A	N						
N377	0.3624		A		Y	CL	PR	OX			
N378	0.1424		A		Y	CL	CA				
N379	0.2706		A		Y	CA	CL				
N380	0.0794		A		Y	CA	CL	EP			
N381	0.2477	B			Y	CL	PR	CA	OX		
N382	0.5632	B			Y	EP	CL	CA	OX		
N383	0.4387	B			Y	CL	CA				
N384											No information
N385											No information
N386	0.1347		B		Y	CL					
N387	0.1606		A		Y	EP					

FRACTURE-ID RVS-MODEL	LENGTH OF FRACTURE[m]	OPEN	HEALED	TIGHT	MINERAL FILL	MINERAL1	MINERAL2	MINERAL3	MINERAL4	MINERAL5	REMARK
N388	0.2185			A	N						
N389	0.0997		B		Y	PR	EP				
N390	0.3347			A	N						
N391	0.2304	B			Y	CL					
N392	0.2692		B		Y	PR	EP	CA			
N393	0.2795		A		Y	PR	CA	OX			
N394	0.1796			A	N						
N395	0.1855			A	N						
N396	0.1231	B			Y	CL	EP				
N397	0.0656			A	N						
N398	0.1126	B			Y	CL					
N399	0.0944			A	N						
N400	0.1035		A		Y	PR	CL				
N401	0.2708	B			Y	CL					
N402	0.2002			A	N						
N403	0.1021		A		Y	CL					
N404	0.0729	B			Y	CL					
N405	0.1801	B			Y	CL					
N406	0.0888	B			Y	CL	PR				
N407	0.2591		B		Y	CL					
N408	0.2354		A		Y	EP	CA				
N409	0.1532		A		Y	CL	EP				
N410											No information
n501	0.5587			A	N						
n502	0.1876			A	N						
n503	0.093			A	N						
n504	0.1008		A		Y	CL					
n505	0.1049		A		Y	EP					
n506	0.1154		A		Y	CL					
n507	0.0771		A		Y	CA	RF				
n508	0.2469		B		Y	CL	PR	CA			
n509	0.0852			A	N						
n510	0.1225			A	N						
n511	0.1352		A		Y	EP					
n512	0.264		A		Y	CL					
n513	0.1355			A	N						
n514	0.1152			A	N						
n515	0.1325			A	N						
n516											No information
n517	0.3826			A	N						
n518											No information
n519a											No information
n519b											No information
n520	0.134		B		Y	CL					
n521	0.1342		B		Y	CL					
n522	0.1264		A		Y	CA					
n523	0.1301			A	N						
n524	0.2843		A		Y	OX	EP				
n525											No information
n526											No information
n527											No information
n528	0.1276		A		Y	EP					
n529											No information
n530	0.0783			A	N						
n531	0.0826		A		Y	RF	CA	OX			
n531b	0.0964		A		Y	RF	CA	OX			
n531c	0.1089		A		Y	RF	CA				
n531d	0.1982		A		Y	CA					
n532											No information
n533	0.2226			A	N						
n534	0.109			A	N						
n535											No information
n536	0.0527			A	N						
n537	0.0687			A	N						

FRACTURE-ID RVS-MODEL	LENGTH OF FRACTURE[m]	OPEN	HEALED	TIGHT	MINERAL FILL	MINERAL1	MINERAL2	MINERAL3	MINERAL4	MINERAL5	REMARK
n538	0.0544			A	N						
n539	0.0853			A	N						
n540	0.1062		A		Y	EP					
n541				A	N						
n542	0.1086			A	N						
n543	0.2992	B			Y	CL	CA	OX			
n544	0.0841			A	N						
n545	0.0658			A	N						
n546				A	N						
n547	0.0974		A		Y	PR	CL				
n548	0.0823			A	N						
n549	0.2			A	N						
n550	0.3877		A		Y	EP					
n551	0.1161		A		Y	EP					
n552	0.0666			A	N						
n553	0.0685			A	N						
n554	0.1857		B		Y	CL					
n555	0.1299			A	N						
n556	0.0879		A		Y	PR					
n557	0.0833			A	N						
n558	0.1947		A		Y	CL					
n559	0.0734			A	N						
n560	0.1194		A		Y	PR					
n561	0.1998			A	N						
n562	0.0735			A	N						
n563	0.1192		A		Y	CL					
n564											No information
n565											No information
n566											No information
n567											
n568			A		Y	CL	CA				
n569	0.0987	B			Y	CL					
n570	0.085		A		Y	CL	PR				
n571	0.1378		A		Y	EP					
n572	0.0879			A	N						
n573	0.0995			A	N						
n574	0.1236			A	N						
n575	0.0964			A	N						
n576	0.095		A		Y	XX					
n577	0.0715			A	N						
n578											No information
n579											No information
n580	0.0601			A	N						
n581											No information
n582											No information
n583	0.1584			A	N						
n584			A		Y	CL					
n585											No information
n586	0.2347		A		Y	EP					
n587	0.1678		A		Y	OX	CL				
n588	0.0749		A		Y	CL	EP	OX			
n589	0.2176	B			Y	CL					
n590	0.1072		B		Y	CA	OX				
n591	0.4254	B			Y	CL					
n592	0.1619		A		Y	EP	CL				
n593	0.1416			A	N						
n594	0.0851			A	N						
n595	0.1159			A	N						
n596	0.1366		B		Y	CL	OX				
n597	0.0794		A		Y	CL	EP				
n598	0.2797	B			Y	CL	PR				
n599	0.2578	B			Y	CL	EP				
n600	0.06		A		Y	EP					
n601	0.1373		A		Y	CL	PR				

FRACTURE-ID RVS-MODEL	LENGTH OF FRACTURE[m]	OPEN	HEALED	TIGHT	MINERAL FILL	MINERAL1	MINERAL2	MINERAL3	MINERAL4	MINERAL5	REMARK
n602	0.0842			A	N						
n603	0.0862			A	N						
n604	0.1095			A	N						
n605	0.2107			A	N						
n606	0.1625			B	N						
n607		B			Y	XX					
n608											No information
n609	0.1612		A		Y	CA	OX				
n610	0.1692		A		Y	CL					
n611	0.159			A	N						
n612	0.2035		A		Y	EP	OX				
n613	0.1478		A		Y	CA					
n614	0.1023			A	N						
n615	0.1019			A	N						
n616	0.1019			A	N						
n617	0.1622	B			Y	CL					
n618	0.1302		B		Y	CL					
n619	0.2216		A		Y	CA	PR				
n620	0.0961		A		Y	CL	PR				
n621	0.0804			A	N						
n622	0.0848			A	N						
n623	0.3127	B			Y	CL					
n624	0.3219	B			Y	CL	CA	OX			
n625	0.06			A	N						
n626	0.1755			A	N						
n627	0.2223		A		Y	CA					
n628l	0.3049	B			Y	CA	CL				
n628u	0.3049	B			Y	CA	CL				
n629	0.1946	B			Y	CA	CL				
n630	0.1279			A	N						
n631	0.138			A	N						
n632	0.0573			A	N						
n633	0.0611			A	N						
n634	0.1015			A	N						
n635	0.099		B		Y	PR					
n636	0.2632	B			Y	CA	CL				
n637	0.3363		A		Y	PR	EP				
n638	0.1056			A	N						
n639	0.0857			A	N						
n640	0.5498	B			Y	CA					
n641	0.2559		B		Y	PR	EP	CA			
n642	0.3869		A		Y	PREP					
n643	0.4467	B			Y	CA	PR				
n644	0.1259	B			Y	PR	CL	CA			
n645	0.148	B			Y	CL	PR				
n646	0.0968			A	N						
n647	0.1318		A		Y	CA	RF				
n648	0.3598			A	N						
n649	0.3024		A		Y	PR	CL	CA			
n650	0.1688			A	N						
n651	0.075			A	N						
n652	0.1027		B		Y	CL					
n653	0.1339			A	N						
n654	0.1075			A	N						
n656	0.1239	B			Y	CL	PR				
n657	0.2274			A	N						
n658	0.1311		A		Y	CL					
n659	0.1926		A		Y	CL					
n660	0.1069			A	N						
n661	0.0832			A	N						
n662	0.0936	B			Y	CL					
n663	0.1055		A		Y	CL					
n664	0.1249	B			Y	CL					
n665	0.1017			A	N						

FRACTURE-ID RVS-MODEL	LENGTH OF FRACTURE[m]	OPEN	HEALED	TIGHT	MINERAL FILL	MINERAL1	MINERAL2	MINERAL3	MINERAL4	MINERAL5	REMARK
n666	0.0875	B			Y	CL					
n667	0.0963			A	N						
n668	0.0884			A	N						
n669	0.1047			A	N						
n670	0.208	B			Y	CL					
n671	0.0737			A	N						
n672	0.108			A	N						
n673											No information
n674											No information
n675	0.0689			A	N						
n676	0.1176			A	N						
n677	0.1498			A	N						
n678	0.1497		A		Y	CL					
n679	0.2613		B		Y	CL					
n680a	0.1918			A	N						
n680b	0.1918			A	N						
n681	0.082		A		Y	CL	PR				
n682	0.0736			A	N						
n683											No information
n684	0.1475		A		Y	CL	OX				
n685	0.1684	B			Y	CL					
n686	0.0934	B			Y	CL					
n687	0.1013			A	N						
n688	0.1238		A		Y	CL					
n689	0.0994		A		Y	CL					
n690	0.2284			A	N						
n691	0.1205		A		Y	CL	OX				
n692			A		Y	EP					
n693				A	N						
n694	0.1973		B		Y	CL	OX	EP			
n695	0.2543		B		Y	EP					
n696	0.0731			B	N						
n697	0.1418		A		Y	CL	OX	PR			
n698	0.0845			A	N						
n699	0.0723			A	N						
n700											No information
n701											No information
n702	0.0893			A	N						
n703											No information
n704											No information
n705											No information
n706	0.26			B	N						
n707	0.1011			A	N						
n708	0.1072			A	N						
n709	0.0641			A	N						
n710											No information
n711											No information
n712											No information
n713	0.0914			A	N						
n714	0.0935			A	N						
n715	0.0664			A	N						
n716											No information
n717											No information
n718	0.1208			A	N						
n719											No information
n720	0.1465			A	N						
n721											No information
n722	0.1963			A	N						
n723	0.0799			A	N						
n724	0.0843			A	N						
n725	0.0987			A	N						
n726	0.0993			A	N						
n727	0.1813		A		Y	EP	PR	CL	OX		
n728	0.1079			A	N						

FRACTURE-ID RVS-MODEL	LENGTH OF FRACTURE[m]	OPEN	HEALED	TIGHT	MINERAL FILL	MINERAL1	MINERAL2	MINERAL3	MINERAL4	MINERAL5	REMARK
n729	0.3791	B			Y	XX					
n730	0.1027			A	N						
n731	0.1			A	N						
n732	0.0921	B			Y	PR					
n733	0.0836			A	N						
n734	0.0685			A	N						
n735	0.0734			A	N						
n736	0.1057			A	N						
n737	0.0639			A	N						
n738											No information
n739	0.2276		A		Y	CL					
n740	0.0599			A	N						
n741	0.087			A	N						
n742	0.273			A	N						
n743	0.1008			A	N						
n744	0.2626			A	N						
n745	0.2996			A	N						
n746	0.079			A	N						
n747	0.0786			A	N						
n748	0.1551			A	N						
n749	0.1233			A	N						
n750	0.0716			A	N						
n751	0.0581		A		Y	CL					
n752	0.0717			A	N						
n753	0.1879	B			Y	CL					
n754	0.2222		B		Y	CA	PR				
n755	0.2222		B		Y	CA	PR				
n756	0.2834			A	N						
n757	0.4113		B		Y	PR	EP				
n758	0.166			A	N						
n759	0.119		A		Y	EP					
n760	0.1298			A	N						
n761	0.2349	B			Y	PR	CL				
n762	0.077			A	N						
n763	0.1049			A	N						
n764											No information
n765	0.1313		A		Y	CA	RF	CL			
n766	0.1074			A	N						
n767	0.1125		A		Y	EP					
n768	0.1572		B		Y	CL					
n769	0.0858		B		Y	CL					
n770	0.0865	B			Y	CL	CA				
n771	0.0658		A		Y	OX	RF				
n772	0.1652		A		Y	EP	CL				
n773											No information
n774											No information
n775	0.1358			A	N						
n776	0.1079			A	N						
n777	0.1051			A	N						
n778	0.1755		A		Y	PR					
n779	0.2237			A	N						
n780											No information
n781	0.2294			A	N						
n782	0.1197			A	N						
n783	0.089			A	N						
n784	0.0902	B			Y	PR	CL				
n785	0.0944		B		Y	PR					
n786	0.1631			A	N						
n787	0.141		A		Y	PR	CL				
n788	0.2036		A		Y	CL					
n789	0.13		A		Y	EP					
n790											No information
n791	0.1504			A	N						
n792	0.1027			A	N						

FRACTURE-ID RVS-MODEL	LENGTH OF FRACTURE[m]	OPEN	HEALED	TIGHT	MINERAL FILL	MINERAL1	MINERAL2	MINERAL3	MINERAL4	MINERAL5	REMARK
n793	0.0868		A		Y	EP					
n794	0.0828			A	N						
n795	0.116			A	N						
n796	0.2565			A	N						
n797	0.1479		A		Y	CL					
n798	0.1002			A	N						
n799	0.1089			A	N						
n800	0.1036			A	N						
n801	0.2177			A	N						
n802	0.1561		A		Y	CL					
n803	0.4702		A		Y	EP	CL	OX	PR		
n804	0.1064			A	N						
n805				A	N						
n806	0.2457	B			Y	CL					
n807											No information
n808	0.2831		A		Y	CA					
n809											No information
n810	0.1691		B?		Y	CL					
n811	0.2034	B			Y	CL					
n812	0.1265			A	N						
n813	0.1998		A		Y	CL	EP				
n814				A	N						
n815	0.3173	B			Y	CL	CA				
n816	0.2807	B			Y	CL					
n817				A	N						
n818				A	N						
n819				A	N						
n820	0.0671			A	N						
n821	0.2042			A	N						
n822											No information
n823											No information
n824	0.122	B			Y	CL					
n825											No information
n826	0.281			B	N						
n827	0.1288			A	N						
n828											No information
n829	0.1422			A	N						
n830	0.0959		B		Y	PR					
n831	0.1964			A	N						
n832	0.2586	B			Y	CL	OX				
n833	0.2869	B			Y	CL	PR	CA			
n834											No information
n835											No information
n836	0.0912		A		2	KL					
n837	0.255		B		Y	PR					
n838	0.1532		A		Y	PR	CA				
n839	0.1361		A		Y	CL	CA				
n840	0.0948		A		Y	PR					
n841	0.1262		A		Y	CL					
n842	0.1572		A		Y	EP	PR				
n843	0.1468		A		Y	EP					
n844											No information
n845											No information
n846	0.6154	B			Y	PR	CA	CL	EP		

Length of fractures in EDZ 3D model

Total number of fractures in 3D-model		Length information available
TOTAL	1223	1187
NATURAL FRACTURES	777	755
DIRECT BLAST INDUCED	262	255
INDUCED	184	177

Large fractures in 3D-model		Length information available
TOTAL	695	677
NATURAL FRACTURES	426	417
DIRECT BLAST INDUCED	169	163
INDUCED	100	97

Small fractures in 3D-model		Length information available
TOTAL	528	510
NATURAL FRACTURES	351	338
DIRECT BLAST INDUCED	93	92
INDUCED	84	80

Length distribution; all natural, direct blast induced and induced

	<15 cm	15-30 cm	30-45 cm	45-60 cm	60-75 cm	>75 cm
Natural	325	246	84	37	26	37
Direct bla:	178	66	8	2	1	0
Induced	121	46	9	1	0	0

Length distribution; small natural, direct blast induced and induced

	<15 cm	15-30 cm	30-45 cm	45-60 cm	60-75 cm	>75 cm
Natural	227	90	17	3	1	0
Direct bla:	84	8	0	0	0	0
Induced	74	6	0	0	0	0

Length distribution; large natural, direct blast induced and induced

	<15 cm	15-30 cm	30-45 cm	45-60 cm	60-75 cm	>75 cm
Natural	98	156	67	34	25	37
Direct bla:	94	58	8	2	1	0
Induced	47	40	9	1	0	0

Natural fractures

FRACTURE-ID RVS-MODEL	LENGTH OF FRACTURE[m]	FRACTURE-ID RVS-MODEL	LENGTH OF FRACTURE[m]	FRACTURE-ID RVS-MODEL	LENGTH OF FRACTURE[m]	FRACTURE-ID RVS-MODEL	LENGTH OF FRACTURE[m]	FRACTURE-ID RVS-MODEL	LENGTH OF FRACTURE[m]
N001	0.6306	N058	0.2009	N107	0.2793	N158	0.1866	N210	0.1217
N002	0.5063	N059a	0.7342	N108	0.1472	N159	0.2409	N211	0.199
N003	0.8116	N059b	0.1371	N109	0.3196	N160	0.2206	N212	0.2565
N004	0.6234	N060	0.2356	N110	0.1707	N161	0.2769	N213	0.0808
N005	0.6577	N061	0.223	N111	0.2191	N162	0.1486	N214	NO INFO
N006	0.6473	N062a	0.2233	N112	0.0872	N163	0.1407	N215	0.1198
N007	0.0689	N062b	0.3559	N113l	0.5102	N164	NO INFO	N216	0.2208
N008	0.2059	N063a	NO INFO	N113u	0.6514	N165	0.3431	N217	0.5068
N009	0.1195	N063b	0.2189	N114l	0.3122	N166	0.7602	N218	0.1564
N010	0.2489	N064	0.2825	N114u	0.339	N167	0.411	N219	0.1297
N011	0.3625	N065	0.1612	N115	0.4063	N168	0.4415	N220	0.2953
N012	0.0716	N066	0.082	N116	0.5656	N169	0.7335	N221	0.3517
N013	0.2998	N067	0.263	N117	1.5241	N170	0.3706	N222	0.2248
N014	0.2409	N068	0.2632	N118	1.566	N171	0.8552	N223	0.5554
N015	0.241	N069	0.2426	N119	0.3422	N172	0.4669	N224	0.4058
N016	0.2481	N070	0.3145	N120	0.405	N173	0.8609	N225	0.1577
N017	0.6038	N071	0.2752	N120b	0.1098	N174	0.6435	N226	0.0817
N018	0.2516	N072	0.0959	N121	0.7836	N175	0.7801	N227	0.3142
N019	0.8175	N073	0.2061	N122	0.3146	N176	0.2323	N228	0.2004
N020	0.1287	N074	0.0925	N123	0.6666	N177	0.4016	N229	0.1104
N021	0.1482	N075l	0.2195	N124	0.4406	N178	0.6651	N230	0.3223
N022	0.092	N075u	0.2892	N125	0.2925	N179	0.2127	N231	1.0112
N023	0.6258	N076	0.544	N126	0.117	N180	0.0671	N232	0.0905
N024	0.9106	N077	0.4062	N127	0.1677	N181	0.2827	N233	0.5874
N025	0.941	N078	0.061	N128	0.1213	N182	0.3993	N234	0.1912
N026	0.6829	N079	0.2898	N129	0.2623	N183	0.1443	N235	0.0959
N027	0.2885	N080	0.231	N130	0.2751	N184	0.1241	N236	0.3897
N028	0.2726	N081	0.1153	N131	0.1373	N185	0.4297	N237	1.0176
N028b	0.1859	N082	0.4841	N132	0.3422	N186	0.2201	N238	1.0306
N029	0.2544	N083	0.1574	N133	0.6954	N187	0.1751	N238b	0.5882
N030	0.3316	N084	0.0294	N134	0.7835	N188	0.1227	N238u	0.5105
N031	0.5179	N085	0.2066	N135	1.7463	N189	0.4383	N239	0.9916
N032	0.3806	N086	0.0811	N136	0.4915	N190	0.5887	N240	0.3164
N033	0.308	N087	0.527	N137	0.4207	N191l	0.62	N241	0.1349
N034	NO INFO	N088a	NO INFO	N138	0.5374	N191u	0.764	N242	0.3697
N035	0.2165	N088b	NO INFO	N139	0.0577	N192	1.4828	N243	0.4846
N036	0.3488	N089	0.1741	N140	0.0468	N193	1.4508	N244	NO INFO
N037	0.2695	N090	0.0549	N141	0.1581	N194	1.2449	N245	1.043
N038	0.2195	N091	0.1316	N142	0.264	N195	0.4034	N246	0.4728
N039	0.258	N092	0.2171	N143	0.2792	N196	0.2864	N247	0.5174
N040	0.3964	N093	0.1269	N144	0.1278	N197	0.6557	N248	0.2295
N041	0.2446	N094	0.0691	N145	0.1054	N198	0.08	N249	0.185
N042	0.0908	N095	0.2274	N146	0.1038	N199	0.5858	N250	0.5877
N043	0.1633	N096	0.2645	N147	0.0839	N200	0.1855	N251	0.4223
N045	0.344	N097	0.1677	N148	0.1959	N201	0.1918	N252	0.3529
N046	0.1819	N098	0.37	N149	0.118	N202	0.2517	N253	0.9675
N048	0.1881	N099	0.2191	N150	0.3815	N203	0.1129	N254	0.9063
N049		N100	0.2218	N151	0.2963	N204a	0.1433	N255	0.3387
N050	0.1284	N101	0.1683	N152	0.3826	N204b	0.2164	N256	0.3332
N052	0.0859	N102	0.1033	N153	0.2667	N205	0.0811	N257	0.1277
N053	0.3015	N103	0.8208	N154	0.2451	N206	0.2964	N258	0.3183
N055	0.1023	N104	0.2358	N155	0.1979	N207	0.2809	N259	0.3093
N056	0.1084	N105	0.2738	N156	0.2823	N208	0.0877	N260	0.4294
N057	0.296	N106	0.1545	N157	0.2951	N209	0.0993	N261	0.2017

Natural fractures

FRACTURE-ID RVS-MODEL	LENGTH OF FRACTURE[m]	FRACTURE-ID RVS-MODEL	LENGTH OF FRACTURE[m]	FRACTURE-ID RVS-MODEL	LENGTH OF FRACTURE[m]	FRACTURE-ID RVS-MODEL	LENGTH OF FRACTURE[m]	FRACTURE-ID RVS-MODEL	LENGTH OF FRACTURE[m]
N262	0.2461	N309b	0.1387	N363	0.1512	n507	0.0771	n557	0.0833
N263	0.2301	N310	0.6625	N364	0.1606	n508	0.2469	n558	0.1947
N264	0.6471	N311	0.1934	N365	0.3893	n509	0.0852	n559	0.0734
N265	0.3298	N312	0.2414	N366	0.2652	n510	0.1225	n560	0.1194
N266	0.1531	N313	0.1385	N367	0.1889	n511	0.1352	n561	0.1998
N267	0.5315	N314	0.1193	N368	0.3064	n512	0.264	n562	0.0735
N268	0.5279	N315	0.2333	N369	0.3518	n513	0.1355	n563	0.1192
N269	0.7583	N316	0.1799	N370	0.19	n514	0.1152	n564	0.2183
N270	1.2009	N317	0.2729	N371	0.1625	n515	0.1325	n565	NO INFO
N271n	0.4701	N318	1.2287	N372	0.2181	n516	0.064	n566	0.061
N271u	0.9922	N319	0.3251	N373	0.1123	n517	0.3826	n567	0.0556
N272	1.023	N320	0.243	N374	0.2204	n518	0.1346	n568	0.3739
N273	0.6292	N321	0.09	N375	0.3734	n519a	0.1668	n569	0.0987
N274	0.703	N322	0.1119	N376	0.1953	n519b	0.1668	n570	0.085
N275	0.1652	N323	0.347	N377	0.3624	n520	0.134	n571	0.1378
N276	0.7818	N324	0.5495	N378	0.1424	n521	0.1342	n572	0.0879
N277	0.2883	N325	0.4232	N379	0.2706	n522	0.1264	n573	0.0995
N278	0.0989	N326	0.1605	N380	0.0794	n523	0.1301	n574	0.1236
N279	0.3256	N327	0.1641	N381	0.2477	n524	0.2843	n575	0.0964
N280	0.4089	N328	0.8647	N382	0.5632	n525	0.1239	n576	0.095
N281	0.5215	N329	0.5443	N383	0.4387	n526	0.0674	n577	0.0715
N282	0.2223	N330	0.1279	N384	NO INFO	n527	0.0569	n578	NO INFO
N283	0.1491	N331	0.0882	N385	0.0685	n528	0.1276	n579	NO INFO
N284	0.1265	N332	0.1068	N386	0.1347	n529	0.0949	n580	0.0601
N285	0.1694	N333	1.0378	N387	0.1606	n530	0.0783	n581	NO INFO
N286	0.1695	N333b	0.2709	N388	0.2185	n531	0.0826	n582	NO INFO
N287	0.1065	N334	0.6998	N389	0.0997	n531b	0.0964	n583	0.1584
N288	0.1172	N335	0.5157	N390	0.3347	n531c	0.1089	n584	0.0806
N289	0.7094	N336	0.2353	N391	0.2304	n531d	0.1982	n585	NO INFO
N290	0.1109	N337	0.1203	N392	0.2692	n532	0.1215	n586	0.2347
N291	0.1536	N338	0.1816	N393	0.2795	n533	0.2226	n587	0.1678
N292	0.4043	N339	0.2067	N394	0.1796	n534	0.109	n588	0.0749
N293	0.2655	N340	0.0861	N395	0.1855	n535	0.0634	n589	0.2176
N294	0.3747	N341	0.1635	N396	0.1231	n536	0.0527	n590	0.1072
N295	0.1861	N342	0.1066	N397	0.0656	n537	0.0687	n591	0.4254
N296	0.1391	N343	0.1501	N398	0.1126	n538	0.0544	n592	0.1619
N297	0.1813	N344	0.0574	N399	0.0944	n539	0.0853	n593	0.1416
N298a	0.176	N345	0.3566	N400	0.1035	n540	0.1062	n594	0.0851
N298b	0.086	N346	0.2597	N401	0.2708	n541	NO INFO	n595	0.1159
N298c	0.1533	N347	0.2038	N402	0.2002	n542	0.1086	n596	0.1366
N298d	0.148	N348	0.5915	N403	0.1021	n543	0.2992	n597	0.0794
N299	1.0981	N349	0.2134	N404	0.0729	n544	0.0841	n598	0.2797
N299b	0.1349	N350	1.2317	N405	0.1801	n545	0.0658	n599	0.2578
N299c	0.1189	N351	0.7415	N406	0.0888	n546	NO INFO	n600	0.06
N300	0.1279	N352	0.6071	N407	0.2591	n547	0.0974	n601	0.1373
N301	1.1566	N353	0.6012	N408	0.2354	n548	0.0823	n602	0.0842
N302	0.2338	N354	0.7766	N409	0.1532	n549	0.2	n603	0.0862
N303	0.4776	N355	0.3358	N410	0.1869	n550	0.3877	n604	0.1095
N304	0.3046	N356	0.4619	n501	0.5587	n551	0.1161	n605	0.2107
N305	0.1762	N358	0.2728	n502	0.1876	n552	0.0666	n606	0.1625
N306	0.4208	N359	0.5257	n503	0.093	n553	0.0685	n607	0.207
N307	0.1685	N360	0.5934	n504	0.1008	n554	0.1857	n608	0.0388
N308	0.3396	N361	0.241	n505	0.1049	n555	0.1299	n609	0.1612
N309a	0.151	N362	0.1179	n506	0.1154	n556	0.0879	n610	0.1692

Natural fractures

FRACTURE-ID RVS-MODEL	LENGTH OF FRACTURE[m]	FRACTURE-ID RVS-MODEL	LENGTH OF FRACTURE[m]	FRACTURE-ID RVS-MODEL	LENGTH OF FRACTURE[m]	FRACTURE-ID RVS-MODEL	LENGTH OF FRACTURE[m]	FRACTURE-ID RVS-MODEL	LENGTH OF FRACTURE[m]
n611	0.159	n665	0.1017	n718	0.1208	n772	0.1652	n826	0.281
n612	0.2035	n666	0.0875	n719	0.0483	n773	0.0567	n827	0.1288
n613	0.1478	n667	0.0963	n720	0.1465	n774	0.0678	n828	NO INFO
n614	0.1023	n668	0.0884	n721	0.1417	n775	0.1358	n829	0.1422
n615	0.1019	n669	0.1047	n722	0.1963	n776	0.1079	n830	0.0959
n616	0.1019	n670	0.208	n723	0.0799	n777	0.1051	n831	0.1964
n617	0.1622	n671	0.0737	n724	0.0843	n778	0.1755	n832	0.2586
n618	0.1302	n672	0.108	n725	0.0987	n779	0.2237	n833	0.2869
n619	0.2216	n673	0.0692	n726	0.0993	n780	0.3347	n834	0.2
n620	0.0961	n674	0.0627	n727	0.1813	n781	0.2294	n835	0.0654
n621	0.0804	n675	0.0689	n728	0.1079	n782	0.1197	n836	0.0912
n622	0.0848	n676	0.1176	n729	0.3791	n783	0.089	n837	0.255
n623	0.3127	n677	0.1498	n730	0.1027	n784	0.0902	n838	0.1532
n624	0.3219	n678	0.1497	n731	0.1	n785	0.0944	n839	0.1361
n625	0.06	n679	0.2613	n732	0.0921	n786	0.1631	n840	0.0948
n626	0.1755	n680a	0.1918	n733	0.0836	n787	0.141	n841	0.1262
n627	0.2223	n680b	0.1918	n734	0.0685	n788	0.2036	n842	0.1572
n628l	0.3049	n681	0.082	n735	0.0734	n789	0.13	n843	0.1468
n628u	0.3049	n682	0.0736	n736	0.1057	n790	NO INFO	n844	0.0806
n629	0.1946	n683	0.0658	n737	0.0639	n791	0.1504	n845	0.165
n630	0.1279	n684	0.1475	n738	0.0497	n792	0.1027	n846	0.6154
n631	0.138	n685	0.1684	n739	0.2276	n793	0.0868		
n632	0.0573	n686	0.0934	n740	0.0599	n794	0.0828		
n633	0.0611	n687	0.1013	n741	0.087	n795	0.116		
n634	0.1015	n688	0.1238	n742	0.273	n796	0.2565		
n635	0.099	n689	0.0994	n743	0.1008	n797	0.1479		
n636	0.2632	n690	0.2284	n744	0.2626	n798	0.1002		
n637	0.3363	n691	0.1205	n745	0.2996	n799	0.1089		
n638	0.1056	n692	NO INFO	n746	0.079	n800	0.1036		
n639	0.0857	n693	NO INFO	n747	0.0786	n801	0.2177		
n640	0.5498	n694	0.1973	n748	0.1551	n802	0.1561		
n641	0.2559	n695	0.2543	n749	0.1233	n803	0.4702		
n642	0.3869	n696	0.0731	n750	0.0716	n804	0.1064		
n643	0.4467	n697	0.1418	n751	0.0581	n805	0.0629		
n644	0.1259	n698	0.0845	n752	0.0717	n806	0.2457		
n645	0.148	n699	0.0723	n753	0.1879	n807	0.1739		
n646	0.0968	n700	0.0642	n754	0.2222	n808	0.2831		
n647	0.1318	n701	0.0539	n755	0.2222	n809	NO INFO		
n648	0.3598	n702	0.0893	n756	0.2834	n810	0.1691		
n649	0.3024	n703	0.1199	n757	0.4113	n811	0.2034		
n650	0.1688	n704	0.0602	n758	0.166	n812	0.1265		
n651	0.075	n705	0.0604	n759	0.119	n813	0.1998		
n652	0.1027	n706	0.26	n760	0.1298	n814	0.1479		
n653	0.1339	n707	0.1011	n761	0.2349	n815	0.3173		
n654	0.1075	n708	0.1072	n762	0.077	n816	0.2807		
n656	0.1239	n709	0.0641	n763	0.1049	n817	0.171		
n657	0.2274	n710	0.092	n764	0.0616	n818	0.162		
n658	0.1311	n711	0.0744	n765	0.1313	n819	0.1047		
n659	0.1926	n712	0.0708	n766	0.1074	n820	0.0671		
n660	0.1069	n713	0.0914	n767	0.1125	n821	0.2042		
n661	0.0832	n714	0.0935	n768	0.1572	n822	0.0762		
n662	0.0936	n715	0.0664	n769	0.0858	n823	0.0638		
n663	0.1055	n716	0.0687	n770	0.0865	n824	0.122		
n664	0.1249	n717	0.0706	n771	0.0658	n825	0.059		

Direct blast induced fractures

FRACTURE-ID RVS-MODEL	LENGTH OF FRACTURE[m]	FRACTURE-ID RVS-MODEL	LENGTH OF FRACTURE[m]	FRACTURE-ID RVS-MODEL	LENGTH OF FRACTURE[m]	FRACTURE-ID RVS-MODEL	LENGTH OF FRACTURE[m]	FRACTURE-ID RVS-MODEL	LENGTH OF FRACTURE[m]
A001	0.1504	B019	0.2105	E007	0.1016	F032	0.1366	f514	0.0572
A002	0.1721	B020	0.0629	E008	0.0537	F033	0.1712	f517	0.0792
A003	0.3111	B021	0.1946	E009	0.2262	F034	0.1416	f520	0.0339
A004	0.1817	B022	0.1229	E010	0.1027	F035	0.0538	f521	0.196
A005	0.1385	B023	0.1071	E011	0.1007	F036	0.1302	f522a	0.1122
A006	0.2009	B024	NO INFO	E012	0.0983	F037	0.1546	f522b	0.1122
A007	0.1476	b502	0.178	E013	0.0693	F038	0.1057	f523	0.0858
A008	0.1984	b503	0.0733	E014	0.5688	F039	0.0787	f524	0.0281
A009	0.1973	b504	0.0913	E015	0.2517	F040	0.0227	f525	0.0499
A010	0.1218	b505	0.149	E016	0.0844	F041	0.0795	f526	0.0472
A011	0.1191	b506	0.2285	E017	0.2871	F042	0.2143	f527	0.0771
A012	0.1006	b507	0.0865	E018	0.254	F043	0.0698	f528	0.0485
A013	0.1612	b511	0.2623	e501	0.0557	F044	0.1329	f529	0.0653
a501	0.0973	b512	0.0706	e502	0.0419	F045	0.1959	f530	0.1692
a502	0.1478	b513	NO INFO	e503	0.0566	F046	0.0831	G002	0.1117
a503	0.0437	b514	0.1473	e504	0.1033	F047	0.0806	G003	0.1284
B001	0.1723	C001	0.0834	e506	0.1006	F048	0.246	G004	0.0782
B002	0.0897	C002	0.1835	e507	0.0683	F049	0.1261	G005	NO INFO
B003	0.1985	ci501	0.068	e508	0.0799	F050	0.1316	g501	0.0428
B004	0.2443	D001	0.0743	e509	0.0677	F051	0.0346	g502	0.0389
B005	0.1467	D002	0.1181	e510	0.0369	F052	NO INFO	g503	0.034
B006	0.2298	D003	0.0402	e511	0.1506	F053	0.2122	g504	0.0499
B007	0.0993	d501	0.0432	e512	0.0498	F054	0.0712	g505	0.0406
B008	0.1462	d502	0.0526	F001	0.0845	F055	0.3052	H002	0.1386
B009	0.2666	d503	0.0356	F002	0.1276	F056	0.1449	H004	0.1889
B010	0.2309	d504	0.0498	F003	0.2605	F057	0.0868	h501	0.1073
B011	0.155	d505	0.0359	F004	0.1305	F058	0.0871	h502	0.1011
B012	0.2395	d506	0.0692	F005	0.2015	F059	0.1529	h503	0.0652
B013	0.1838	E001	0.2456	F006	0.163	F060	0.1804	h504	0.1473
B014	0.0784	E002	0.0573	F007	0.0984	F061	0.2075	h505	0.108
B015	0.1666	E003	0.0413	F008	0.1321	F062	0.0574	h506	0.0554
B016	0.4056	E004	0.0299	F009	0.2663	F063	0.0241	I001	0.1801
B017	0.0931	E005	0.522	F010	0.1491	F064	0.1942	I002	0.0697
B018	0.1034	E006	0.6192	F011	0.1244	F065	0.2176	I003	NO INFO
F012	0.266	F066	0.2429	f531	0.0338	F091	0.1475	I004	0.1223
F013	0.0446	F067	0.2905	f532	0.1489	F092	NO INFO	I005	0.1768
F014	0.1284	F068	0.4283	f533	0.0738	F093	0.09	I006	0.1107
F015	0.3462	F069	0.3754	f534	0.0531	F094	0.1203	I007	0.2367
F016	0.142	F070	0.2423	f535	0.0491	F095	0.0554	i501	0.0528
F017	0.152	F071	0.1357	f536	0.0626	F096	0.0611	i502	0.016
F018	0.3959	F072	0.0477	f537	0.0373	F098	0.0674	i503	0.1086
F019	0.3738	F073	0.1249	f538	0.0931	F099	0.0431	i504	0.0266
F020	0.2546	F074	0.2242	f539	0.0268	F100	0.1289	i505	0.053
F021	0.0934	F075	0.1266	f540	0.1108	F101	NO INFO	i506	0.1264
F022	0.0723	F076	0.2026	f542	0.0687	f501	0.0514	i507	0.0819
F023	0.1301	F077	0.1414	f543	0.1139	f503	0.0876	i511	0.056
F024	0.2379	F080	0.1805	f544	0.0974	f504	0.0853		
F026	0.1768	F081	0.049	f545	0.0333	f505	0.0995		
F027	0.1672	F082	0.1129	f546	0.1654	f507	0.0354		
F028	0.1104	F083	0.1213	f547	0.2469	f508	0.0773		
F029	0.1597	F084	0.1359	f548	0.0702	f510	0.1018		
F029b	0.0737	F085	0.0852	f549	0.0779	f511	0.083		
F030	0.1443	F086	0.1842	f550	0.0465	f512	0.138		
F031	0.1199	F090	0.1155	G001	0.0563	f513	0.064		

Induced fractures

FRACTURE-ID RVS-MODEL	LENGTH OF FRACTURE[m]	FRACTURE-ID RVS-MODEL	LENGTH OF FRACTURE[m]	FRACTURE-ID RVS-MODEL	LENGTH OF FRACTURE[m]	FRACTURE-ID RVS-MODEL	LENGTH OF FRACTURE[m]
AI001	0.1338	di507	0.0617	FI017	0.0903	fi529	0.0623
AI002	0.2645	di508	0.0438	FI018	0.1398	fi530	0.048
AI003	0.101	di509	0.1	FI019	0.0736	fi532	0.0482
AI004	0.1943	di510	0.106	FI020	0.3002	fi533	0.0717
AI005	0.142	di511	0.0885	FI021	0.1034	fi534	0.1029
AI006	0.2091	di512	0.066	FI022	0.1601	fi535	0.1597
AI007	0.2109	di513	0.0563	FI023	0.1137	fi536	0.0845
AI008	0.1585	EI001	0.3748	FI024	0.2243	fi540	0.0666
AI009	0.1825	EI002	0.0664	FI025	0.1805	fi541	0.0607
AI010	0.2565	EI003	0.098	FI026	0.0608	fi542	NO INFO
AI011	0.3144	EI004	0.0882	FI027	0.557	fi543	0.0828
AI012	0.2005	EI009	0.25	FI028	0.256	fi544	0.0906
AI013	0.2276	EI010	0.1439	FI029	0.0715	fi545	0.1087
ai502	0.1943	EI011	0.1801	FI030	0.3103	fi546	NO INFO
ai503	0.0495	EI012	0.0636	FI031	0.1381	GI001	0.1262
ai504	0.0501	EI013	0.0972	FI032	0.0476	GI002	0.1371
ai506	0.0703	EI015	0.1028	FI033	0.1821	GI003	0.242
BI001	NO INFO	ei501	0.0769	FI034	0.0642	gi501	0.1846
BI004	0.1161	ei503	0.0734	FI036	0.1695	gi502	0.0929
BI006	0.2732	ei504	0.0562	FI037	0.3448	HI001	0.2433
BI007	0.2405	ei505	NO INFO	FI038	0.1209	HI002	0.4016
BI008	0.1575	ei506	0.121	FI039	0.2811	HI003	0.2078
BI009	0.133	ei507	0.123	FI040	0.0363	HI004	0.2995
BI010	0.1706	ei508	0.1564	FI041	0.2337	hi501	0.2217
BI011	0.2003	ei509	0.1204	FI042	0.0818	hi502	0.0478
BI012	0.1747	ei510	0.0672	FI043	0.2203	hi503	NO INFO
BI013	0.0936	ei511	0.0387	FI044	0.1878	II001	0.4017
BI014	0.2789	ei512	0.1418	FI045	0.0761	ii501	0.0239
BI015	0.0983	ei513	0.0923	FI046	0.0893		
BI016	0.1716	ei514	0.0156	FI047	0.3428		
BI017	0.1912	ei515	0.0376	FI048	0.112		
BI018	0.1121	ei516	0.0878	fi501	0.0909		
BI019	0.0801	ei517	0.0177	fi502	0.0468		
BI020	0.1146	ei518	0.0839	fi503	0.0305		
BI021	NO INFO	ei519	0.0363	fi505	0.0188		
BI022	0.2184	ei520	0.0527	fi507	0.0485		
BI023	0.1982	ei521	0.0139	fi508	0.1288		
BI024	0.1093	ei522	0.0479	fi509	0.0283		
bi503	0.1269	FI001	0.2718	fi510	0.0354		
bi504	0.1093	FI002	0.0934	fi511	0.1569		
bi505	0.0743	FI003	0.1802	fi512	0.1083		
bi506	0.0428	FI004	0.0723	fi515	0.1268		
bi507	0.0625	FI005	0.2081	fi517	0.1388		
bi508	0.0484	FI008	0.079	fi520	0.0763		
bi509	0.1395	FI009	0.0732	fi521	0.1262		
DI001	0.07	FI010	0.0938	fi522	0.0663		
DI003	0.0556	FI011	0.2317	fi523	0.1311		
DI004	0.0979	FI012	0.1416	fi524	0.1127		
di501	0.0836	FI013	0.094	fi525	0.0609		
di502	0.0455	FI014	0.0695	fi526	0.0577		
di504	0.1158	FI015	0.3156	fi527	0.123		
di506	0.0445	FI016	NO INFO	fi528	0.049		

Length of the sorted natural fractures

Total number of sorted natural fractures in 3D-model		Length information available
TOTAL	713	685
OPEN	214	206
HEALED	261	254
TIGHT	238	225

Large sorted natural fractures		Length information available
TOTAL	413	397
OPEN	176	169
HEALED	158	154
TIGHT	79	74

Small sorted natural fractures		Length information available
TOTAL	300	288
OPEN	38	37
HEALED	103	100
TIGHT	159	151

Length distribution; all natural fractures

	<15 cm	15-30 cm	30-45 cm	45-60 cm	60-75 cm	>75 cm
Tight	145	67	10	2	1	0
Healed	97	101	30	10	7	9
Open	33	62	41	24	18	28

Length distribution; large natural fractures

	<15 cm	15-30 cm	30-45 cm	45-60 cm	60-75 cm	>75 cm
Tight	28	36	8	1	1	0
Healed	38	67	24	9	7	9
Open	21	46	34	23	17	28

Length distribution; small natural fractures

	<15 cm	15-30 cm	30-45 cm	45-60 cm	60-75 cm	>75 cm
Tight	117	31	2	1	0	0
Healed	59	34	6	1	0	0
Open	12	16	7	1	1	0

Open natural fractures

FRACTURE-ID RVS-MODEL	LENGTH OF FRACTURE[m]	FRACTURE-ID RVS-MODEL	LENGTH OF FRACTURE[m]	FRACTURE-ID RVS-MODEL	LENGTH OF FRACTURE[m]	FRACTURE-ID RVS-MODEL	LENGTH OF FRACTURE[m]
N001	0.6306	N168	0.4415	N268	0.5279	N361	0.241
N002	0.5063	N169	0.7335	N269	0.7583	N373	0.1123
N003	0.8116	N170	0.3706	N270	1.2009	N375	0.3734
N004	0.6234	N171	0.8552	N272	1.023	N381	0.2477
N005	0.6577	N172	0.4669	N273	0.6292	N382	0.5632
N006	0.6473	N173	0.8609	N274	0.703	N383	0.4387
N007	0.0689	N174	0.6435	N275	0.1652	N391	0.2304
N008	0.2059	N175	0.7801	N276	0.7818	N396	0.1231
N014	0.2409	N176	0.2323	N277	0.2883	N398	0.1126
N015	0.241	N177	0.4016	N279	0.3256	N401	0.2708
N019	0.8175	N178	0.6651	N280	0.4089	N404	0.0729
N028	0.2726	N180	0.0671	N288	0.1172	N405	0.1801
N028b	0.1859	N185	0.4297	N289	0.7094	N406	0.0888
N031	0.5179	N189	0.4383	N292	0.4043	n543	0.2992
N033	0.308	N191l	0.62	N294	0.3747	n569	0.0987
N034	NO INFO	N191u	0.764	N295	0.1861	n589	0.2176
N038	0.2195	N192	1.4828	N296	0.1391	n591	0.4254
N043	0.1633	N196	0.2864	N297	0.1813	n598	0.2797
N053	0.3015	N199	0.5858	N299	1.0981	n599	0.2578
N058	0.2009	N202	0.2517	N299b	0.1349	n607	NO INFO
N059a	0.7342	N206	0.2964	N299c	0.1189	n617	0.1622
N062b	0.3559	N212	0.2565	N301	1.1566	n623	0.3127
N068	NO INFO	N214	NO INFO	N303	0.4776	n624	0.3219
N070	NO INFO	N215	0.1198	N304	0.3046	n628l	0.3049
N075l	0.2195	N217	0.5068	N306	0.4208	n628u	0.3049
N087	0.527	N221	0.3517	N308	0.3396	n629	0.1946
N089	0.1741	N222	0.2248	N316	0.1799	n636	0.2632
N095	0.2274	N223	0.5554	N317	0.2729	n640	0.5498
N098	0.37	N224	0.4058	N318	1.2287	n643	0.4467
N104	0.2358	N227	0.3142	N319	0.3251	n644	0.1259
N105	0.2738	N231	1.0112	N320	0.243	n645	0.148
N113l	0.5102	N233	0.5874	N322	0.1119	n656	0.1239
N113u	0.6514	N234	0.1912	N323	0.347	n662	0.0936
N117	1.5241	N238	1.0306	N324	0.5495	n664	0.1249
N118	1.566	N238b	0.5882	N325	0.4232	n666	0.0875
N120	0.405	N239	0.9916	N326	0.1605	n670	0.208
N121	0.7836	N240	0.3164	N327	0.1641	n685	0.1684
N126	0.117	N242	0.3697	N328	0.8647	n686	0.0934
N129	0.2623	N243	0.4846	N332	0.1068	n732	0.0921
N133	0.6954	N244	NO INFO	N333	1.0378	n753	0.1879
N134	0.7835	N245	1.043	N333b	0.2709	n761	0.2349
N135	1.7463	N246	0.4728	N335	0.5157	n770	0.0865
N136	0.4915	N247	0.5174	N336	0.2353	n784	0.0902
N138	0.5374	N252	0.3529	N340	0.0861	n806	0.2457
N144	0.1278	N253	0.9675	N341	0.1635	n811	0.2034
N146	0.1038	N254	0.9063	N342	0.1066	n815	0.3173
N148	0.1959	N255	0.3387	N344	0.0574	n816	0.2807
N154	0.2451	N256	0.3332	N347	0.2038	n824	0.122
N156	0.2823	N259	0.3093	N348	0.5915	n832	0.2586
N159	0.2409	N260	0.4294	N351	0.7415	n833	0.2869
N161	0.2769	N264	0.6471	N352	0.6071	n846	0.6154
N162	0.1486	N265	0.3298	N354	0.7766		
N164	NO INFO	N266	0.1531	N358	0.2728		
N165	0.3431	N267	0.5315	N359	0.5257		

Healed natural fractures

FRACTURE-ID RVS-MODEL	LENGTH OF FRACTURE[m]	FRACTURE-ID RVS-MODEL	LENGTH OF FRACTURE[m]	FRACTURE-ID RVS-MODEL	LENGTH OF FRACTURE[m]	FRACTURE-ID RVS-MODEL	LENGTH OF FRACTURE[m]	FRACTURE-ID RVS-MODEL	LENGTH OF FRACTURE[m]
N009	0.1195	N106	0.1545	N237	1.0176	n508	0.2469	n679	0.2613
N010	0.2489	N107	0.2793	N248	0.2295	n511	0.1352	n681	0.082
N011	0.3625	N108	0.1472	N250	0.5877	n512	0.264	n684	0.1475
N012	0.0716	N109	0.3196	N251	0.4223	n520	0.134	n688	0.1238
N013	0.2998	N111	0.2191	N262	0.2461	n521	0.1342	n689	0.0994
N016	0.2481	N112	0.0872	N271n	0.4701	n522	0.1264	n691	0.1205
N017	0.6038	N114l	0.3122	N271u	0.9922	n524	0.2843	n692	NO INFO
N018	0.2516	N116	0.5656	N284	0.1265	n528	0.1276	n694	0.1973
N023	0.6258	N119	0.3422	N298d	0.148	n531	0.0826	n695	0.2543
N024	0.9106	N120b	0.1098	N302	0.2338	n531b	0.0964	n697	0.1418
N025	0.941	N122	0.3146	N307	0.1685	n531c	0.1089	n727	0.1813
N026	0.6829	N123	0.6666	N309a	0.151	n531d	0.1982	n729	0.3791
N029	0.2544	N124	0.4406	N310	0.6625	n540	0.1062	n739	0.2276
N032	0.3806	N127	0.1677	N311	0.1934	n547	0.0974	n751	0.0581
N035	0.2165	N128	0.1213	N312	0.2414	n550	0.3877	n754	0.2222
N036	0.3488	N130	0.2751	N314	0.1193	n551	0.1161	n755	0.2222
N037	0.2695	N131	0.1373	N315	0.2333	n554	0.1857	n757	0.4113
N039	0.258	N132	0.3422	N329	0.5443	n556	0.0879	n759	0.119
N040	0.3964	N137	0.4207	N330	0.1279	n558	0.1947	n765	0.1313
N041	0.2446	N139	0.0577	N331	0.0882	n560	0.1194	n767	0.1125
N042	0.0908	N141	0.1581	N334	0.6998	n563	0.1192	n768	0.1572
N045	0.344	N143	0.2792	N338	0.1816	n568	NO INFO	n769	0.0858
N046	0.1819	N145	0.1054	N339	0.2067	n570	0.085	n771	0.0658
N048	0.1881	N147	0.0839	N349	0.2134	n571	0.1378	n772	0.1652
N052	0.0859	N149	0.118	N350	1.2317	n576	0.095	n778	0.1755
N055	0.1023	N150	0.3815	N356	0.4619	n584	NO INFO	n785	0.0944
N060	0.2356	N151	0.2963	N360	0.5934	n586	0.2347	n787	0.141
N061	0.223	N152	0.3826	N362	0.1179	n587	0.1678	n788	0.2036
N062a	0.2233	N155	0.1979	N363	0.1512	n588	0.0749	n789	0.13
N063a	NO INFO	N157	0.2951	N364	0.1606	n590	0.1072	n793	0.0868
N063b	0.2189	N158	0.1866	N365	0.3893	n592	0.1619	n797	0.1479
N066	0.082	N160	0.2206	N366	0.2652	n596	0.1366	n802	0.1561
N067	NO INFO	N166	0.7602	N368	0.3064	n597	0.0794	n803	0.4702
N069	NO INFO	N167	0.411	N369	0.3518	n600	0.06	n808	0.2831
N072	0.0959	N182	0.3993	N370	0.19	n601	0.1373	n810	0.1691
N074	0.0925	N187	0.1751	N374	0.2204	n609	0.1612	n813	0.1998
N075u	0.2892	N190	0.5887	N377	0.3624	n610	0.1692	n830	0.0959
N076	0.544	N193	1.4508	N378	0.1424	n612	0.2035	n836	0.0912
N077	0.4062	N194	1.2449	N379	0.2706	n613	0.1478	n837	0.255
N079	NO INFO	N197	0.6557	N380	0.0794	n618	0.1302	n838	0.1532
N080	0.231	N198	0.08	N386	0.1347	n619	0.2216	n839	0.1361
N081	0.1153	N200	0.1855	N387	0.1606	n620	0.0961	n840	0.0948
N082	0.4841	N201	0.1918	N389	0.0997	n627	0.2223	n841	0.1262
N084	0.0294	N203	0.1129	N392	0.2692	n635	0.099	n842	0.1572
N085	0.2066	N204b	0.2164	N393	0.2795	n637	0.3363	n843	0.1468
N092	0.2171	N207	0.2809	N400	0.1035	n641	0.2559		
N093	0.1269	N211	0.199	N403	0.1021	n642	0.3869		
N094	0.0691	N213	0.0808	N407	0.2591	n647	0.1318		
N096	0.2645	N216	0.2208	N408	0.2354	n649	0.3024		
N097	0.1677	N220	0.2953	N409	0.1532	n652	0.1027		
N099	0.2191	N226	0.0817	n504	0.1008	n658	0.1311		
N100	0.2218	N228	0.2004	n505	0.1049	n659	0.1926		
N102	0.1033	N230	0.3223	n506	0.1154	n663	0.1055		
N103	0.8208	N236	0.3897	n507	0.0771	n678	0.1497		

Tight natural fractures

FRACTURE-ID RVS-MODEL	LENGTH OF FRACTURE[m]	FRACTURE-ID RVS-MODEL	LENGTH OF FRACTURE[m]	FRACTURE-ID RVS-MODEL	LENGTH OF FRACTURE[m]	FRACTURE-ID RVS-MODEL	LENGTH OF FRACTURE[m]	FRACTURE-ID RVS-MODEL	LENGTH OF FRACTURE[m]
N027	0.2885	N293	0.2655	n561	0.1998	n561	0.1998	n690	0.2284
N030	0.3316	N298a	0.176	n562	0.0735	n562	0.0735	n693	
N049	NO INFO	N298b	0.086	n572	0.0879	n572	0.0879	n696	0.0731
N050	0.1284	N298c	0.1533	n573	0.0995	n573	0.0995	n698	0.0845
N056	0.1084	N300	0.1279	n574	0.1236	n574	0.1236	n699	0.0723
N057	0.296	N305	0.1762	n575	0.0964	n575	0.0964	n702	0.0893
N059b	0.1371	N313	0.1385	n577	0.0715	n577	0.0715	n706	0.26
N064	0.2825	N321	0.09	n580	0.0601	n580	0.0601	n707	0.1011
N065	0.1612	N337	0.1203	n583	0.1584	n583	0.1584	n708	0.1072
N071	NO INFO	N343	0.1501	n593	0.1416	n593	0.1416	n709	0.0641
N073	0.2061	N345	0.3566	n594	0.0851	n594	0.0851	n713	0.0914
N078	NO INFO	N346	0.2597	n595	0.1159	n595	0.1159	n714	0.0935
N083	0.1574	N353	0.6012	n602	0.0842	n602	0.0842	n715	0.0664
N086	0.0811	N355	0.3358	n603	0.0862	n603	0.0862	n718	0.1208
N090	0.0549	N367	0.1889	n604	0.1095	n604	0.1095	n720	0.1465
N091	0.1316	N371	0.1625	n605	0.2107	n605	0.2107	n722	0.1963
N101	0.1683	N372	0.2181	n606	0.1625	n606	0.1625	n723	0.0799
N110	0.1707	N376	0.1953	n611	0.159	n611	0.159	n724	0.0843
N114u	0.339	N388	0.2185	n614	0.1023	n614	0.1023	n725	0.0987
N115	0.4063	N390	0.3347	n615	0.1019	n615	0.1019	n726	0.0993
N125	0.2925	N394	0.1796	n616	0.1019	n616	0.1019	n728	0.1079
N140	0.0468	N395	0.1855	n621	0.0804	n621	0.0804	n730	0.1027
N142	NO INFO	N397	0.0656	n622	0.0848	n622	0.0848	n731	0.1
N153	0.2667	N399	0.0944	n625	0.06	n625	0.06	n733	0.0836
N163	0.1407	N402	0.2002	n626	0.1755	n626	0.1755	n734	0.0685
N179	0.2127	n501	0.5587	n630	0.1279	n630	0.1279	n735	0.0734
N181	0.2827	n502	0.1876	n631	0.138	n631	0.138	n736	0.1057
N183	0.1443	n503	0.093	n632	0.0573	n632	0.0573	n737	0.0639
N184	0.1241	n509	0.0852	n633	0.0611	n633	0.0611	n740	0.0599
N186	0.2201	n510	0.1225	n634	0.1015	n634	0.1015	n741	0.087
N188	0.1227	n513	0.1355	n638	0.1056	n638	0.1056	n742	0.273
N195	0.4034	n514	0.1152	n639	0.0857	n639	0.0857	n743	0.1008
N204a	0.1433	n515	0.1325	n646	0.0968	n646	0.0968	n744	0.2626
N205	NO INFO	n517	0.3826	n648	0.3598	n648	0.3598	n745	0.2996
N209	0.0993	n523	0.1301	n650	0.1688	n650	0.1688	n746	0.079
N218	0.1564	n530	0.0783	n651	0.075	n651	0.075	n747	0.0786
N219	0.1297	n533	0.2226	n653	0.1339	n653	0.1339	n748	0.1551
N225	0.1577	n534	0.109	n654	0.1075	n654	0.1075	n749	0.1233
N229	0.1104	n536	0.0527	n657	0.2274	n657	0.2274	n750	0.0716
N235	0.0959	n537	0.0687	n660	0.1069	n660	0.1069	n752	0.0717
N241	0.1349	n538	0.0544	n661	0.0832	n661	0.0832	n756	0.2834
N249	0.185	n539	0.0853	n665	0.1017	n665	0.1017	n758	0.166
N258	0.3183	n541	NO INFO	n667	0.0963	n667	0.0963	n760	0.1298
N261	0.2017	n542	0.1086	n668	0.0884	n668	0.0884	n762	0.077
N263	0.2301	n544	0.0841	n669	0.1047	n669	0.1047	n763	0.1049
N278	0.0989	n545	0.0658	n671	0.0737	n671	0.0737	n766	0.1074
N281	0.5215	n546	NO INFO	n672	0.108	n672	0.108	n775	0.1358
N282	0.2223	n548	0.0823	n675	0.0689	n675	0.0689	n776	0.1079
N283	0.1491	n549	0.2	n676	0.1176	n676	0.1176	n777	0.1051
N285	0.1694	n552	0.0666	n677	0.1498	n677	0.1498	n779	0.2237
N286	0.1695	n553	0.0685	n680a	0.1918	n680a	0.1918	n781	0.2294
N287	0.1065	n555	0.1299	n680b	0.1918	n680b	0.1918	n782	0.1197
N290	0.1109	n557	0.0833	n682	0.0736	n682	0.0736	n783	0.089
N291	0.1536	n559	0.0734	n687	0.1013	n687	0.1013	n786	0.1631

Tight natural fractures

FRACTURE-ID RVS-MODEL	LENGTH OF FRACTURE[m]
n791	0.1504
n792	0.1027
n794	0.0828
n795	0.116
n796	0.2565
n798	0.1002
n799	0.1089
n800	0.1036
n801	0.2177
n804	0.1064
n805	NO INFO
n812	0.1265
n814	NO INFO
n817	NO INFO
n818	NO INFO
n819	NO INFO
n820	0.0671
n821	0.2042
n826	0.281
n827	0.1288
n829	0.1422
n831	0.1964